The Synthesis and Characterization of Diastereomeric Phosphorus Mustards Derived from Chiral Amino Alcohols

by

Bernard Louis Adjei

Submitted in Partial Fulfilment of the Requirements

For the Degree of

Master of Science

In the

Chemistry

Program

Youngstown State University

August, 2019

The Synthesis and Characterization of Diastereomeric Phosphorus Mustards Derived from Chiral Amino Alcohols

Bernard Louis Adjei

I hereby release this thesis to the public. I understand that this thesis will be made available from the OHIOLINK ETD Center and the Maag Library Circulation Desk for public access. I also authorize the university or other individuals to make copies of this thesis as needed for scholarly research.

Signature:

Bernard Louis Adjei Date

Approvals:

Dr. John A. Jackson Date

Thesis Advisor

Dr. Peter Norris Date

Committee Member

Dr. Douglas T Genna Date

Committee Member

Dr. Salvatore A. Sanders Date

Dean of Graduate Studies

Abstract

Chiral diastereomeric phosphorus mustards were synthesized using enantiomerically pure chiral amino alcohols with bis(2-chloroethyl) phosphoramidic dichloride. Flash column chromatography afforded enantiopure products, confirmed by ^{31}P, ^{13}C, and ^{1}H NMR.

Determination of absolute stereochemistry at phosphorus by X-ray diffraction analysis was carried out to confirm the initial assignments which were done based on the syn / anti relationship inferred from literature references, with respect to the position of the chiral substituents present on the nitrogen mustard moiety.

Acknowledgment

The great success of this thesis work would not have been possible without the chance to enroll at the Youngstown State University. I would like to thank the chemistry department for giving me the opportunity to pursue my master's degree here. I am grateful to all those with whom I had the privilege of interacting and working with during my thesis and other related work.

To my thesis committee members, Professor Peter Norris and Professor Douglas T Genna for their invaluable suggestions, comments and constructive criticisms. I am especially indebted to Professor John A. Jackson, my thesis advisor for allowing me study under him and to carry out this interesting research work.

As my mentor and teacher, I can't thank him enough for his believe in me and for the enthusiasm exuded which made everything possible. And to all my friends and family for helping me survive throughout all these changing scenes of my life.

Most of all, I am extremely thankful to my Maker for the undeserving knowledge, strength and favor in pursuing my academic goals.

Table of Contents

List of Figures

List of Schemes

List of Tables

List of Abbreviations

Abbreviations	Description
# a chromatography	fast diastereomer obtained through flash column
Å	Angstrom
$[\alpha]_D^{20}$	specific rotation
# b chromatography	slow diastereomer obtained through flash column
^{13}C	Carbon-13
c	concentration
$CDCl_3$	deuterated chloroform
δ	chemical shift in parts per million (ppm)
d	doublet
dd	doublet of doublets
ddd	doublet of doublets of doublet
dddd	doublet of doublet of doublet of doublets
DMSO-d_6	deuterated dimethyl sulfoxide
DNA	deoxyribonucleic acid
Et_3N	triethylamine
EtOAc	ethyl acetate
FDA	Food and Drug Administration
g	gram
^1H	Proton-1
h	hour
Hz	Hertz
J	coupling constant
q	quartet
m	multiplet
MHz	megahertz
mL	milliliter

mmol	millimoles
mol eq.	mole equivalent
mp	melting point
NMR	nuclear magnetic resonance
^{31}P	Phosphorus-31
$P(O)Cl_3$	phosphoryl chloride
PMA	phosphomolybdic acid
ppm	parts per million
R_f	retention factor
s	singlet
S_N2	biomolecular nucleophilic substitution in the second order
t	triplet
TMS	tetramethylsilane
UV	ultraviolet
XRD	X-ray diffraction

Dedication

To the memory of my late dad Cletus Kwasi Adjei

Whose optimism and dedication made it possible for me to come this far.

Even though you are gone to be with our Maker,

We are still a team and I shall strive to keep moving on in this life, until the dreams of the future come to pass.

Chapter One (1)

Introduction

History of Mustard Agents:

Bis(2-chloroethyl) amine moieties, also called nitrogen mustards, interact with deoxyribonucleic acid (DNA), which results in an interstrand crosslink that inhibit or stop the mitotic process of cancerous cells.[1] Cyclophosphamide and melphalan (**Figure 1**) are among this unique class of mustards with approval from the FDA and are known to possess alkylating potential which makes them useful as anti-proliferative agents.[2] The chemical properties of these mustards became apparent in recent times even though the sulfur analog (sulfur mustard) had been previously utilized as a vesicant during the first world war (WWI).

The sulfur mustard (mustard gas) was applied as an aerosol and had the ability to impair the normal functioning of soldiers as target enemies which inevitably caused their death.[3]

Latter day discovery of anti-cancer activity of nitrogen mustards was born out of both clinical investigations and serendipity following the failure of sulfur mustards which were observed to be too toxic and injurious for clinical applications.[3]

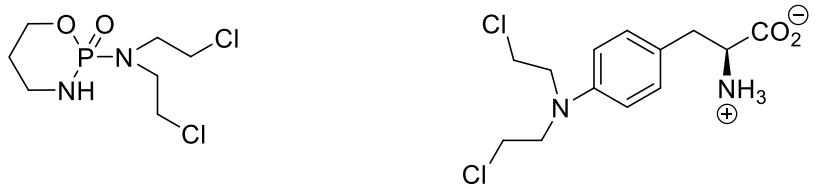

Cyclophosphamide Melphalan

Figure 1. Structure of cyclophosphamide and melphalan.[2]

Bis(2-chloroethyl) (methyl) amine, also called chlormethine, was the first FDA approved chemotherapeutic obtained from a nitrogen mustard. This bifunctional electrophile can undergo both intramolecular and intermolecular S_N2 reactions (**Scheme 1**). The intramolecular reaction generates a heterocyclic cation known as an aziridinium ring (intermediate) which undergoes a subsequent ring opening reaction when attacked by a nucleophilic DNA molecule.[2] The N-3 of adenine (a purine) and N-7 of guanine (a pyrimidine) are mostly the target sites for the DNA's alkylation (**Figure 2**).

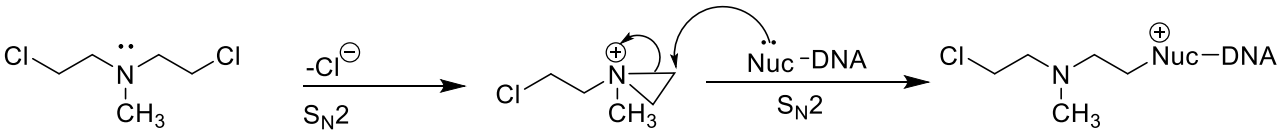

Scheme 1: Alkylation of DNA in chlormethine.[3]

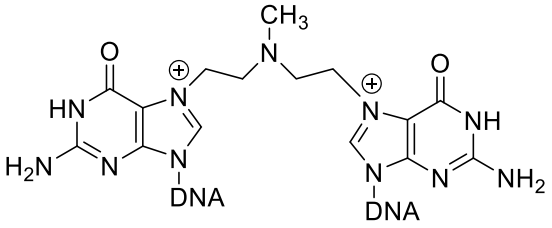

Figure 2. Interstrand crosslink formation of methchlormethine with N-**7** of guanine.[3]

DNA replication and transcription are prevented as a result of the alkylating nature of nitrogen mustards and consequently become effective cytotoxins in the reduction towards proliferation of cancer cells.[2] Some examples of mustards used in clinical practice are listed in (**Figure 3**) below.

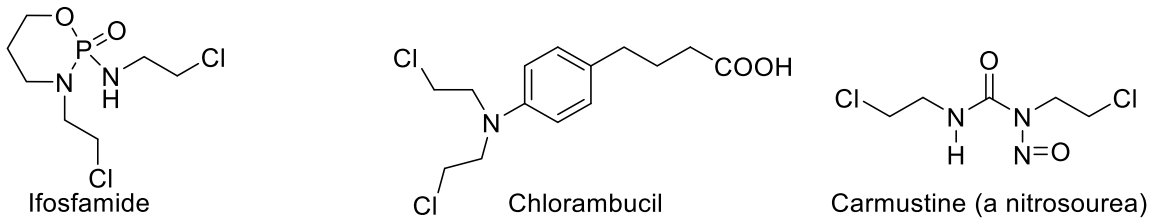

Figure 3. Examples of mustards and a nitrosourea used clinically.[3]

1.1 **Cyclophosphamide**

Cyclophosphamide, a nitrogen mustard derivative, gained prominence as a chemotherapeutic and immunosuppressive agent following FDA approval in 1959 after it had been used extensively in a series of clinical trials.[2] The mode of action and bioactive materials from the metabolism of this compound (**Scheme 2**) below, became known between the late 60's and early 1970's. Samples of metabolites obtained from animal urine suggested that hydroxylation occurred at the C-4 position (**Figure 4**).

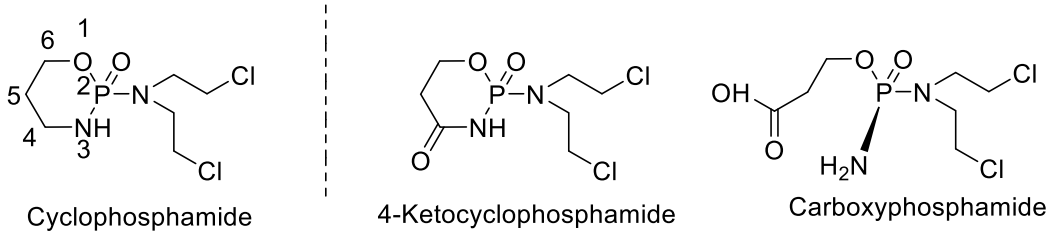

Figure 4. Cyclophosphamide (left) and observed metabolites (right).[3, 4]

Even though the bioactive material of cyclophosphamide was thought to be the observed metabolite 4-ketocyclophosphamide, it's *in vitro* activity proved less cytotoxic than cyclophosphamide.[4] The generation of the bioactive form of cyclophosphamide is by the aliphatic oxidation by hepatic cytochrome P450 enzyme (CYP 2B6, 2C9 and 3A4) to give 4-hydroxycyclophosphamide a tautomeric form of aldophosphamide (**Figure 4**) above.[3]

However, a major drawback for the synthesis of this bioactive material is for the cytochrome P450 to be present in the tumor itself, the absence of which will result in the problem of cellular uptake, resistance and the alkylation of normal cell.[2] The base - induced abstraction of one of the protons on the α-carbons results in phosporodiamidic acid after the elimination of acrolein.

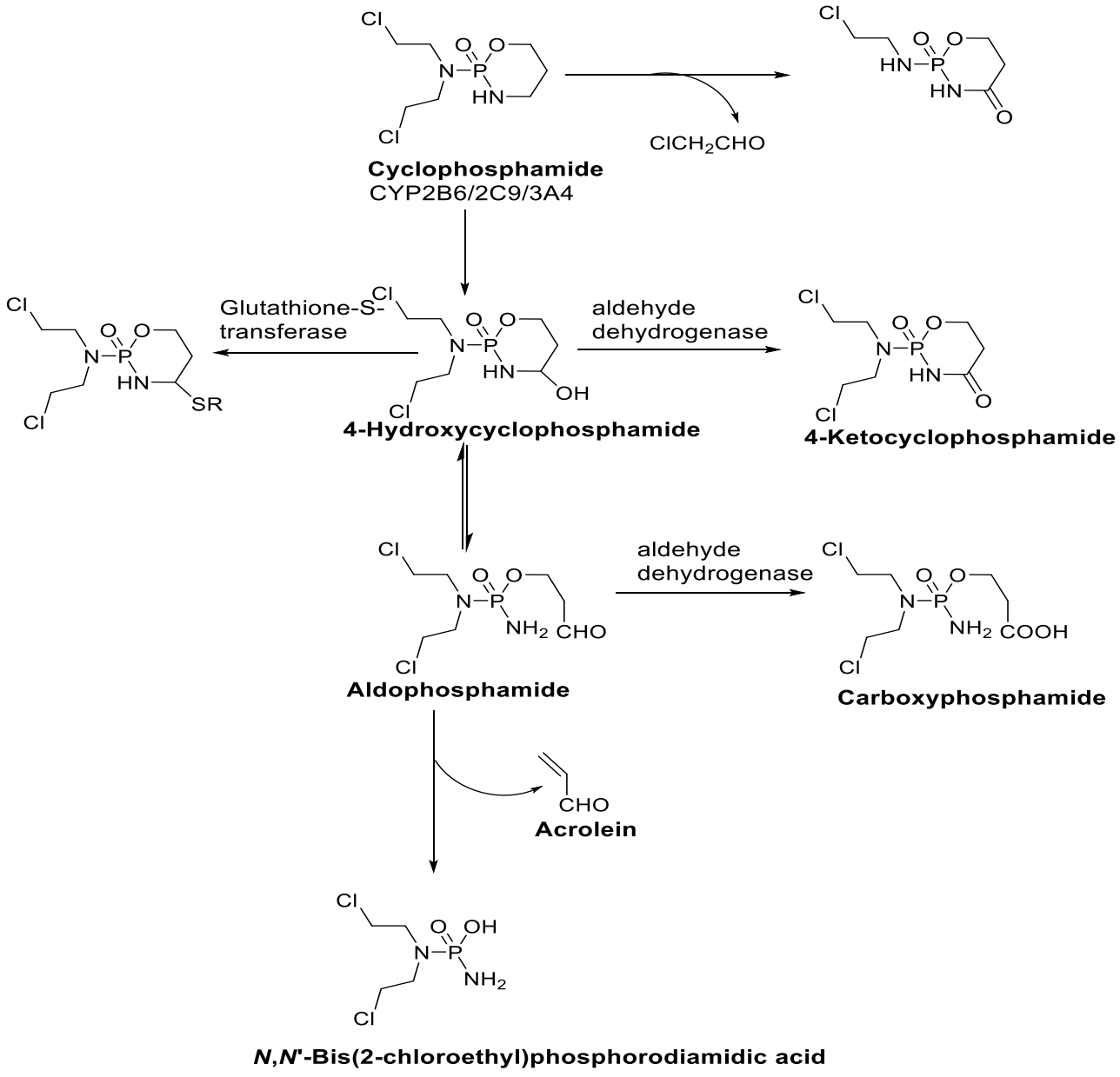

Scheme 2. The metabolic activation of cyclophosphamide.[3]

1.3 **Melphalan**

Melphalan is synthesized from (*S*)-4-nitrophenylalanine with the α-amino group having been protected and later converted back into the amino group, retaining the stereochemistry in the synthetic route. The esterification of the alkanoic acid group of (*S*)-4-nitrophenylalanine into an ethyl ester marks the first step transformation. Phthalic anhydride is utilized as a protecting group for the α-amino group in the reaction which affords the formation of the phthalimide **(Scheme 3)**.[5]

The phthalimido group remains unreactive under the reaction conditions and is removed in a later step. The nitro group is reduced to an aromatic amine, and subsequently with two equivalents of ethylene oxide to afford bis(2-hydroxyethyl) amino adduct.[5] The amino group behaves as a nucleophile and is involved in the epoxide ring opening.[2] The final step is the deactivation of the phthalimido protecting group via chlorination of the diol that affords the dichloro derivative melphalan.[5] Hydrolysis of the ester results in the formation of a molecule with the same stereochemistry as the starting material.

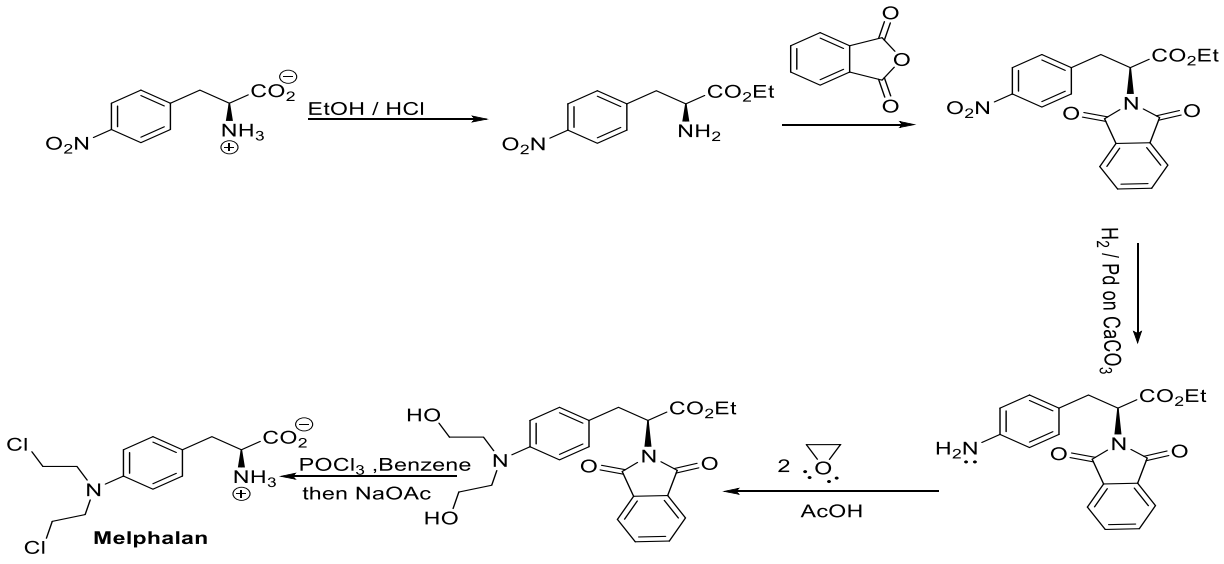

Scheme 3: Original synthesis of Melphalan.[3]

1.4 **Importance of chirality in pharmaceuticals**

Many pharmaceuticals have at least one stereocenter and with one isomer desired over the other. For instance, DOPA has two enantiomers, D-DOPA and L-DOPA (**Figure 5**). Whilst the l-enantiomer is administered to treat Parkinson's disease, the D-DOPA reduces white blood cell count (agranulocytosis), which is essential in fighting infections.

Enantioselectivity of pharmaceuticals in biological systems accounts for the differences in their effect, while one enantiomer binds onto a specific site better.[6, 7, 10]

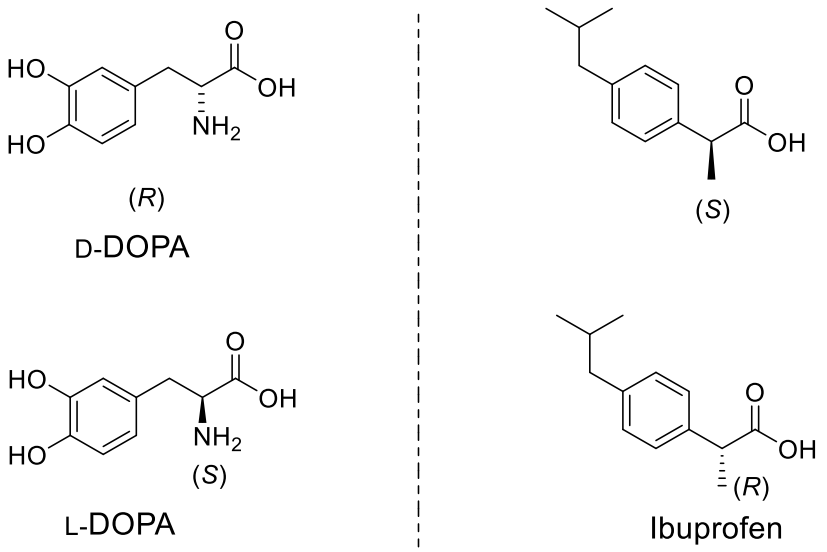

Figure 5. Enantiomers of DOPA and Ibuprofen.[6]

Differences in configuration among enantiomers results in selective activity, the effects which can be either medicinally useful, inactive or injurious in pharmaceutical products as such purity of these pharmaceuticals are critical. For example L-DOPA is sold as an enantiomerically pure product. In some cases, however, if an enantiomer is inactive or less toxic, the pharmaceutical is sold as a mixture to offset the cost of production.[5, 6] For

example, in order to minimize cost of production, ibuprofen is sold as a racemic mixture, the *S* enantiomer is active biologically and the *R* is inactive.

Moreover, studies have shown that there is epimerization of the *R* enantiomer into the *S* form through a stereoselective enzymatic route,[8-9] which prevents the conversion of the *S* enantiomer back into the *R* enantiomer. Cyclophosphamide, which has one chiral center, is also administered as a racemate.[5]

Tetramisole, a nematocide, was first administered as a racemate but due to the many side effects (headache, vomiting, abdominal pain, vertigo) of its D-isomer, whose role is a xenobiotic and an environmental contaminant, only the L-isomer, levamisole, has a therapeutic use; highly effective against Ascaris lumbricoides in humans (**Figure 6**).[10] Simialarly, *R*-(-)-ketamine; less active (distomer), accounts for hallucination, restlessness and agitation when administered, but in variance with the *S*-(+)-ketamine isomer; more active (eutomer) is used as an anesthetic drug in the treatment of rheumatic disorder.

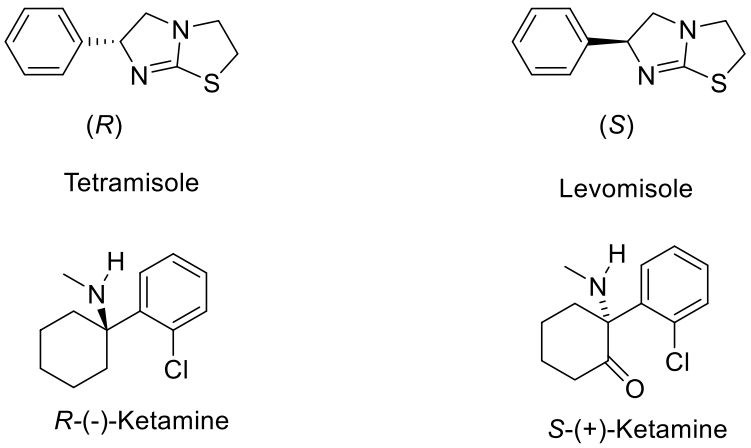

Figure 6. Some examples of chiral pharmaceutical agents administered as a racemate.[10]

Previous work

The synthesis and characterization of oxazaphospholidinones had been previously explored at Youngstown State University by Kelly Madison and Laurence Rohde Jr. respectively.

Table1: Summarized yields of previously synthesized oxazaphospholidinones by Madison YSU Thesis (1996).[11]

Table 1. Summarized Yields of Previously synthesized Oxazaphospholidinones						
Amino alcohol[a]	Overall Yield (%)			Observed Ratio (*A*: *S*)[b]		
	THF	CH_2Cl_2	Toluene	THF	CH_2Cl_2	Toluene
(1*S*,2*R*)-(+)-Ephedrine Hydrochloride	41.4	50.2	60.9	1.6:1	2.4:1	1.1:1
(1*R*,2*S*)-(-)Ephedrine	45.2	50.7	60.7	1.1:1	1.5:1	1.6:1
(*S*)-(-)-2-Amino-3-Phenyl-1-Propanol	53.6	59.5	64.0	1.1:1	1:1	1.9:1
(*R*)-(+)-2-Amino-3-Phenyl-1-Propanol	64.6	73.2	54.0	1.3:1	0.9:1	1.3:1
Ethanolamine[c]	62.0	84.8	30.7	-	-	-
[a] The chiral amino alcohol used generates their respective diastereomers						
[b] *A* : *S* refer to the anti and syn-configuration						
[c] Generates a racemic mixture, as confirmed via polarimetry						

Varying yields for synthesized oxazaphospholidinones and diastereomeric ratios were accordingly reported with the anti-configurations in greater yields than the syn-configurations. These descriptions were based on the spatial relationship of the chiral center on the C-4 position of the heterocyclic mustard moiety.

Characterization of these compounds using ^{31}P, ^{13}C, ^{1}H NMR spectroscopy was relied upon. Single crystal X-ray diffraction (XRD) was not the focus at the time of Madison, however Rohde Jr, in 2018 obtained for some of these compounds X-ray data which was used in solving the crystal structures and subsequently for the determination of absolute configuration at phosphorus in various oxazaphospholidinones synthesized.[8]

Table 2. Summarized Yields of Oxazaphospholidinones by Rohde, Jr. (2018).[8]

Amino Alcohol Used[a]	Yield (%)	^{31}P NMR (ppm)[c]	
		OAPa	OAPb
Ethanolamine	75	27.15	
(*R*)-(+)-2-Amino-3-Phenyl-1-Propanol	71.8	27.03	28.57
(*S*)-(-)-2-Amino-3-phenyl-1-propanol	75.3	27.04	28.54
(1*R*, 2*S*)-(-)Ephedrine	64.6	24.30	24.63
(*S*)-(+)-2-Amino-1-Butanol	68.7	27.87	29.72
(*R*)-(-)-2-Amino-1-Butanol	65.0	27.56	29.30
(*S*)-2-Amino-3,3-Dimethyl-1-Propanol	75.0	27.55	29.93
(*S*)-(+)-2-Amino-4-Methyl-1-Propanol	79.2	27.56	29.00
(*R*)-(-)-2-Amino-4-Methyl-1-Pentanol	72.8	27.58	28.98
[a]Each amino alcohol generates their aforementioned oxazaphospholidinone			
[c]a and b refer to the diastereomer's order of elution upon purification.			

All diastereomers that eluted first from the column were observed to have upfield ^{31}P NMR chemical shift and were assigned anti-configuration and syn-configuration was assigned to diastereomers that eluted last with a downfield ^{31}P NMR chemical shift. Polarimetry was used to obtain the specific rotation of the diastereomerically pure products, these were the basis of the characterization made by Rohde Jr. (**Figure 7**). Diastereomeric 2-[bis(2-chloroethyl)]-1,3,2-oxazaphospholidin-2-ones derived from *l*- and *d*-serine had been previously synthesized by [Foster 1978; Jackson et al., (1992)][2,12] but lacked X-ray

diffraction data to determine the absolute configuration at the phosphorus atom even though a previous assignment based on analogy had been put forward by Thompson et al., (1990).[13]

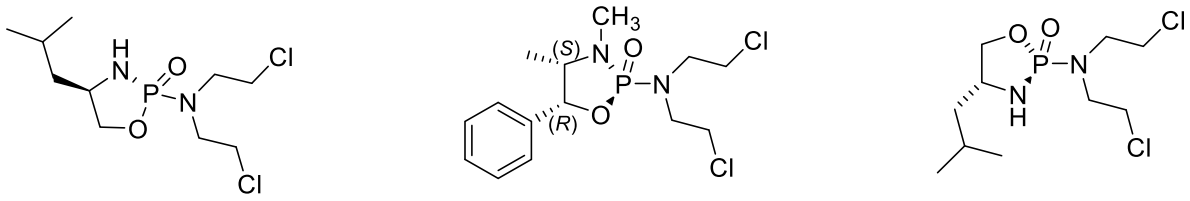

Figure 7. Some single crystal structures obtained by Rohde, Jr. et al., (2018).[8]

STATEMENT OF PURPOSE

This thesis work seeks to explore, further, the works of two predecessors at YSU via the synthesis of diastereomeric phosphorus mustards using selected chiral amino alcohols. Additional structural assignments were made using NMR spectroscopy (^{1}H, ^{13}C, ^{31}P), XRD data collected will build on what Jackson and co-workers (1992) obtained, and polarimetry will be utilized to determine the specific rotation of the compounds to be synthesized. The products obtained, will be tested for their anti-cancer potentials.

Chapter Two (2)

Results and Discussion

Synthesis of Bis(2-chloroethyl)phosphoramidic Dichloride

Since Phosphoramide **1** (**Scheme 4**) is not readily available commercially for purchase, therefore attempts have been made to synthesize this starting material using the experimental procedure put forward by Friedman and Seligman.[14]

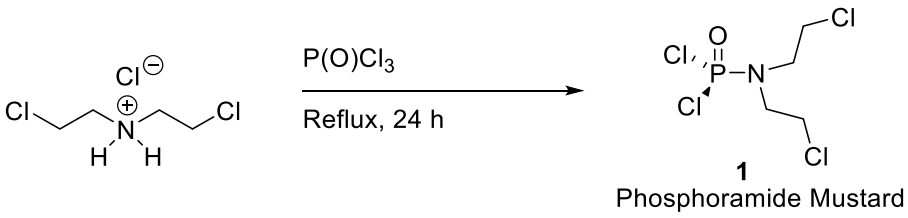

Scheme 4. Synthesis of Phosphoramide Mustard **1**.

The crude product was recrystallized to afford phosphoramide **1** in 75.6% yield. ^{31}P NMR is a powerful tool used in the characterization of compounds, which produces unique singlet peaks that corresponds with the number of phosphorus atoms present in a compound. ^{31}P NMR of phosphoramide mustard **1** gave a single peak at 17.49 ppm (**Figure 9**) whilst that of the phosphoryl chloride gave a peak at 2.9 ppm. The change in the chemical shift value of the single peak observed confirmed the formation of the new product. ^{1}H NMR showed a very distinct multiplet from 3.99 - 3.61 ppm and ^{13}C NMR gave two doublets at 49.44 and 40.81 ppm, indicating the two unique carbons in the product formed. The most downfield peak in the ^{13}C NMR relates to the carbon closer to phosphorus, whereas the most upfield peak relates to the carbon closest to chlorine.

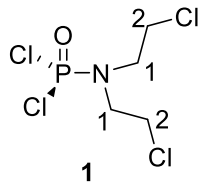

1

Figure 8. Phosphoramide Mustard **1**.

Table 3. ^{13}C NMR of Phosphoramide Mustard **1**

^{13}C	δ(ppm) in $CDCl_3$
C1	49.44 (d, J = 4.31 Hz)
C2	40.81 (d, J = 2.96 Hz)

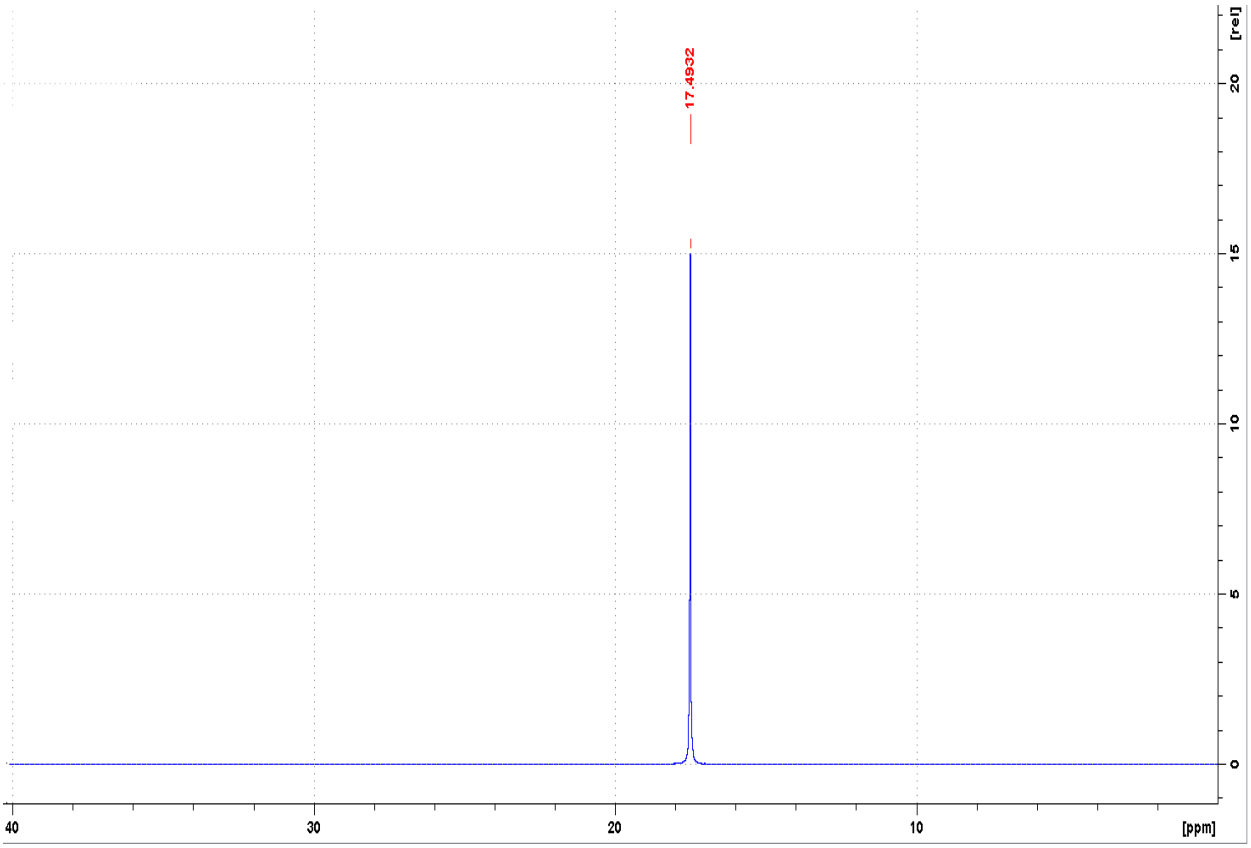

Figure 9. ^{31}P NMR spectrum of Phosphorus Mustard **1**.

Synthesis of 1, 3, 2 - Oxazaphospholidinone Derivatives

Experimental practice using a cheap non-chiral amino alcohol ethanolamine afforded the result below (**Scheme 5**).

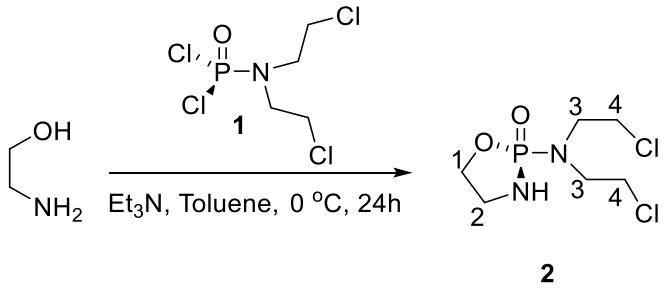

Scheme 5. Synthesis of Oxazaphospholidin-2-one **2**.[14]

A single peak at 30.69 ppm was observed in the ^{31}P NMR of compound **2**. ^{13}C NMR revealed four carbon peaks with chemical shift values at 66.32, 42.31, 49.09, 42.19 ppm with two of the peaks splitting to give doublets. With oxazaphospholidinone **2** synthesized in a good yield, the synthesis of selected chiral amino alcohols and serine methyl esters were carried out and the products subsequently characterized using NMR spectroscopy. XRD data was collected in an attempt to solve the crystal structures of these new diastereomers.

Table 4. ^{13}C NMR of Oxazaphospholidinone **2**

^{13}C	δ(ppm) in $CDCl_3$
C1	66.32 (d, J = 2.64 Hz)
C2	42.31
C3	49.09 (d, J = 4.78 Hz),
C4	42.19

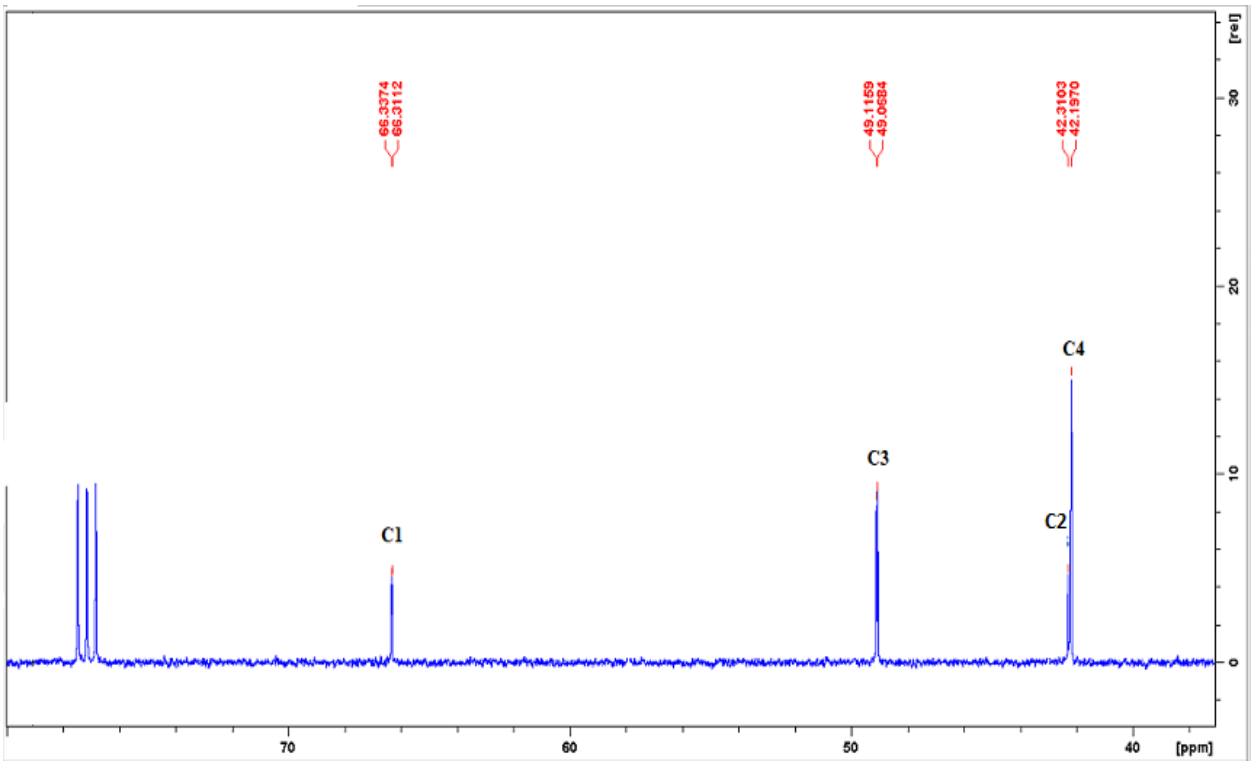

Figure 10. ^{13}C NMR Spectrum of Oxazaphospholidinone **2**.

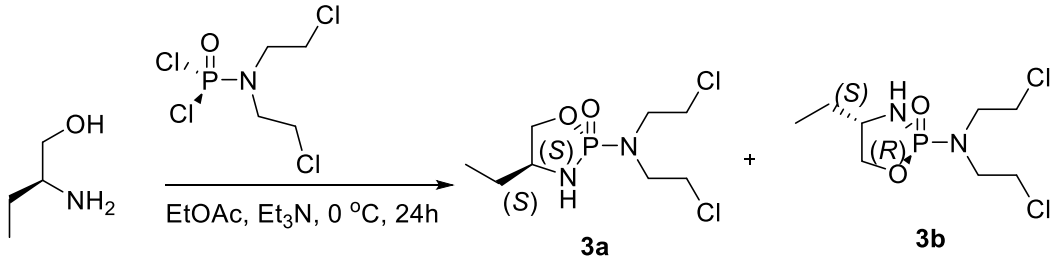

Scheme 6. Synthesis of Oxazaphospholidinones **3a** and **3b**.

Synthesis of oxazaphospholidinones **3a** and **3b** from (*S*)-(+)-2-amino-1-butanol gave an overall yield of 75.9% with the ^{31}P NMR chemical shift values of 27.59 and 29.43 ppm respectively based on their order of elution from the flash column. The other diastereomeric pair **4a** and **4b** (**Scheme 7**) were synthesized from (*R*)-(-)-2-amino-1-butanol and gave an overall yield of 55.7% also with ^{31}P NMR chemical shift values of 28.08 and 29.20 ppm, respectively.

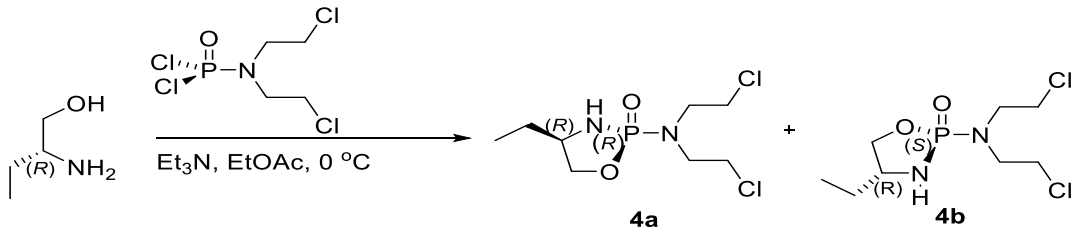

Scheme 7: Synthesis of oxazaphospholidinones **4a** and **4b**.

The slight difference in the chemical shift values of **3a** and **4a** could possibly be due to water contamination from exposure of the deuterated chloroform to moisture. As implemented by earlier researchers (Foster, 1978, Jackson et al., 1992) a syn configuration corresponds with a chemical shift value which is downfield while an anti-configuration is assigned to peaks with an upfield chemical shift values (**Figure 12**). This relationship is based on the relative position of the mustard moiety and the amino alcohol groups of the synthesized oxazaphospholidinones.

In this regard, the absolute configuration at phosphorus for **3a** and **4b** is expected to be *S* and that of **3b** and **4a** would be *R*.

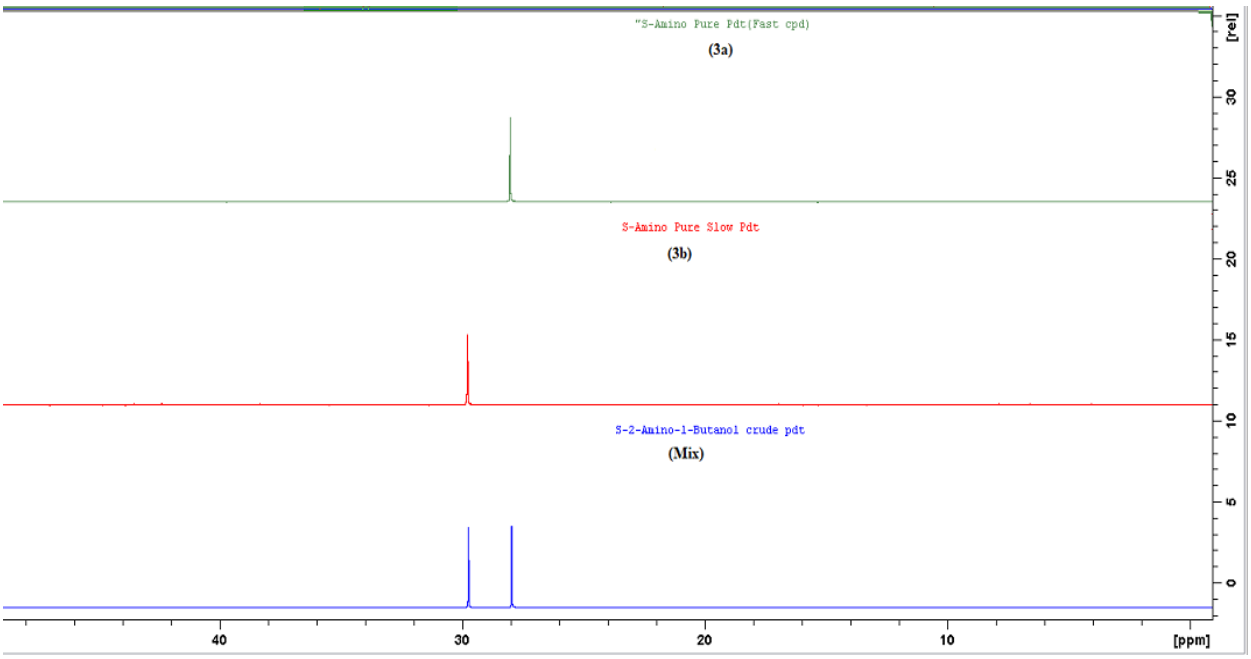

Figure 11.^{31}P NMR of Oxazaphospholidinone **3a** and **3b**.

Green peak = fast / anti diastereomer (**3a**)

Red peak = slow / syn diastereomer (**3b**)

Blue peaks = combined peaks obtained from crude product (**Mixture**) in (**Figure 11**).

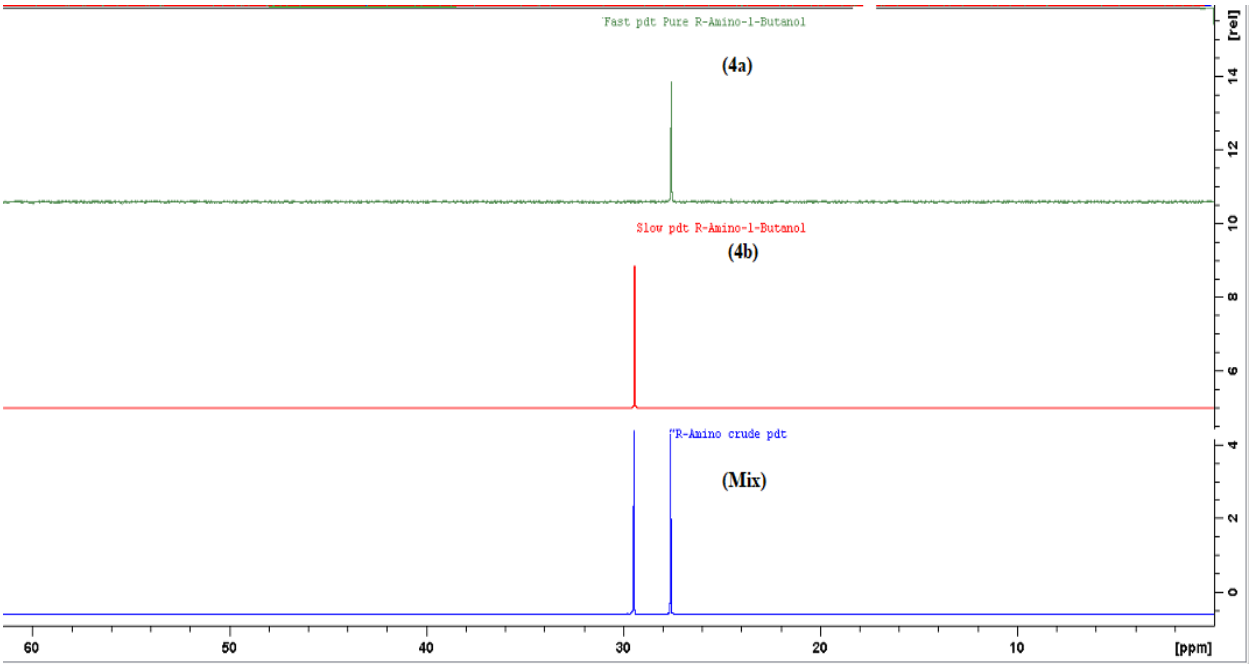

Figure 12.^{31}P NMR of Oxazaphospholidinone **4a** and **4b**.

Green peak = fast /anti diastereomer (**4a**)

Red peak = slow / syn diastereomer (**4b**)

Blue peaks = combined peaks obtained from crude product (**Mixture**) in (**Figure 12**)

Structural assignments made for oxazaphospholidinones **3a**, an enantiomeric pair of **4a** based on ^{1}H, ^{13}C, ^{31}P and COSY NMR spectroscopy, revealed an integration of the proton signals in ^{1}H NMR which added up to seventeen protons and six uneven carbon signals as expected in the compounds. Both **3a** and **4a** were analogous to each other structurally due to their enantiomeric relationship.

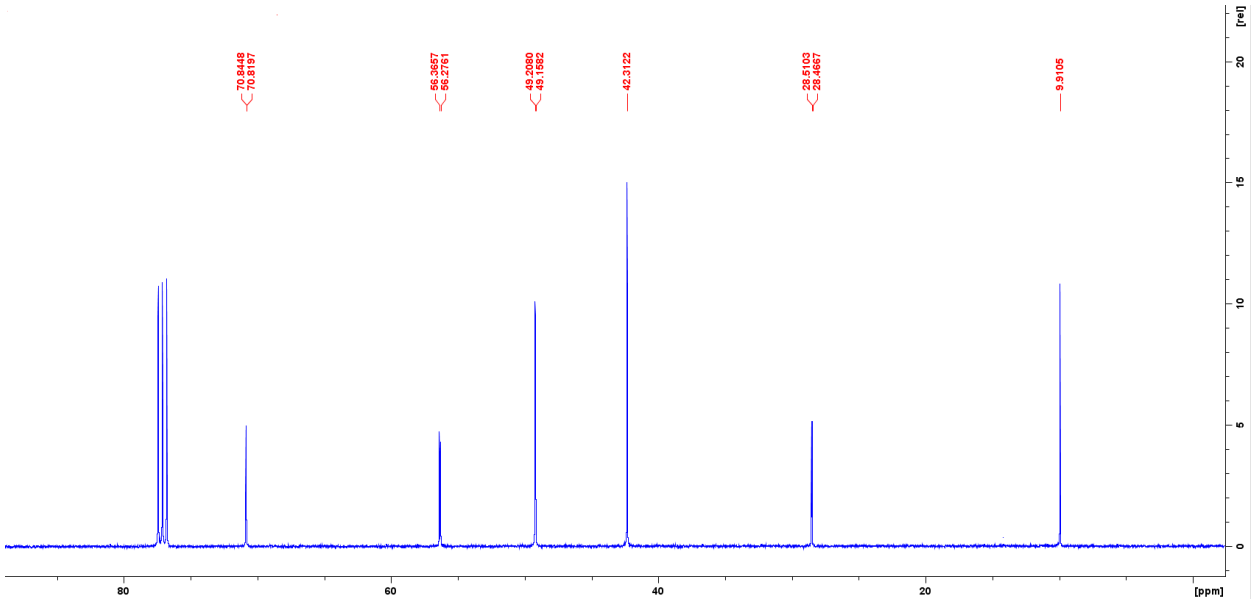

Figure 13.[13]C NMR of Oxazaphospholidinone **3a**.

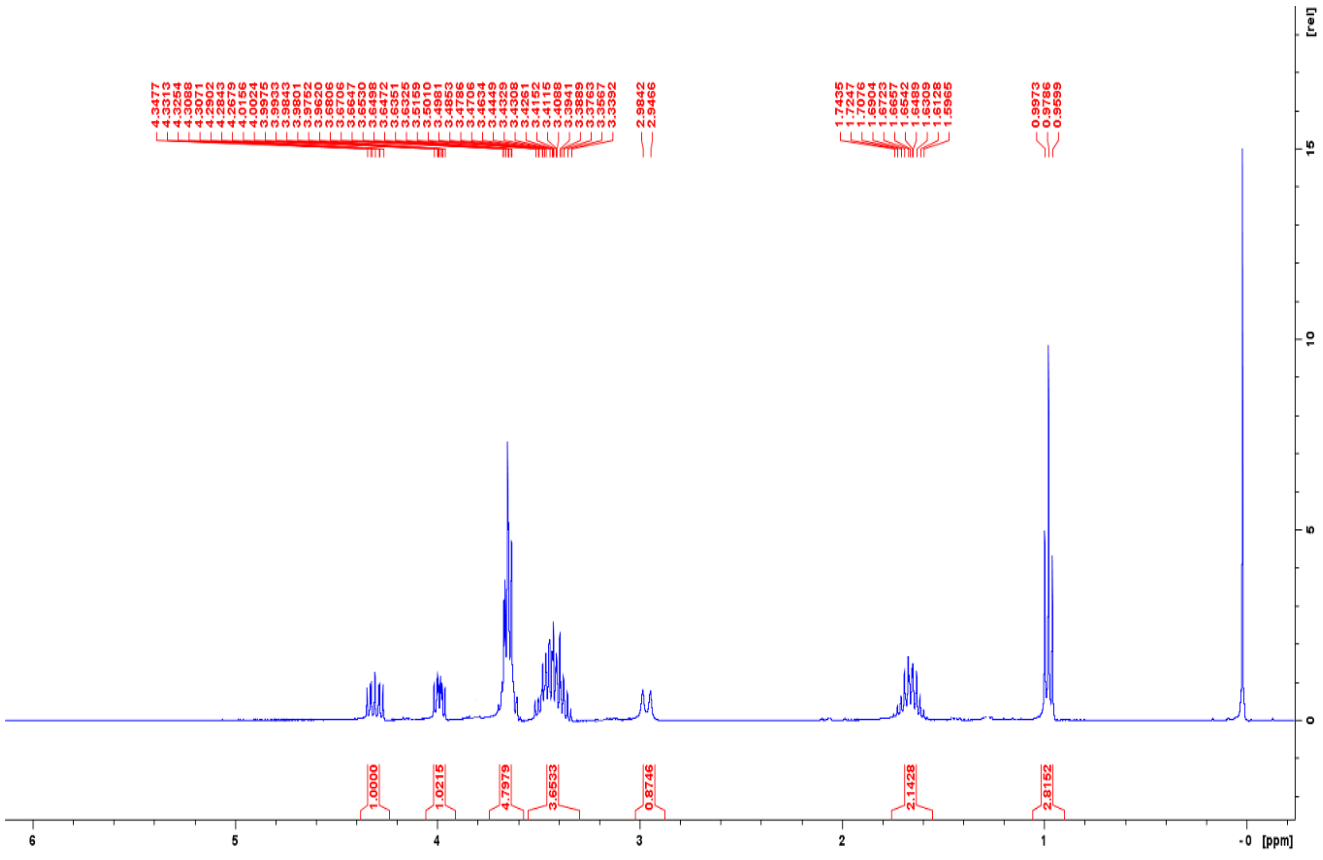

Figure 14. [1]H NMR of Oxazaphospholidinone **3a**.

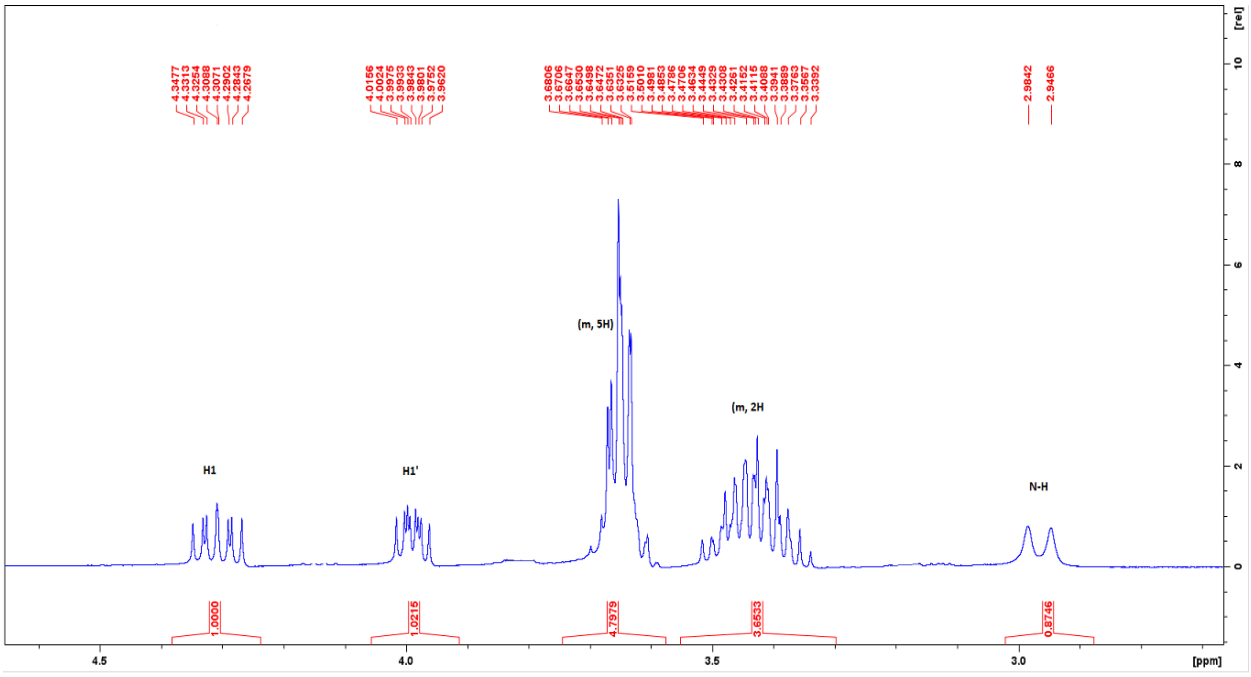

Figure 15. Expanded ^{1}H NMR of Oxazaphospholidinone **3a**.

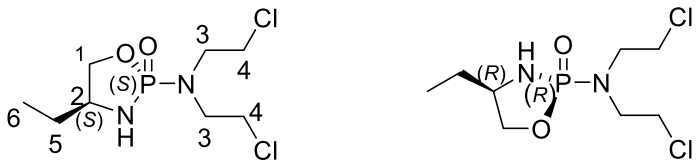

3a **4a**

Figure 16. Enantiomeric pair of oxazaphospholidinones **3a** and **4a**.

Table 5. ^{13}C NMR and ^{1}H NMR assignments of oxazaphospholidinone **3a**.

^{13}C	δ (ppm)	^{1}H	δ (ppm)
C1	70.79 (d, *J* = 2.19 Hz)	H1 & H1'	4.31 (ddd, 1H, *J* = 16.31 Hz, 8.90 Hz, 3.81 Hz) 3.99 (ddd, 1H, *J* = 8.92 Hz, 7.24 Hz, 5.27 Hz)
C2	56.40 (d, *J* = 8.88 Hz)	H2	3.69-3.53 (m, 5H)
C3	49.13 (d, *J* = 4.94 Hz)	H3	3.51-3.33 (m, 4H)
C4	42.37	H4	3.69-3.53 (m, 5H)
C5	28.49 (d, *J* = 4.38 Hz)	H5	1.74-1.59 (m, 2H)
C6	9.92	H6	0.97 (t, 3H, *J* = 7.48 Hz)
		N-H	2.97 (d, 1H, *J* = 15.05 Hz)

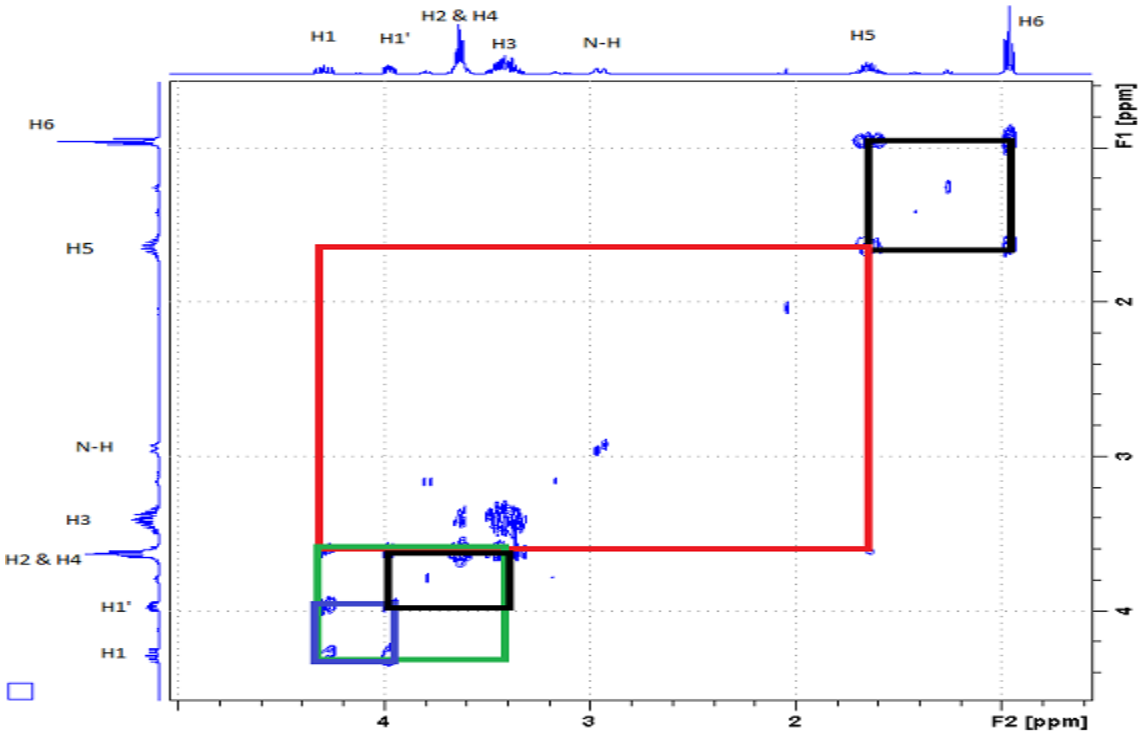

Figure 17. COSY of Oxazaphospholidinone **3a**

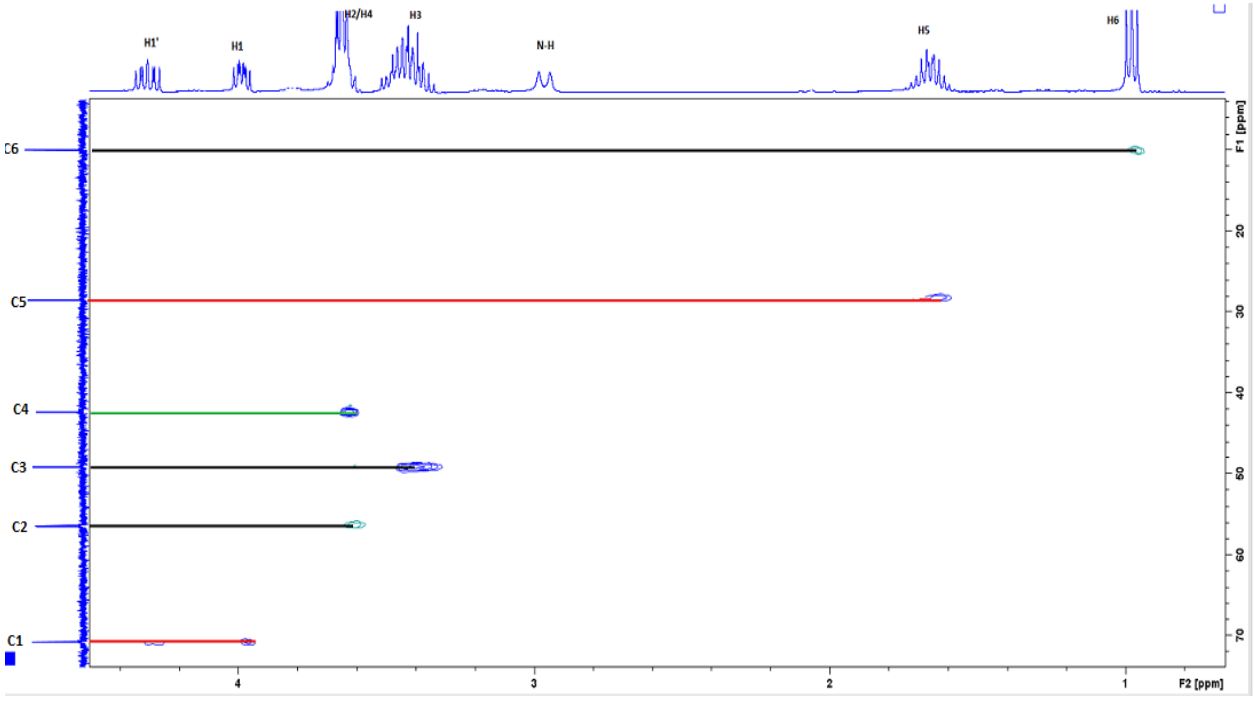

Figure 18. HSQC NMR of Oxazaphospholidinone **3a**

COSY NMR was used to assign the proton signals in oxazaphospholidinone **3a** (**Figure 17**). The oxygen atom has the greatest deshielding effect in the heterocycle. H1 and H1' were labelled as the most deshielded proton signals at 4.31 and 3.99 ppm. A careful observation of the COSY NMR spectrum revealed that H1 / H1' are coupled to each other through geminal coupling, and to H2 by vicinal coupling.

HSQC NMR confirmed that H2 and H4 proton signals were overlapping with each other (**Figure 18**). The labelling of the carbon peaks was based on the COSY NMR assignment of the protons and comparison made using the ACD / LAB. The doublet at 2.97 ppm in the ^{1}H NMR was labelled as the hydrogen attached to the nitrogen in the heterocycle as it lacked any direct correlation to the carbon peaks in the HSQC NMR spectrum.

The C3 and C4, were assigned to the nitrogen mustard when compared with the previously synthesized phosphorus mustard **1**.

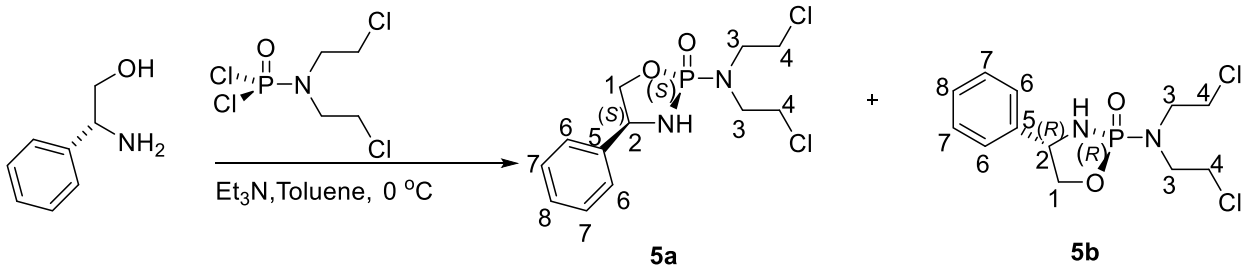

Scheme 8. Synthesis of Oxazaphospholidinones **5a** and **5b**.

The ^{31}P NMR of oxazaphospholidinones **5a** and **5b** are 27.02 and 28.52 respectively with an overall yield of 77.9%. The individual yield for **5a** and **5b** isolated as white crystalline solids gave 43.4% and 34.5% respectively. Assignment of anti / syn

configurations to the compounds were based on the same relationship utilized earlier. The chirality at phosphorus for **5a** is expected to be *S* and that at **5b** expected to be *R*. Oxazaphospholidinone **5a** has a melting point of 156-159 ºC with a specific rotation of +42.7º and that of **5b** gave a melting point of 121-124 ºC with a specific rotation of -22.8º.

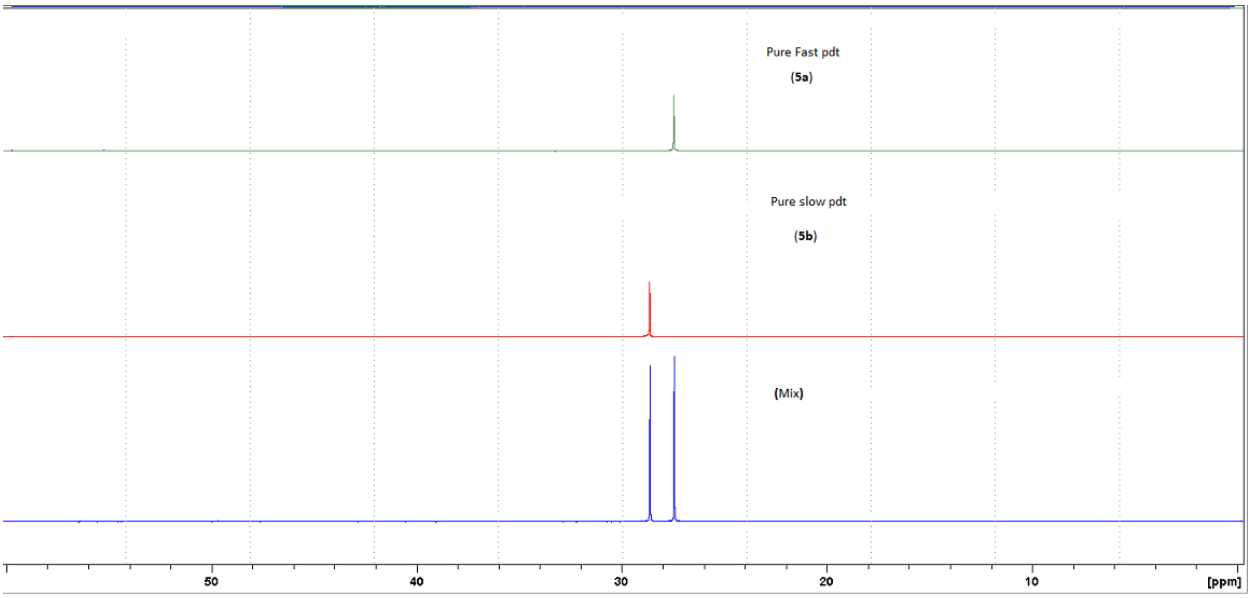

Figure 19. ^{31}P NMR of Oxazaphospholidinone **5a** and **5b**.

Green peak= fast / anti diastereomer (**5a**)

Red peak = slow / syn diastereomer (**5b**)

Blue peaks = combined peaks obtained from crude product (**Mixture**) in (**Figure 19**).

The oxazaphospholidinones **5a** and **5b** are expected to have diastereomeric relationship with a pair of diastereomers when the (*R*)-(-)-2-phenylglycinol starting material is used.

An integration of the proton signals in ^{1}H NMR afforded 17 protons with a total of eight inequivalent carbon signals as predicted with the ACD/LAB and confirmed by ^{13}C NMR from the final product obtained.

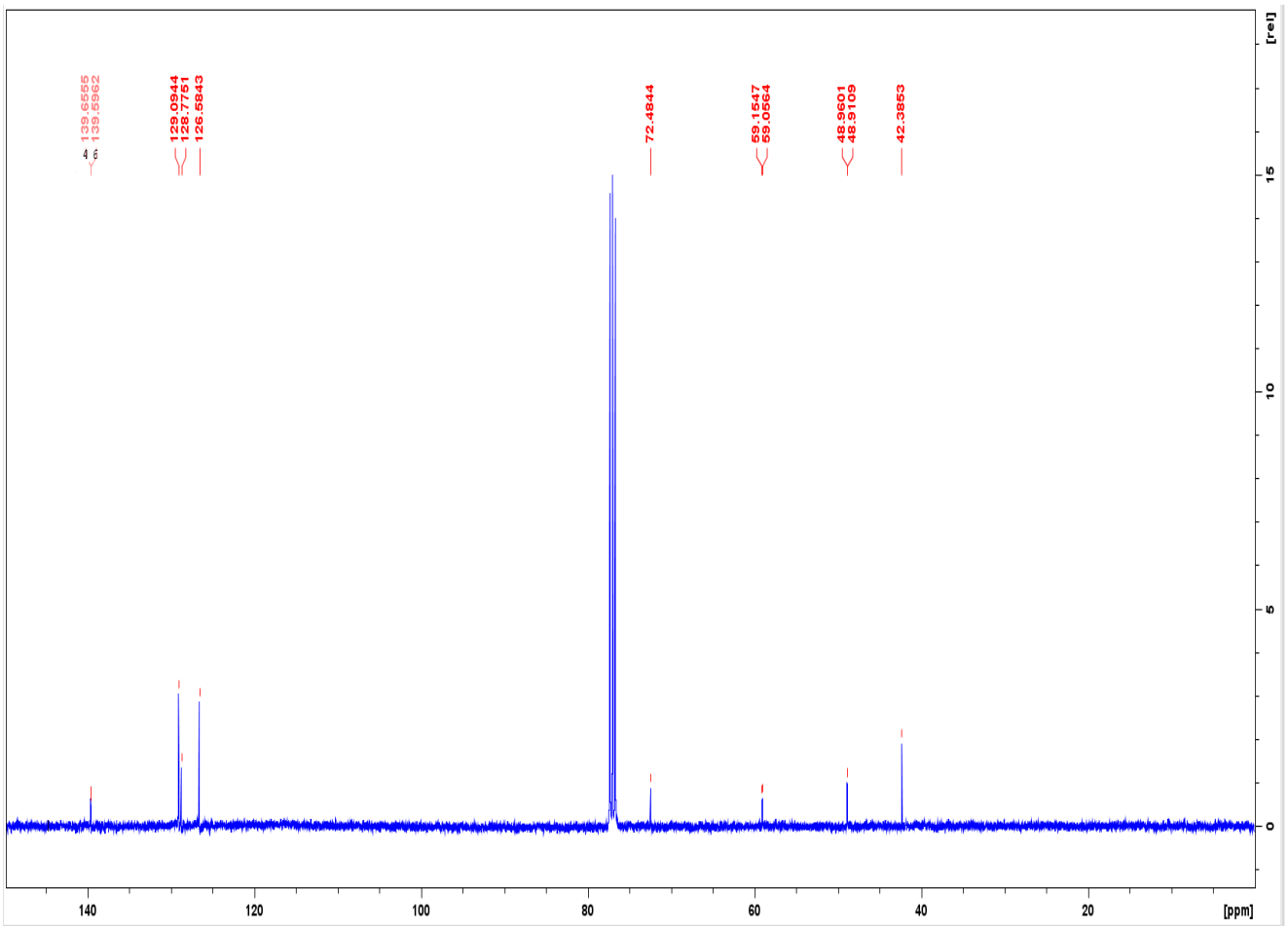

Figure 20. ^{13}C NMR of Oxazaphospholidinone **5a**.

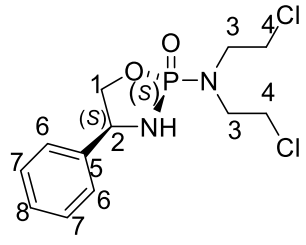

5a

Figure 21. Structure of Oxazaphospholidinone **5a**.

Table 6. ^{13}C NMR and ^{1}H NMR assignments of Oxazaphospholidinone **5a**.

^{13}C	δ (ppm)	^{1}H	δ (ppm)
C1	72.48	H1 & H1'	4.48 (ddd, 1H, *J* = 18.59 Hz, 9.12 Hz, 7.02 Hz) 4.11 (ddd, 1H, *J* = 8.98 Hz, 8.42 Hz, 3.48 Hz)
C2	59.11(d, *J*= 9.88 Hz)	H2	4.80 (apparent quartet)
C3	48.94 (d, *J*= 4.85 Hz)	H3	3.58-3.39 (m, 4H)
C4	42.39	H4	3.70-3.66 (m, 4H)
C5	139.63 (d, *J*= 5.97 Hz)		
C6	126.58	H6	7.48-7.46 (m, 2H)
C7	129.09	H7 & H8	7.37-7.26 (m, 3H)
C8	128.78		
		N-H	3.15 (d, *J* = 17.21 Hz)

The most downfield proton signal was assigned to the proton adjacent to the oxygen atom in the heterocycle owing to its deshielding effect. The H2 proton signal from COSY NMR is expected to be a doublet of doublet of doublet of doublets (dddd) but was observed to be an apparent quartet with very broad peaks. H2 is coupled to H1 / H1', N-H and phosphorus resulting in an apparent quartet.

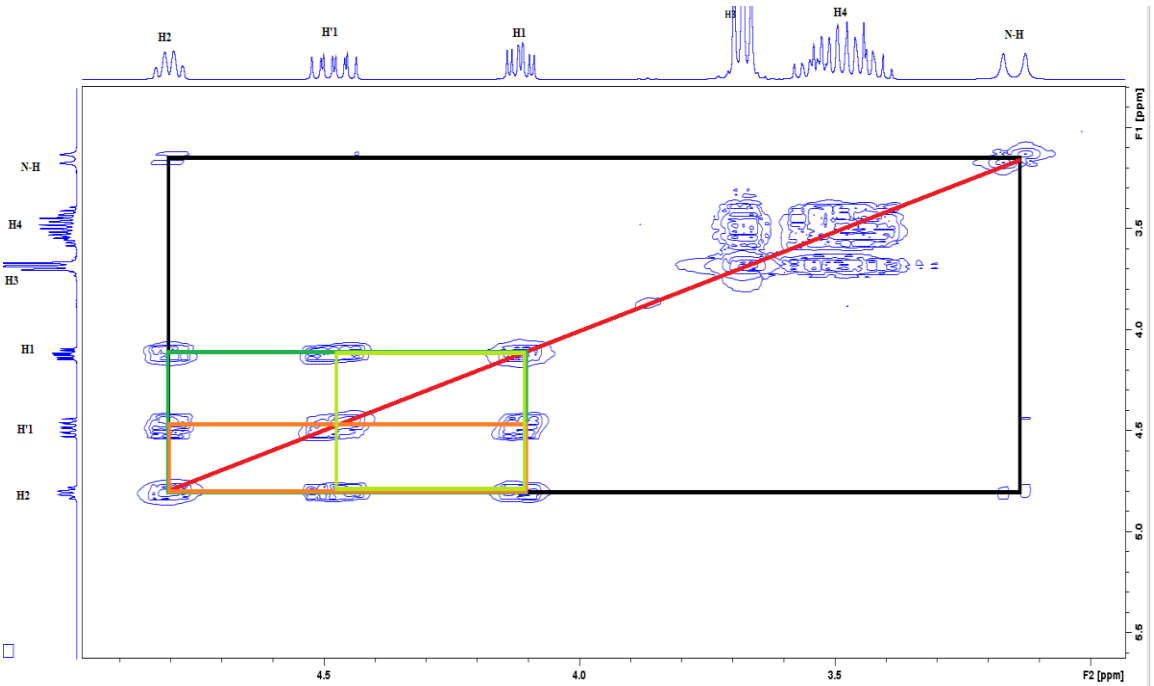

Figure 22. COSY NMR of oxazaphospholidinone **5a**.

The N-H proton signal is observed to be coupled to H2 and phosphorus (P). H2 proton is also coupled to the H1 /H1' proton signals that appears to be coupled to the phosphorus atom in the heterocycle. H3 and H4 are the proton signals on the nitrogen mustard and are not linked to any of the other proton signals observed from the spectral analysis.

A single crystal structure of diastereomer **5a** confirms the chiral center at phosphorus as *S*, as the phenyl group is in the anti - relationship to the nitrogen mustard moiety which leaves the *R* configuration to **5b**.

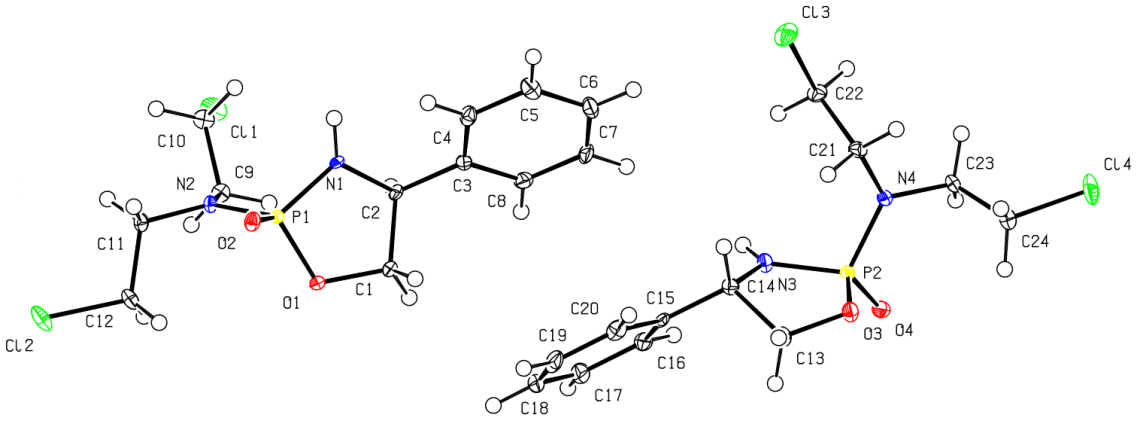

Figure 23. Preliminary X-Ray structure of Oxazaphospholidinone **5a**

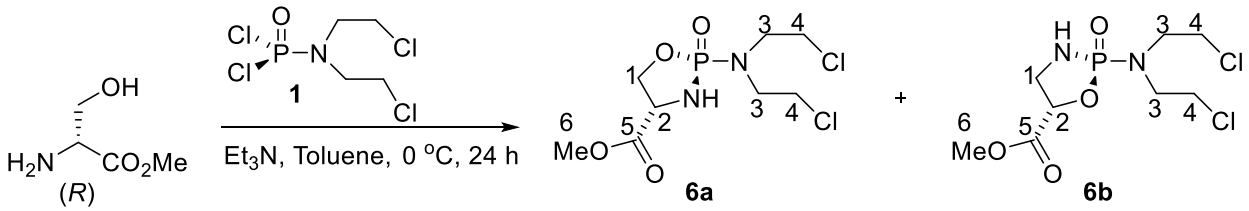

Scheme 9. Synthesis of Oxazaphospholidinones **6a** and **6b**.

The ^{31}P NMR of oxazaphospholidinones **6a** and **6b** are 28.17 and 28.84 ppm respectively. The diastereomers were formed in an overall yield of 77.7%. The individual yield for **6a** and **6b** isolated as white crystalline solids gave 38.9% and 38.9% respectively. Assignment of anti / syn configurations to the compounds were based on the same relationship utilized earlier. The chirality at phosphorus for **6a** is expected to be *S* and that at **6b** expected to be *R*.

The oxazaphospholidinones **6a** and **6b** are expected to have a diastereomeric relationship with a pair of diastereomers when the *l*-Serine methyl ester hydrochloride is used as a starting material. Oxazaphospholidinone **6a** has a melting point of 154-157 ^{o}C with a specific rotation of -3.9^{o} and that of **6b** gave a melting point of 166-169 ^{o}C with a specific rotation of -42.8^{o}.

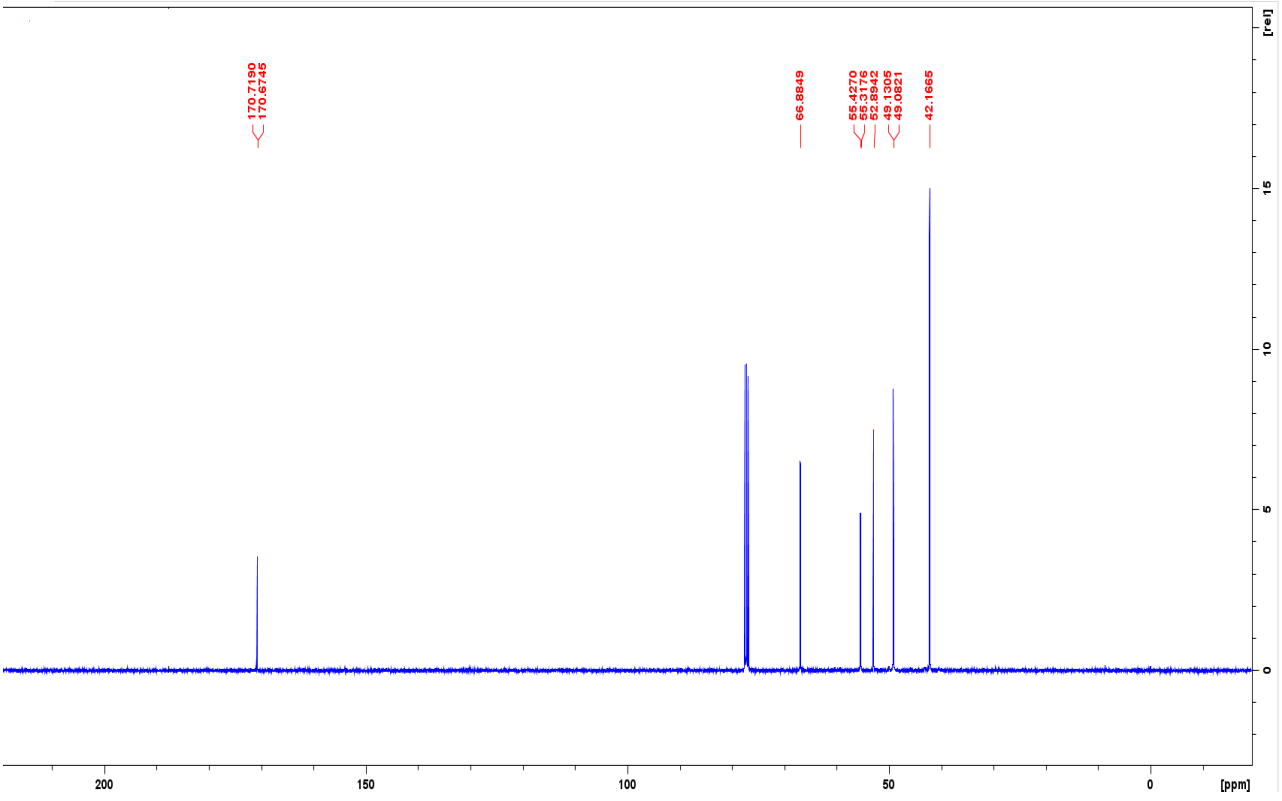

Figure 24. ^{13}C NMR of Oxazaphospholidinone **6a**.

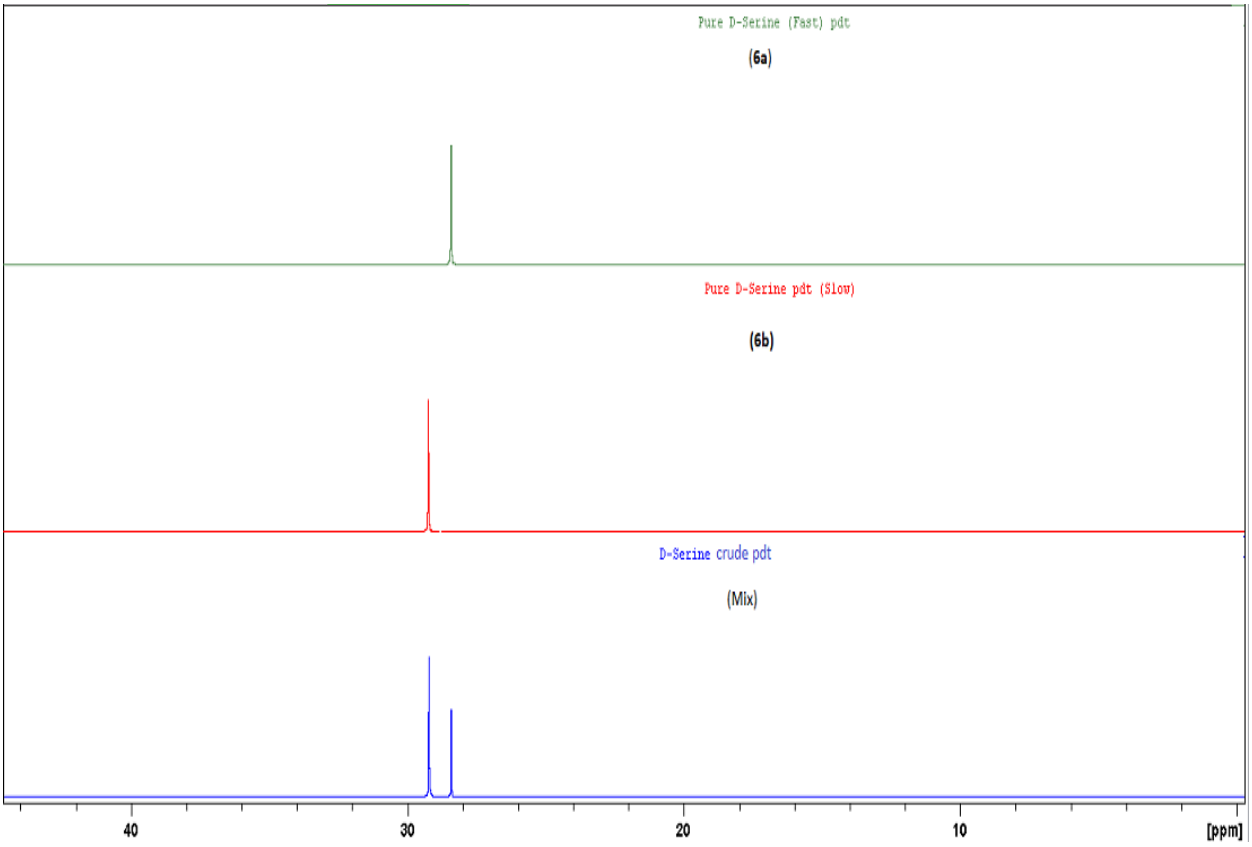

Figure 25. ^{31}P NMR of Oxazaphospholidinone **6a** and **6b**.

Green peak = fast / anti diastereomer (**6a**)

Red peak = slow / syn diastereomer (**6b**)

Blue peaks = combined peaks obtained from crude product (**Mixture**) in (**Figure 25**)

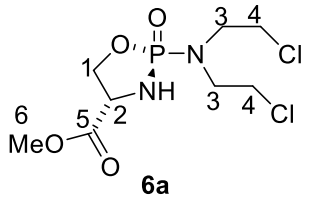

6a

Figure 26. Oxazaphospholidinone **6a**

Table 7. ^{13}C NMR and ^{1}H NMR assignments of Oxazaphospholidinone **6a**

^{13}C	δ (ppm)	^{1}H	δ (ppm)
C1	66.88	H1 / H1'	4.45-4.33 (m, 1H)
C2	55.37 (d, *J* = 11.01 Hz)	H2	4.30-4.24 (m, 2H)
C3	49.11 (d, *J* = 4.87 Hz)	H3	3.61-3.58 (m, 4H)
C4	42.16	H4	3.40-3.35 (m, 4H)
C5	170.69 (d, *J* = 4.48 Hz)	N-H	3.69 (d, *J* = 5.48 Hz)
C6	52.89	H6	3.76 (s, 3H)

Like previously utilized, the most downfield proton signal was assigned to the protons adjacent to the oxygen in the heterocycle due to it having the greatest deshielding effect. An integration of the protons gave a total of 15 inequivalent proton signals with 6 unequal carbon peaks.

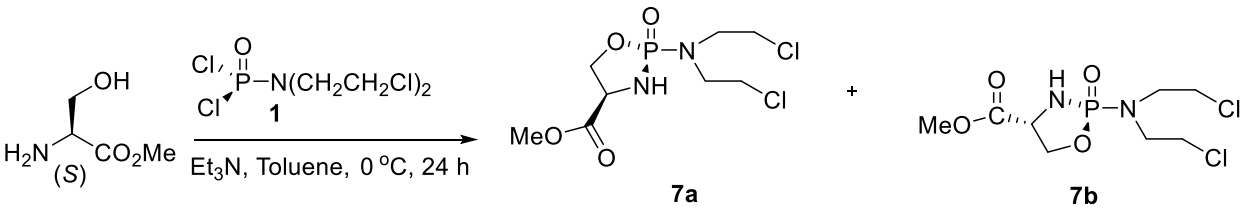

Scheme 10: Synthesis of Oxazaphospholidinones **7a** and **7b**.

The ^{31}P NMR of oxazaphospholidinones **7a** and **7b** are 28.22 and 28.75 ppm respectively with an overall yield of 64.7%. The individual yield for **7a** and **7b** isolated as white crystalline solids gave 37.7% and 27.0% respectively.

Assignment of anti / syn configurations to the compounds were based on the same relationship utilized earlier. The chirality at phosphorus for **7a** is expected to be *S* and that at **7b** expected to be *R*.

Table 8. ^{13}C NMR and ^{1}H NMR assignments of Oxazaphospholidinone **7a**

^{13}C	δ (ppm)	^{1}H	δ (ppm)
C1	66.88	H1 / H1'	4.50-4.41 (m, 1H)
C2	55.42 (d, J = 10.83 Hz)	H2	4.34-4.28 (m, 2H)
C3	49.12 (d, J = 4.93 Hz)	H3	3.67-3.63 (m, 4H)
C4	42.15	H4	3.47-3.38 (m, 4H)
C5	170. 48 (d, J = 4.68 Hz)	N-H	3.86 (d, J = 13.57 Hz)
C6	53.01	H6	3.81 (s, 3H)

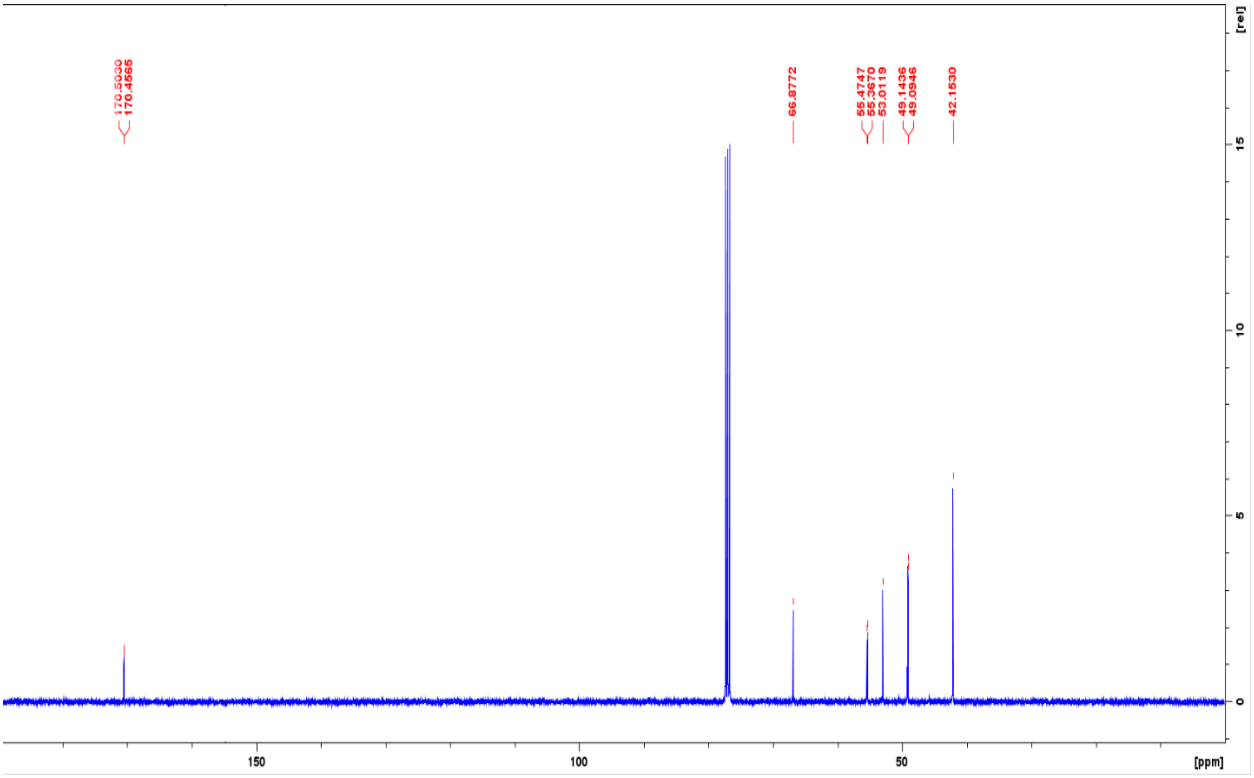

Figure 27. ^{13}C NMR of Oxazaphospholidinone **7a**

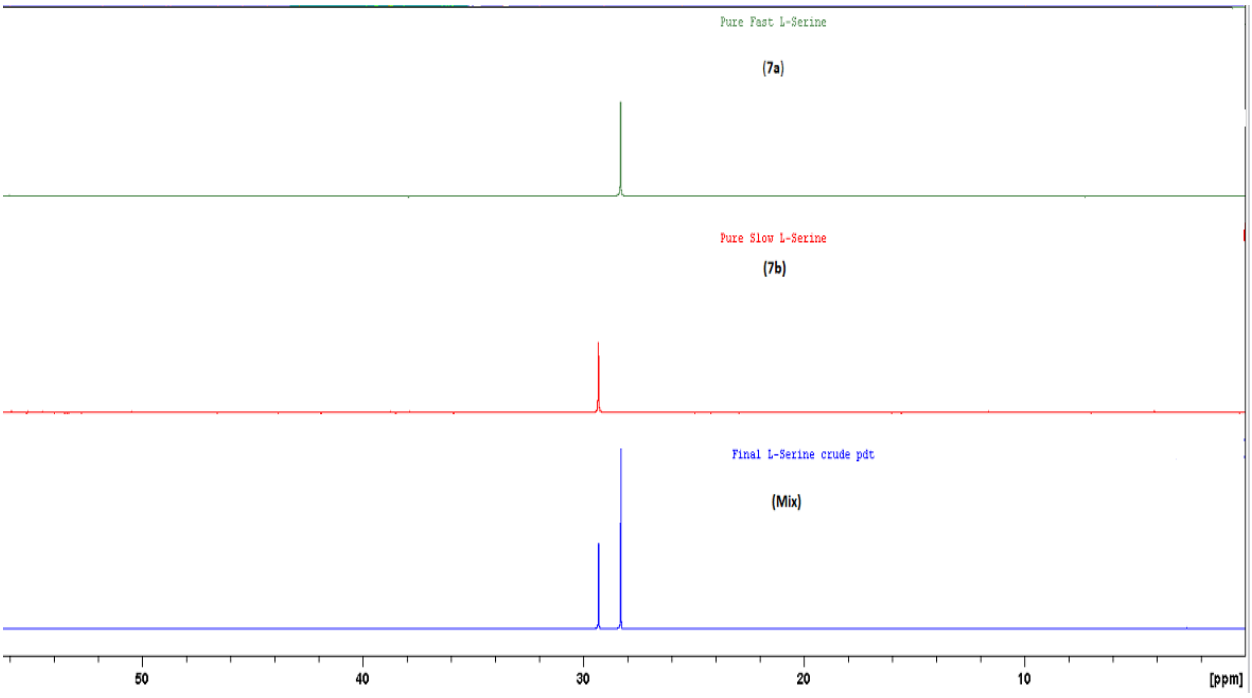

Figure 28. ^{31}P NMR of Oxazaphospholidinone **7a** and **7b**

Green peak = fast / anti diastereomer (**7a**)

Red peak = slow / syn diastereomer (**7b**)

Blue peaks = combined peaks obtained from crude product (**Mixture**) in (**Figure 27**)

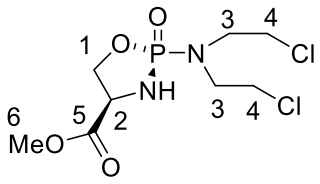

7a

Figure 29. Oxazaphospholidinone **7a**

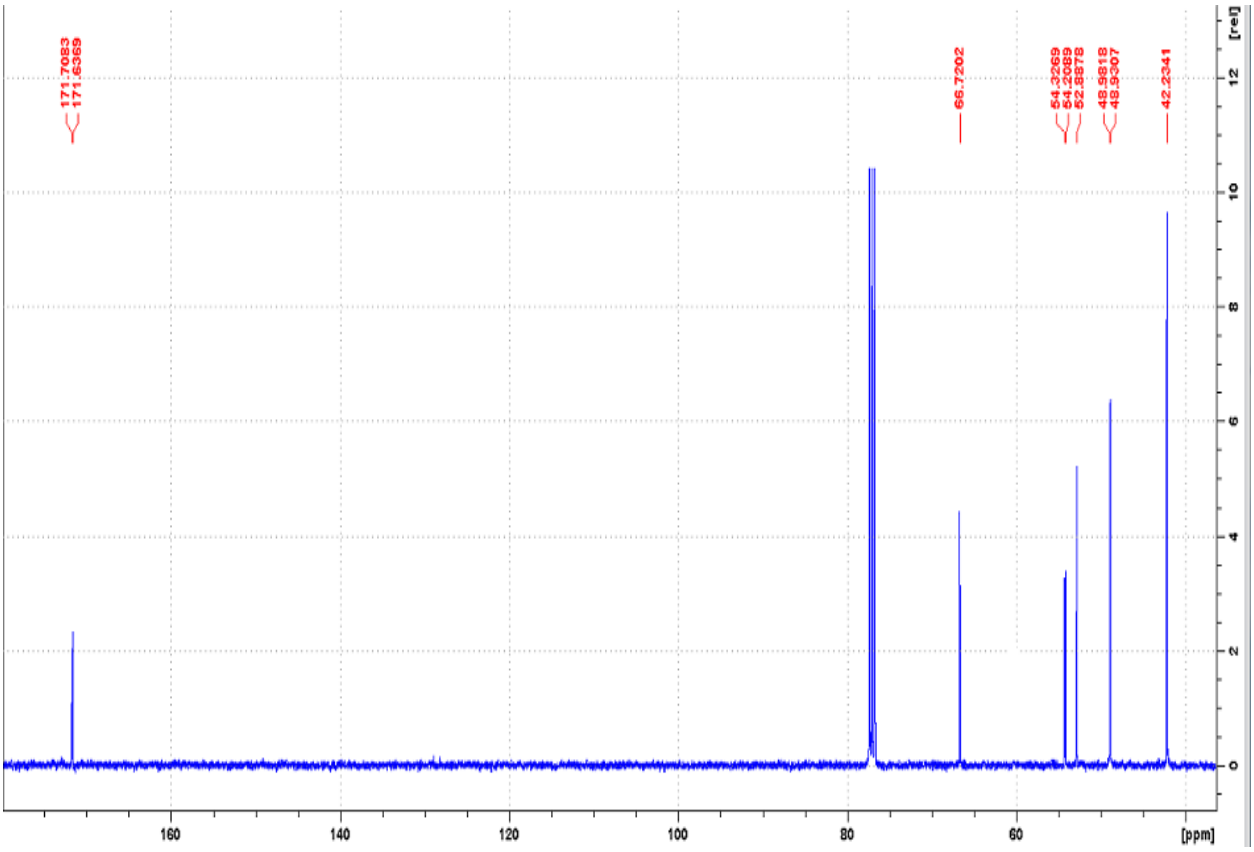

Figure 30. ^{13}C NMR of Oxazaphospholidinone **7b.**

Both diastereomers **7a** and **7b** were isolated as white crystalline solids. Structural assignments were based on the same method employed earlier in the labelling of the proton signals and carbon peaks.

The melting point of **7a** was at 156-158 ^{o}C while that of **7b** was at 169-172 ^{o}C. The ^{1}H NMR integration of the protons gave a total of 15 inequivalent proton signals and 6 uneven carbon peaks.

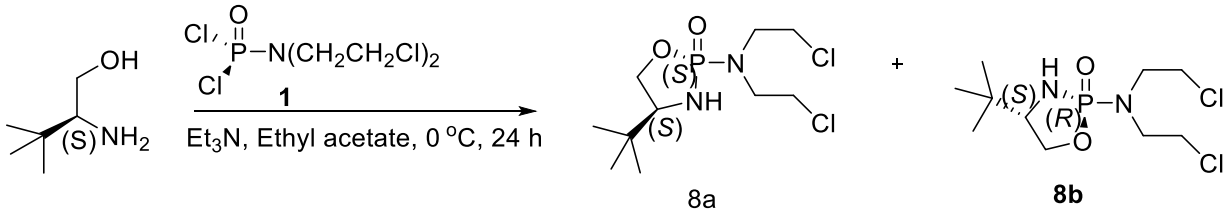

Scheme 11: Synthesis of Oxazaphospholidinones **8a** and **8b**.

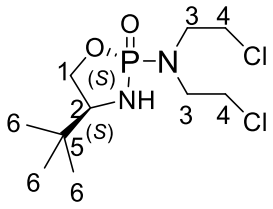

8a

Figure 31. Oxazaphospholidinone 8a

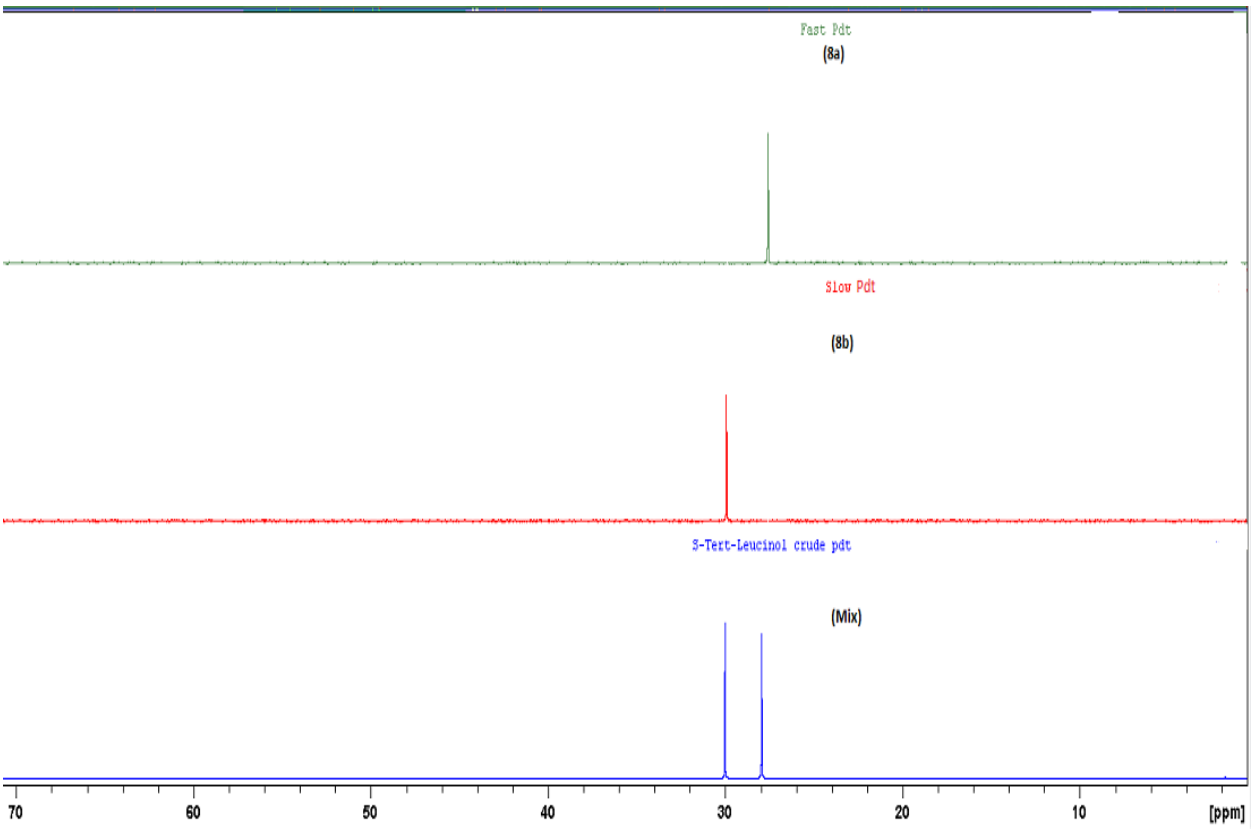

Figure 32. ^{31}P NMR of Oxazaphospholidinone **8a** and **8b**

Green peak = fast / anti diastereomer (**7a**)

Red peak = slow / syn diastereomer (**7b**)

Blue peaks = combined peaks obtained from crude product (**Mixture**) in (**Figure 32**).

Table 9. ^{13}C NMR and ^{1}H NMR assignments of Oxazaphospholidinone **8a**

^{13}C	δ (ppm)	^{1}H	δ (ppm)
C1	67.80	H1 / H1'	4.30-4.12 (m, 2H)
C2	63.82 (d, *J* = 8.84 Hz)	H2	3.45-3.07 (m, 1H)
C3	49.36 (d, *J* = 4.66 Hz)	H3	3.91-3.63 (m, 4H)
C4	42.44	H4	3.45-3.07 (m, 4H)
C5	33.42 (d, *J* = 4.39 Hz)	N-H	2.71 (d, *J* = 5.04 Hz)
C6	25.20	H6	0.93 (s, 9H)

^{31}P NMR chemical shifts for oxazaphospholidinone **8a** and **8b** are 27.58 and 29.93 ppm respectively. The same relationship adopted for assignment of syn / anti configurations were used as before, where the most downfield chemical shift relates to the syn configuration and vice versa.

Therefore, the chirality at phosphorus for **8a** is expected to be *S* and that at phosphorus for **8b** is expected to be *R*. With both diastereomers isolated as white crystals, the melting point of **8a** is 89-91 ^{o}C, with a specific rotation of +8.4 and that of **8b** was at 112-114 ^{o}C also with a specific rotation of +6.2^{o}.

Also, the ^{1}H NMR proton signal that was most downfield was labelled as that which was adjacent the oxygen atom in the heterocycle owing to the higher deshielding effect.

CONCLUSION

Several diastereomeric oxazaphospholidinones were synthesized in a moderate overall yield (55-75%) and purified. The absolute configurations of the diastereomers were assigned based on ^{1}H, ^{13}C, ^{31}P and COSY NMR spectroscopy. The synthesis of these oxazaphospholidinones has progressed, with reagent and reaction conditions being altered occasionally to achieve some desired results. The treatment of silica with varying amount of triethylamine by volume to prevent acidic decompositions of some of the diastereomers is worthy of note during chromatography.

Diastereomers that eluted first from the column upon purification were assigned anti configuration to correspond with its upfield chemical shift value and vice-versa.

Polarimetry was employed to determine the specific rotation of the diastereomers synthesized.

The physical appearance of the oxazaphospholidinones synthesized were observed to be mostly white crystalline solids, with **3a** and **4a** appearing as a yellow syrupy product, the syn- configuration diastereomers having mostly high melting point as against the low melting point of the anti-configuration isolated compounds.

Crystal growth of the oxazaphospholidinones made via the slow evaporation and vacuum diffusion methods both yielded white crystals in plates and narrow rod shapes. Suitable crystals were obtained for analysis leading to the resolution, and refinement of the single crystal structure of the oxazaphospholidinone **5a** (**Appendix B**).

Table 10. Summarized Yields of Oxazaphospholidinones.

Amino Alcohol Used [x]		OAP[y]	Overall Yield (%)	^{31}P NMR (ppm)[z]	
				OAP[a]	OAP[b]
1	Ethanolamine	**2a**	75.2	30.69	
2	(*S*)-(+)-2-Amino-1-butanol	**3a** and **3b**	75.9	27.59	29.43
3	(*R*)-(-)-2-Amino-1-butanol	**4a** and **4b**	55.7	28.08	29.20
4	(*S*)-(+)-2-Phenylglycinol	**5a** and **5b**	77.9	27.02	28.52
5	(*d*)-Serine methyl ester hydrochloride	**6a** and **6b**	77.7	28.17	28.84
6	(*l*)-Serine methyl ester hydrochloride	**7a** and **7b**	64.7	28.22	28.75
7	(*S*)-2-Amino-3,3-Dimethyl-1-butanol	**8a** and **8b**	74.8	27.58	29.93

[x] Each amino alcohol generates the above mentioned oxazaphospholidinone

[y] OAP = Oxazaphospholidinone.

[z] a and b refer to the order of elution of the diastereomers upon purification by flash column chromatography.

Experimentals

General Methods

All reagents were ordered from Sigma-Aldrich and utilized without any additional purification unless otherwise stated. Melting points were determined using a closed end glass capillary tube, and were uncorrected for, from the Stuart SMP10 (2 ^{o}C / min) used. All reactions performed at 0 ^{o}C were achieved using an ice water bath. All reactions were carried out in an oven- dried glassware and performed under an inert argon gas atmosphere unless otherwise indicated.

Flash column chromatography was carried out on Merck grade 9385, 240-400 mesh, 60 Å (particle size) silica. Thin layer chromatography (TLC) was carried out on aluminum backed plates. The TLC plates were viewed by ultraviolet (UV) lamp or PMA stain. NMR (^{1}H, ^{13}C, ^{31}P, COSY and HSQC) spectra were recorded on a Bruker Avance 400 MHz spectrometer using $CDCl_3$ as a solvent, unless otherwise indicated.

^{1}H NMR chemical shifts (ppm) reported are relative to the internal standard TMS peak at 0.00 ppm, while the ^{13}C NMR chemical shifts (ppm) are described relative to the internal $CDCl_3$ peaks at 77.00 ppm. ^{31}P NMR chemical shifts (ppm) are outlined relative to the external standard, phosphoric acid. All coupling constant values are reported in Hertz (Hz).

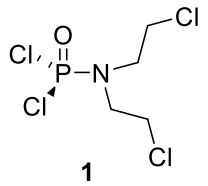

1

Bis(2-chloroethyl) phosphoramidic dichloride (**1**).

Method 1

Bis (2-chloroethyl)amine hydrochloride (3.00 g, 16.77 mmol) was suspended in a solution of freshly distilled phosphoryl chloride (10 mL, 107 mmol) in a 100 mL round bottom flask and refluxed overnight. Once the suspension dissolved, excess phosphoryl chloride was distilled off to leave behind a dark brown oily residue. The oily residue was then dissolved in a solution of petroleum ether: acetone (50:50) while in a 50 ^{o}C hot water bath. The hot solution was then filtered under gravity to remove any solids present and the remaining solvent removed under vacuum.

The crude solid obtained was then recrystallized from a solution of petroleum ether: acetone (50:50), which gave the product, phosphoramide mustard **1** (4.68 g, 86%) as an off-white crystalline solid (m.p = 54-55 ^{o}C).

Method 2

Bis (2-chloroethyl)amine hydrochloride (9.00 g, 50.31 mmol) was suspended in freshly distilled phosphorus oxychloride (30.0 mL, 321 mmol) in a 100 mL round bottom flask and refluxed overnight. Once the suspension dissolved, excess phosphorus oxychloride was distilled off which left a dark brown oily residue. The dark brown oily residue was fractionally distilled under reduced pressure that afforded a pale brown oil in the collection flasks. The fractions were allowed to stand in the fume hood for 1-3 days

and gave a pink/grey solid which was recrystallized using a solution of petroleum ether: acetone (50:50). This gave phosphoramide mustard **1** (6.07 g, 68%) as an off - white crystalline solid (m.p = 52-55 ºC).

^{31}P NMR (162 MHz, $CDCl_3$): δ 17.49.

^{13}C NMR (100 MHz, $CDCl_3$): δ 49.44 (d, J = 4.31 Hz), 40.81 (d, J = 2.96 Hz).

^{1}H NMR (400 MHz, $CDCl_3$): δ 3.99-3.61 (m, 8H).

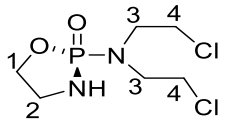

2

(±)-2-[Bis(2-chloroethyl)amino]-1,3,2-oxazaphospholidin-2-one (2)

Phosphoramide mustard 1 (1.29 g, 4.96 mmol), ethanolamine (0.30 mL, 4.97 mmol), toluene (20 mL) and triethylamine 91.6 mL, 11.47 mmol) were added to a 100 mL round bottom flask at 0 ºC under argon atmosphere. The solution was allowed to stir and warm to room temperature for 24 hours. The reaction mixture was vacuum filtered through a 2 cm layer of celite packed in a fritted glass funnel and the reaction flask washed with 60-80 mL of methylene chloride. The solvent was removed though rotary evaporation and gave an off-white crystalline solid. The solid was purified by flash column chromatography (60 g silica, 1:1 of ethanol: hexane, R_f = 0.56) and yielded oxazaphospholidinone **2** (0.94, 75.2%) as an off-white crystalline solid (m. p = 99-101 ºC).

$[\alpha]_D^{20}$= 0.00 º, (c = 0.025 g/mL).

^{31}P NMR (162 MHz, $CDCl_3$): δ 30.69.

^{13}C NMR (100MHz, $CDCl_3$): δ 66.32 (d, J = 2.64 Hz), 49.09 (d, J = 4.78 Hz), 42.31, 42.19.

^{1}H NMR (400MHz, $CDCl_3$): δ 4.37-4.29 (m, 1H), 4.23-4.15 (m, 2H), 3.71-3.48 (m, 4H), 3.43-3.28 (m, 4H), 3.05 (t, 1H, J = 5.48 Hz).

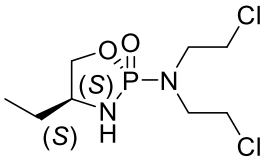

3a

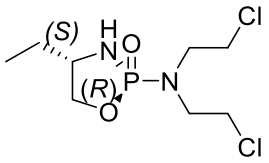

3b

(2*S*,4*S* and 2*R*,4*S*)-2-[Bis(2-chloroethyl) amino]-4-ethyl-1,3,2-Oxazaphospholidin-2-one (3a and 3b)

Phosphoramide **1** (0.52 g, 2.00 mmol), (*S*)-(+)-2-amino-1-butanol (0.18 mL, 2.12 mmol), ethyl acetate (40 mL) and triethylamine (1.0 mL, 5.38 mmol) were added to a 100 mL round bottom flask at 0 ^{o}C under inert argon atmosphere. The reaction mixture was made to stir and warm up to room temperature overnight. The resulting solution was vacuumed filtered via a 2 cm bed of celite packed on a fritted glass funnel and then washed with about 60-80 mL of ethyl acetate.

The solvent was removed through rotary evaporation, which afforded a yellow syrupy product. The syrupy product was purified by flash column chromatography (125 g silica treated with 1% triethylamine), 100% ethyl acetate eluting solvent, R_f = 0.47 and 0.31

and afforded oxazaphospholidinones **3a** and **3b** (0.22 g, 50.3%) with reference to their order of elution.

Fast diastereomer (**3a**): 0.11 g (25.1%), yellow viscous syrup

R_f = 0.47 in 100% ethyl acetate

$[\alpha]_D^{20}$ = +13.1° (c = 0.025 g/mL).

^{31}P NMR (162 MHz, $CDCl_3$): δ 27.59.

^{13}C NMR (100MHz, $CDCl_3$): δ 70.79 (d, *J* = 2.17 Hz), 56.40 (d, *J* = 8.88 Hz), 49.13 (d, *J* = 4.94 Hz), 42.37, 28.49 (d, *J* = 4.38 Hz), 9.92.

^{1}H NMR (400MHz, $CDCl_3$): δ 4.31 (ddd, 1H, *J* = 16.31 Hz, 8.90 Hz, 3.81 Hz), 3.99 (ddd, 1H, *J* = 8.92 Hz, 7.24 Hz, 5.29 Hz), 3.69-3.53 (m, 5H), 3.51-3.33 (m, 4H), 2.97 (d, 1H, *J* = 15.05 Hz), 1.74-1.59 (m, 2H), 0.97 (t, 3H, *J* = 7.48 Hz).

Slow diastereomer (**3b**): 0.11 g (25.21%), white crystalline solid (m.p = 92-94 °C)

R_f = 0.31 in 100% ethyl acetate

$[\alpha]_D^{20}$ = -1.7°, (c = 0.025 g/mL).

^{31}P NMR (162 MHz, $CDCl_3$): δ 29.43.

^{13}C NMR (100 MHz, $CDCl_3$): δ 71.17 (s), 54.49 (d, *J* = 9.35 Hz), 49.22 (d, *J* = 4.82 Hz,), 42.27 (s), 28.56 (d, *J* = 8.88 Hz), 9.93.

^{1}H NMR (400 NMR, $CDCl_3$): δ 4.50 (m, 1H), 3.79-3.63 (m, 2H), 3.62-3.53 (m, 4H), 3.52-3.35 (m, 4H), 2.86 (d, 1H, *J* = 11.35 Hz), 1.58-1.54 (m, 2H), 0.97 (t, *J* = 7.45 Hz).

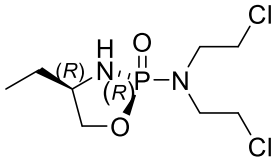

4a

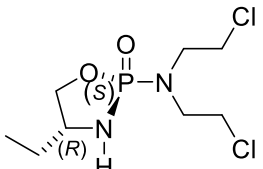

4b

(2*R*, 4*R* and 2*S*, 4*R*)-2-[Bis(2-chloroethyl) amino-4-ethyl-1,3,2-oxazaphospholidin-2-one (4a & 4b)

Phosphoramide Mustard **1** (0.52 g, 2.02 mmol), (*R*)-(-)-2-amino-1-butanol (0.19 mL, 2.01 mmol), ethyl acetate (10 mL) and triethylamine (0.90 mL, 6.45 mmol) were added to a 100 mL round bottom flask at 0 ^{o}C under argon atmosphere and stirred overnight. The reaction mixture was vacuum filtered through a 2 cm bed of celite packed on a fritted glass funnel and was washed with an additional 60-80 mL of ethyl acetate.

The solvent was removed via rotary evaporation, which yielded a yellow viscous oil. The crude oily product was purified by flash column chromatography (125 g silica treated with 1% triethylamine), 100% ethyl acetate, R_f = 0.31 and 0.18 for fast and slow, respectively, and gave oxazaphospholidinones **4a** and **4b** (0.53 g, 55.7%), based on the order of elution.

Fast diastereomer (**4a**): 0.14 g (26.89%), white crystalline solid.

R_f = 0.31 in 100% ethyl acetate.

$[\alpha]_D^{20}$ = -12.9^{o}, (c = 0.025 g/mL).

^{31}P NMR (162 MHz, $CDCl_3$): δ 27.59.

^{13}C NMR (100MHz, $CDCl_3$): δ 70.79 (d, *J* = 2.52 Hz), 56.40 (d, *J* = 9.02 Hz), 49.13 (d, *J* = 5.01 Hz), 42.37, 28.49 (d, *J* = 4.38 Hz), 9.92.

^{1}H NMR (400 MHz, $CDCl_3$): δ 4.26 (ddd, 1H, *J* = 16.25 Hz, 8.89 Hz, 6.47 Hz), 3.92 (ddd, 1H, *J* = 8.83 Hz, 7.14 Hz, 5.68 Hz), 3.62-3.55 (m, 5H), 3.46 - 3.30 (m, 4H), 2.96 (d, 1H, *J* = 15.23 Hz), 1.67-1.56 (m, 2H), 0.97 (t, 3H, *J* = 7.47 Hz).

Slow diastereomer (**4b**): 0.15 g (28.81%), white crystalline solid (m.p = 91-93 ^{o}C)

R_f = 0.18 in 100% ethyl acetate.

$[\alpha]_D^{20}$ = 1.9^{o}, (c = 0.025 g/mL).

^{31}P NMR (162 MHz, $CDCl_3$): δ 29.20.

^{13}C NMR (100MHz, $CDCl_3$): δ 71.17, 54.49 (d, *J* = 9.04 Hz), 49.22 (d, *J* = 5.04 Hz), 42.28, 28.56 (d, *J* = 8.96 Hz), 9.93.

^{1}H NMR (400 MHz, $CDCl_3$): δ 4.49-4.40 (m, 1H), 3.83-3.75 (m, 2H), 3.69 - 3.59 (m, 4H), 3.54 - 3.36 (m, 4H), 2.90 (d, 1H, *J* = 11.22 Hz), 1.69-1.53 (m, 2H), 0.97 (t, 3H, *J* = 7.45 Hz).

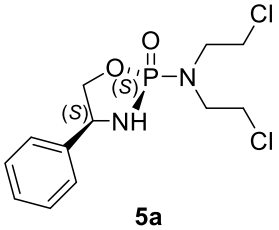

5a

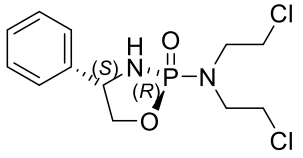

5b

(2*S*, 4*S* and 2*R*, 4*S*)-2-[Bis(2-chloroethyl)amino-4-phenyl-1, 3, 2-oxazaphospholidine -2-oxide (5a & 5b).

The synthesis of **5a** and **5b** was via (*S*)-(+)-2-phenylglycinol and afforded an overall yield of (1.13 g, 77.9%).

Phosphoramide mustard **1** (0.52 g, 2.02 mmol), (*S*)-(+)-2-phenylglycinol (0.68 g, 5.00 mmol), ethyl acetate (20 mL) and triethylamine (1.60 mL, 11.47 mmol) were added to a 100 mL round bottom flask at 0 ^{o}C under argon atmosphere and stirred overnight. The reaction mixture was vacuum filtered through a 2 cm layer of celite packed on a fritted glass funnel and was washed with an additional 60-80 mL of ethyl acetate.

The solvent was removed via rotary evaporation, which yielded a yellow viscous oil. The crude oily product was purified by flash column chromatography (100 g silica treated with 1% triethylamine, 100% ethyl acetate, R_f = 0.4 and 0.3 in ethyl acetate) and gave oxazaphospholidinones **5a** and **5b** (1.13 g, 77.9%), based on the order of elution.

Fast diastereomer (**5a**): 0.22 g (36.5%), white crystalline solid (m.p = 155-159 ^{o}C).

R_f = 0.4 in 100% ethyl acetate.

$[\alpha]_D^{20}$ = +42.7^{o}, (c = 0.020 g/mL).

^{31}P NMR (162 MHz, $CDCl_3$): δ 27.02.

^{13}C NMR (100MHz, $CDCl_3$): δ 139.63 (d, *J* = 5.97 Hz), 129.09, 128.78, 126.58, 72.48, 59.11 (d, *J* = 9.88 Hz), 48.94 (d, *J* = 4.95 Hz), 42.39.

^{1}H NMR (400 MHz, $CDCl_3$): δ 7.48-7.46 (m, 2H), 7.39-7.26 (m, 3H), 4.80 (apparent q, 1H, *J* = 7.17 Hz), 4.48 (ddd, 1H, *J* = 18.59 Hz, 9.12 Hz, 7.02 Hz), 4.11 (ddd, 1H, *J* = 8.98 Hz, 8.42 Hz, 3.48 Hz), 3.70 - 3.66 (m, 4H), 3.58 - 3.39 (m, 4H), 3.15 (d, 1H, *J* = 17.21 Hz).

Slow diastereomer (**5b**): 0.25 g (41.4%), white crystalline solid (m.p = 121-125 ^{o}C).

R_f = 0.3 in 100% ethyl acetate.

$[\alpha]_D^{20}$ = -22.8°, (c = 0.020 g/mL).

^{31}P NMR (162 MHz, $CDCl_3$): δ 28.52.

^{13}C NMR (100 MHz, $CDCl_3$): δ 138.79 (d, *J* = 12.43 Hz), 129.16, 128.78, 126.18, 73.32, 56.84 (d, *J* = 10.73 Hz), 49.06 (d, *J* = 4.95 Hz), 42.24.

^{1}H NMR (400 MHz, $CDCl_3$): δ 7.43–7.33 (m, 5H), 4.99 - 4.95 (m, 1H), 4.57 (ddd, 1H, *J* = 8.83 Hz, 7.14 Hz, 5.68 Hz), 3.92 (ddd, 1H, *J* = 9.28 Hz, 9.28 Hz, 4.46 Hz), 3.73 - 3.59 (m, 4H), 3.58 - 3.47 (m, 4H), 3.25 (d, 1H, *J* = 10.24 Hz).

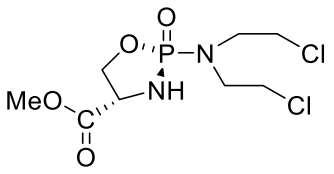

6a

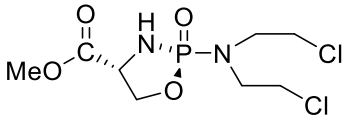

6b

Methyl (2*S*, 4*S* and 2*R*, 4*S*)-2-[bis(2-chloroethyl)amino] -1,3,2-oxazaphospholidine-4-carboxylate-2-oxide (6a and 6b).

To a 100 mL round bottom flask phosphoramide mustard **1** (1.29 g, 4.96 mmol), toluene (20 mL), *d*-Serine methyl ester hydrochloride (0.8 g, 5.0 mmol) and triethylamine (1.60 mL, 11.47 mmol) were added at 0 °C under argon condition and the solution allowed to stir overnight.

The reaction mixture was vacuum filtered via a 2 cm bed of celite packed on a fritted glass funnel, washed with 60-80 mL of methylene chloride. The solvent was removed through rotary evaporation, which yielded a yellow viscous oil.

The oil was purified using flash column chromatography (60 g, silica treated with 1% triethylamine), 95% ethyl acetate: 5% hexane, R_f = 0.2 and 0.1) gave a yield of (2.2 g, 77.7%).

Fast diastereomer (**6a**): 0.34 g (38.9 %), white crystalline solid (m.p = 154-157 ^oC).

R_f = 0.2 in 95% ethyl acetate: 5% Hexane

$[\alpha]_D^{20} = -3.9^o$, (c = 0.025g/mL).

^{31}P NMR (162 MHz, $CDCl_3$): δ 28.17.

^{13}C NMR (100MHz, $CDCl_3$): δ 170.69 (d, *J* = 4.48 Hz), 66.88, 55.37 (d, *J* = 11.01 Hz), 52.89, 49.11 (d, *J* = 4.87 Hz), 42.16.

^1H NMR (400 MHz, $CDCl_3$): δ 4.45 – 4.33 (m, 1H), 4.30 – 4.24 (m, 2H), 3.75 (s, 3H), 3.69 (d, 1H, *J* = 5.84 Hz), 3.61 - 3.58 (m, 4H), 3.40 - 3.35 (m, 4H).

Slow diastereomer (**6b**): 0.34 g (38.9%), white crystalline solid (m.p = 166-169 ^oC).

R_f = 0.1 in 95% ethyl acetate: 5% Hexane

$[\alpha]_D^{20} = -42.8^o$, (c = 0.025 g/mL).

^{31}P NMR (162 MHz, $CDCl_3$): δ 28.84.

^{13}C NMR (100 MHz, $CDCl_3$): δ 171.70 (d, *J* = 7.12 Hz), 66.97, 55.38 (d, *J* = 10.73 Hz), 52.89, 49.11 (d, *J* = 5.06 Hz), 42.18 (d, *J* = 11.83 Hz).

^{1}H NMR (400 MHz, $CDCl_3$): δ 4.62 - 4.57 (m, 1H), 4.34 - 4.31 (m, 2H), 3.96 (d, *J* = 2.80 Hz), 3.92 (s, 3H), 3.92 - 3.58 (m, 4H), 3.48 - 3.41 (m, 4H).

Methyl (2*S*, 4*R* and 2*R*, 4*R*)-2-[bis(2-chloroethyl)amino] -1,3,2-oxazaphospholidine-4-carboxylate-2-oxide (7a and 7b).

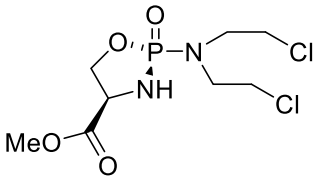

7a

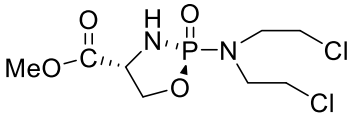

7b

To a 100 mL round bottom flask phosphoramide mustard **1**(1.29 g, 4.96 mmol), toluene (20 mL), *l*-Serine methyl ester hydrochloride (0.80 g, 5.00 mmol) and triethylamine (1.60 mL, 11.47 mmol) were added at 0 ºC under argon condition and the solution allowed to stir overnight.

The reaction mixture was vacuum filtered via a 2 cm bed of celite packed on a fritted glass funnel, washed with 60-80 mL of methylene chloride. The solvent was removed through rotary evaporation, which yielded a yellow viscous oil.

The oil was purified using flash column chromatography (60 g, silica treated with 1% triethylamine), 95% ethyl acetate: 5% hexane, R_f = 0.2, and 0.1) gave a yield of (1.83 g, 64.7%).

Fast diastereomer (**7a**): 0.46 g (37.7 %), white crystalline solid (m.p = 156-158 ^{o}C).

R_f = 0.2 in 95% ethyl acetate: 5% Hexane

$[\alpha]_D^{20}$ = + 4.2^{o} , (c = 0.025g/mL).

^{31}P NMR (162 MHz, $CDCl_3$): δ 28.22.

^{13}C NMR (100MHz, $CDCl_3$): δ 170.48 (d, *J* = 4.68 Hz), 66.88, 55.42 (d, *J* = 10.83 Hz), 53.01, 49.12 (d, *J* = 4.93 Hz), 42.15.

^{1}H NMR (400 MHz, $CDCl_3$): δ 4.50 - 4.40 (m, 1H), 4.32 - 4.28 (m, 2H), 3.81 (s, 3H), 3.67-3.63 (m, 4H), 3.47-3.38 (m, 4H), 3.86 (d, 1H, *J* = 2.56 Hz).

Slow diastereomer (**7b**): 0.33 g (27.0%), white crystalline solid (m.p = 169-172 ^{o}C).

R_f = 0.1 in 95% ethyl acetate: 5% Hexane

$[\alpha]_D^{20}$ = + 42.3^{o}, (c = 0.025 g/mL).

^{31}P NMR (162 MHz, $CDCl_3$): δ 28.74.

^{13}C NMR (100 MHz, $CDCl_3$): δ 171.67 (d, *J* = 7.18 Hz), 66.72, 54.27 (d, *J* = 11.87 Hz), 52.89, 48.96 (d, *J* = 5.14 Hz), 42.23.

^{1}H NMR (400 MHz, $CDCl_3$): δ 4.61 - 4.55 (m, 1H), 4.38 - 4.30 (m, 2H), 3.80 (s, 3H), 3.76 (d, *J* = 5.44 Hz), 3.67 - 3.58 (m, 4H), 3.52 - 3.39 (m, 4H).

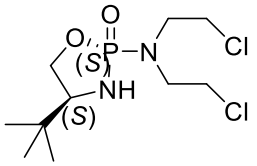

8a

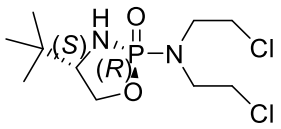

8b

(2*S*, 4*S* and 2*R*, 4*S*)-2-[Bis(2-chloroethyl)amino]-4-(*t*ert-butyl)-1,3,2-oxazaphospholidin-2-ones (8a and 8b)

Phosphoramide mustard **1** (0.65 g, 2.50 mmol), (*S*)-*t*ert-leucinol (0.28 g, 2.50 mmol), 20 mL ethyl acetate and triethylamine (0.8 mL, 5.5 mmol) were added in a 100 mL round bottom flask. The reaction was allowed to stir overnight from 0 ^{o}C to room temperature.

The reaction mixture was vacuum filtered through a 2 cm bed celite packed on a fritted glass funnel and was washed using 60-80 mL methylene chloride. The solvent was removed using a rotary evaporator and yielded a viscous yellow oil.

The oil was then purified by flash column chromatography (60 g silica, 100% ethyl acetate, R_f = 0.4 and 0.3) **8a** and **8b** diastereomers respectively, yield (0.89 g, 74.8%).

Fast diastereomer (**8a**): 0.12 g (42.7%), white crystalline solid (m.p = 89-91 ^{o}C).

R_f = 0.4 in 100% ethyl acetate.

$[\alpha]_D^{20} = +8.4^{o}$, (c = 0.025 g/mL).

^{31}P NMR (162 MHz, $CDCl_3$): δ 27.58.

^{13}C NMR (100MHz, $CDCl_3$): δ 67.80, 63.82 (d, *J* = 8.84 Hz), 49.36 (d, *J* = 4.66 Hz), 42.44, 33.42 (d, *J* = 4.39 Hz), 25.20.

^{1}H NMR (400 MHz, $CDCl_3$): δ 4.30 - 4.12 (m, 2H), 3.91 - 3.63 (m, 4H), 3.45-3.07 (m, 5H), 2.71 (d, 1H, *J* = 5.04 Hz), 0.93 (s, 9H).

Slow diastereomer (**8b**): 0.09g (32.1%), white crystalline solid (m.p = 112-114 ^{o}C).

R_f = 0.3 in 100% ethyl acetate.

$[\alpha]_D^{20}$ = + 6.2^{o}, (c = 0.025 g/mL).

^{31}P NMR (162 MHz, $CDCl_3$): δ 29.93.

^{13}C NMR (100 MHz, $CDCl_3$): δ 67.82, 61.61 (d, *J* = 8.45 Hz), 49.33 (d, *J* = 4.68 Hz), 42.20, 33.17 (d, *J* = 10.54 Hz), 25.30.

^{1}H NMR (400 MHz, $CDCl_3$): δ 4.29 - 4.12 (m, 2H), 3.91 - 3.62 (m, 4H), 3.45 - 3.04 (m, 5H), 2.01 (d, 1H, *J* = 9.48 Hz), 0.91 (s, 9H).

References

1. Einhorn, J. *Int. J. Radiation Oncology Biol. Phys*. **1985**, *11*, 1375 - 1378.
2. Jackson, J. A.; Frick, J. A.; Thompson, C. M.; *Bioorg.Med.Chem. Lett*. **1992**, *2*, 1547 - 1550.
3. Adam, T.; Groundwater, P.W.; Gill, J. H. Anticancer Therapeutic: *From Drug Discovery to Clinical Application*,1st ed. John Wiley & Sons Ltd (2018). pp 83-97.
4. FDA-Approved Drugs. htpp://dtp.cancer.gov/timeline/flash/FDA.htm (accessed November 16, 2018).
5. Thall, E. *J. Chem. Educ.*, **1996**, *73*, 481-483.
6. Takamizawa, A.; Matsumoto, S.; Iwata, T.; Tochino, Y.; Katagiri, K.; Yamaguchi, K.; Shirator, O. *J. Med. Chem.* **1975**, *18*, 376 - 383.
7. Rohde Jr, Laurence. N. The Synthesis and Characterization of Diastereomeric 2-[bis(2-chloroethyl)amino] 1, 3, 2-oxazaphospholidin-2-ones. MS Thesis, Youngstown State University, 2018.
8. Davis, N.M.; Tend. X. W.; *Advances in Pharm*. **2003**, *1*, 242-252.
9. Nguyen, L. A, He, H.; Pharm-Huy, C. *Int. J. Biomed. Sci*. **2006,** *2*, 85-100.
10. Madison, K. A. Synthesis of Chiral Phosphorus Mustards from Chiral Amino Alcohols. MS Thesis, Youngstown State University, 1996.
11. Castro, F. A.; Scatena, G. D.; Rocha, O.P.; Marques, M. P.; Cass, Q. B; Simoes, B. P.; Lanchote, V. L. *J. Chromatogr. B*. **2016**, *1011*, 53-61.
12. Foster, E. *J. Pharm. Sci.***1978**. *67*, 709-710.
13. Thompson, C. M.; Frick, J.A.; Green, D.L.C *J. Org. Chem.* **1990**, *55*, 111-122.
14. Friedman, O. M.; Seligman, A. M. *J. Am. Chem. Soc.* **1954**, *76*, 655-658.

Appendix A

NMR Spectra

Figure 33. ^{13}C NMR Spectrum of Phosphoramide Mustard **1.**

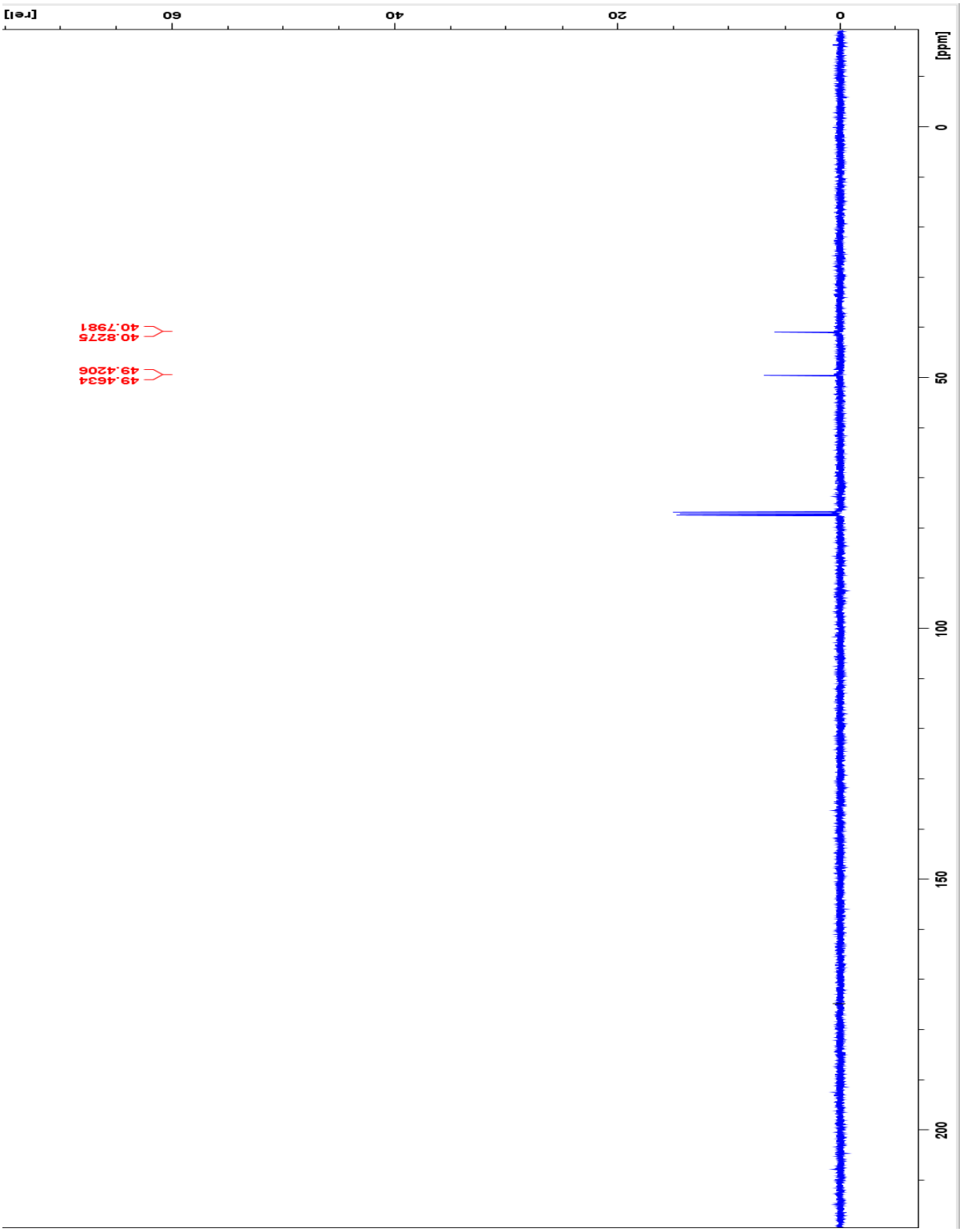

Figure 34. ^{1}H NMR Spectrum of Phosphoramide Mustard **1.**

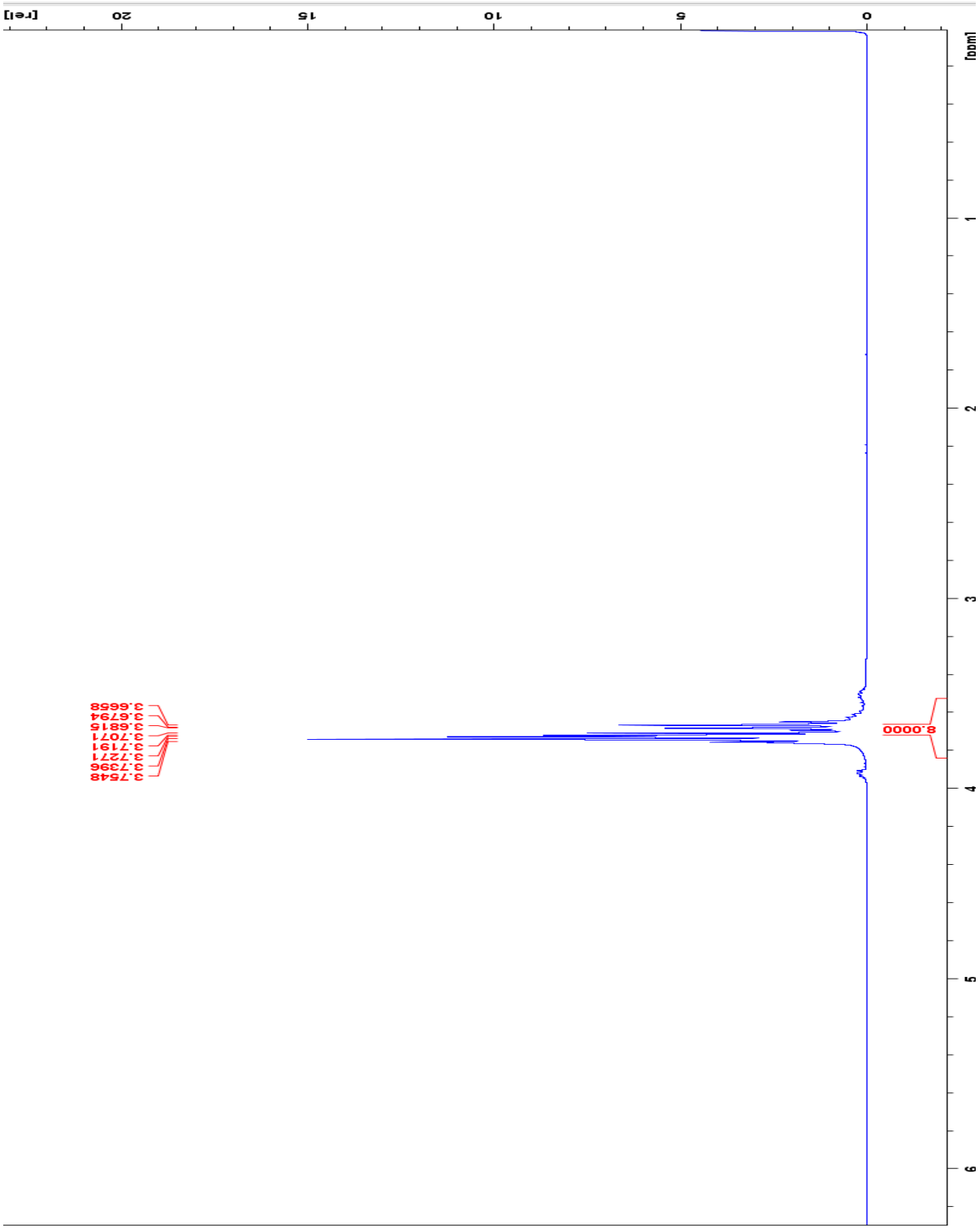

Figure 35. ^{1}H NMR Oxazaphospholidinone **2** in $CDCl_3$.

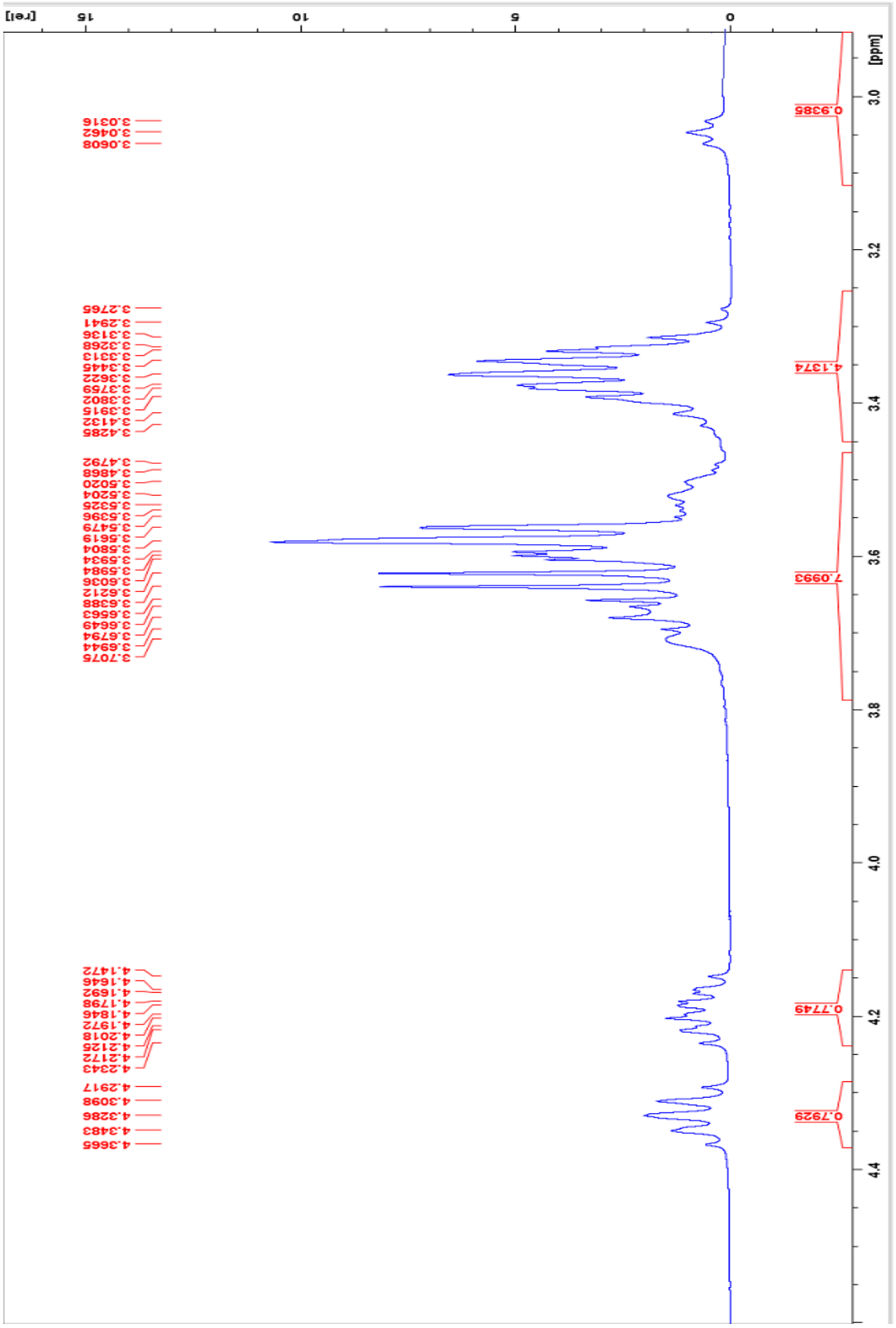

Figure 36. ^{31} P NMR Oxazaphospholidinone **2** in $CDCl_3$.

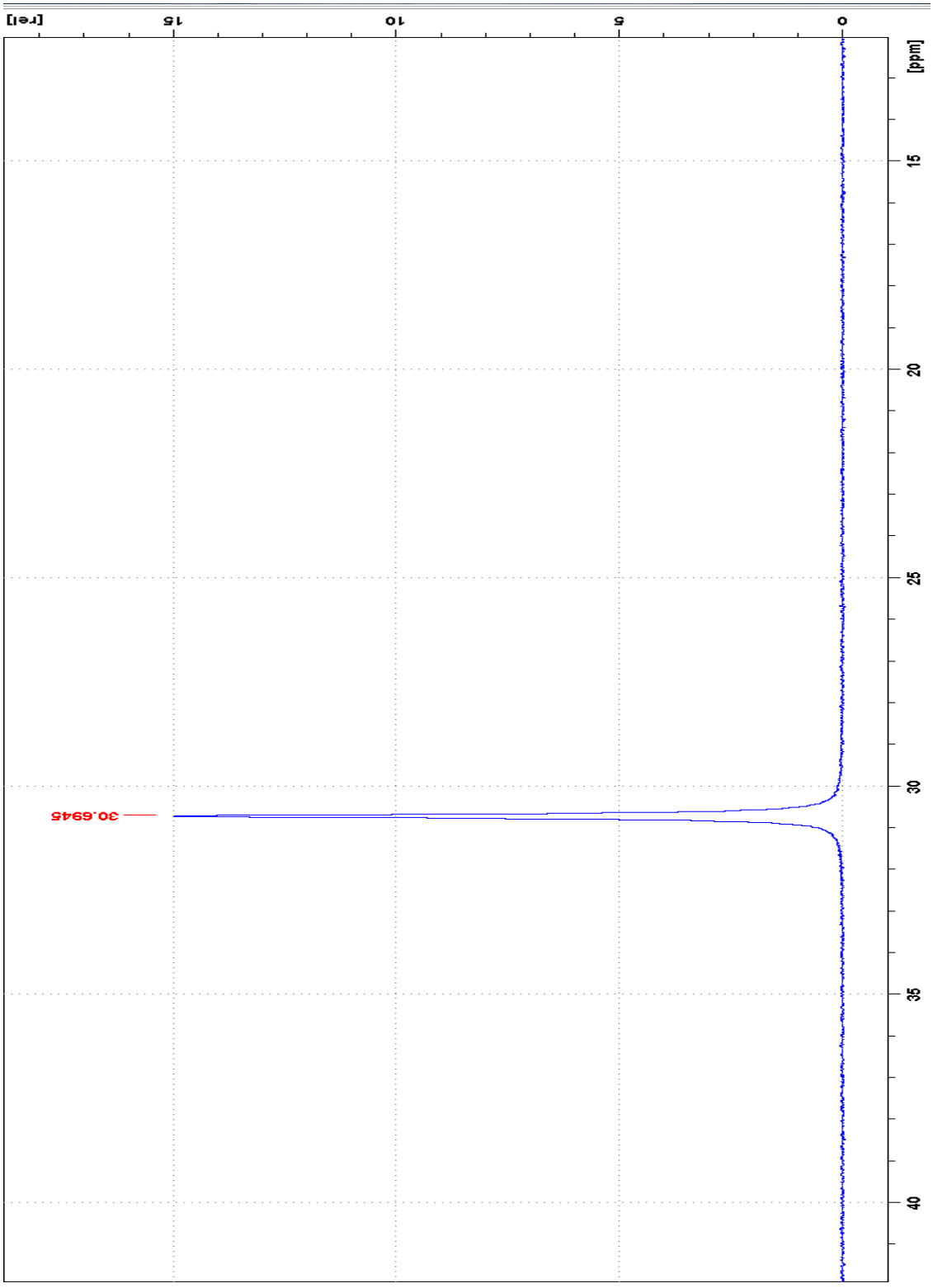

Figure 37. COSY NMR of Oxazaphospholidinone **2** in $CDCl_3$.

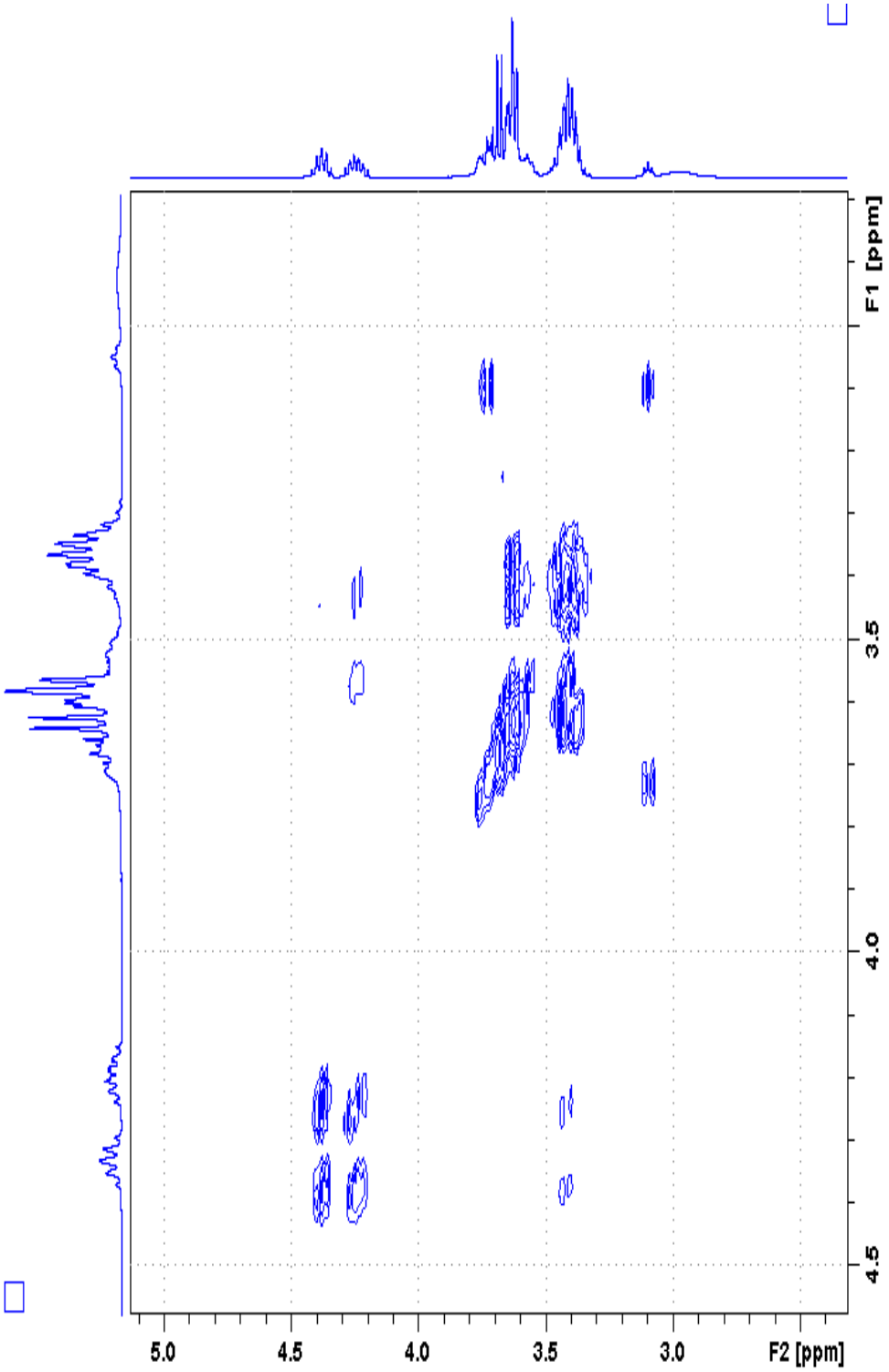

Figure 38. ^{31}P NMR of Oxazaphospholidinone **3a**.

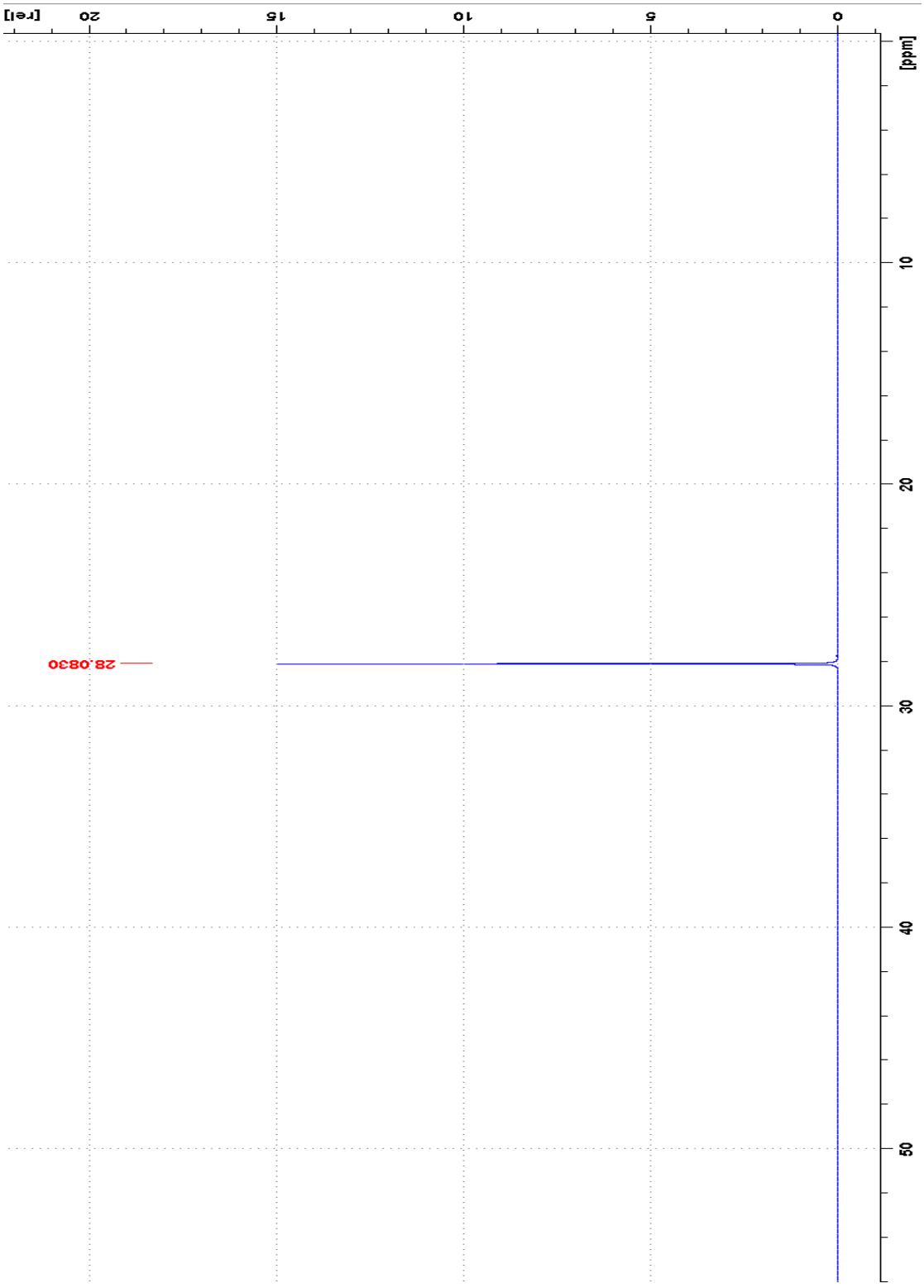

Figure 39. ^{1}H NMR of Oxazaphospholidinone **3b**.

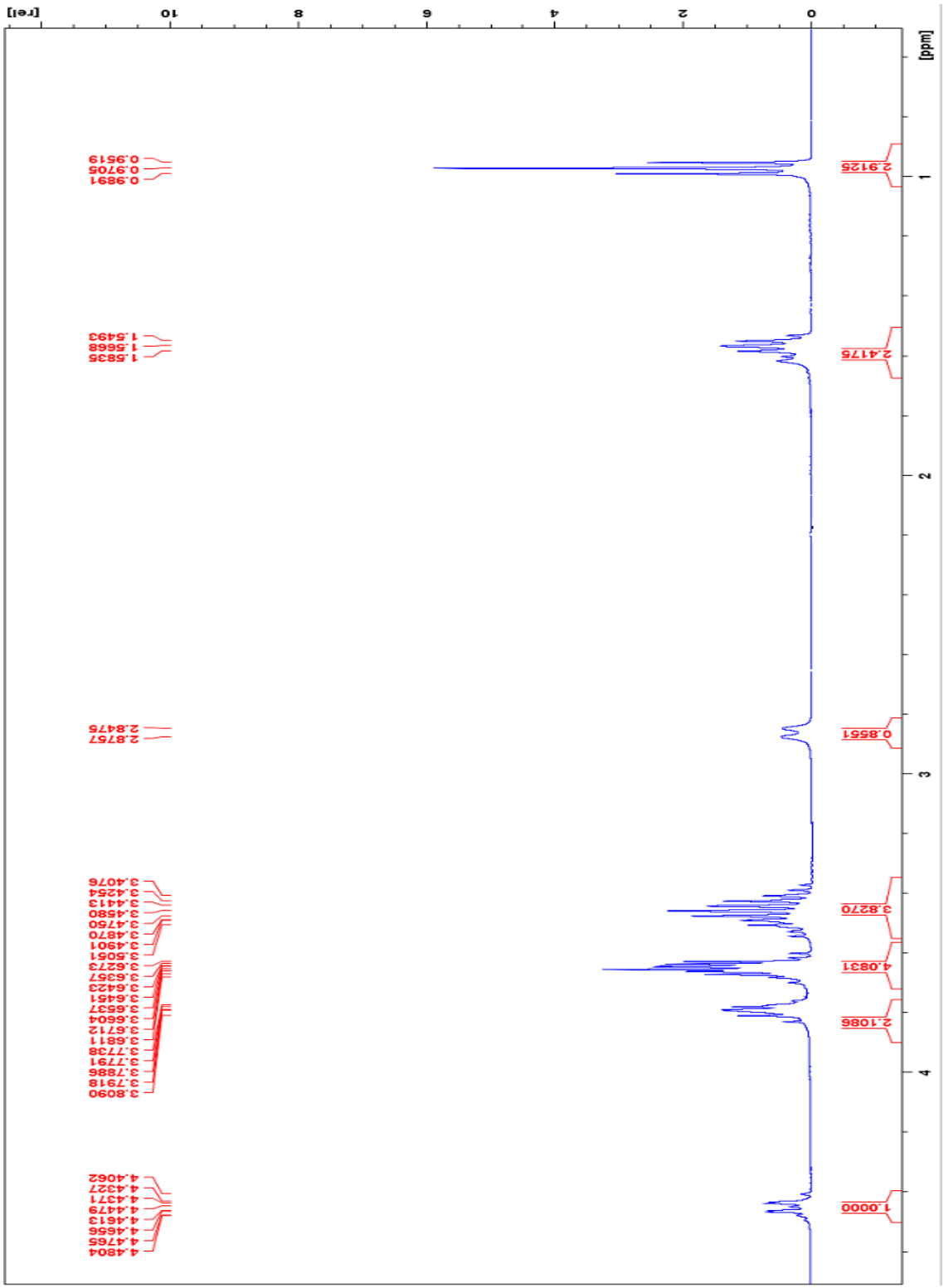

Figure 40. ^{31}P NMR of Oxazaphospholidinone **3b**.

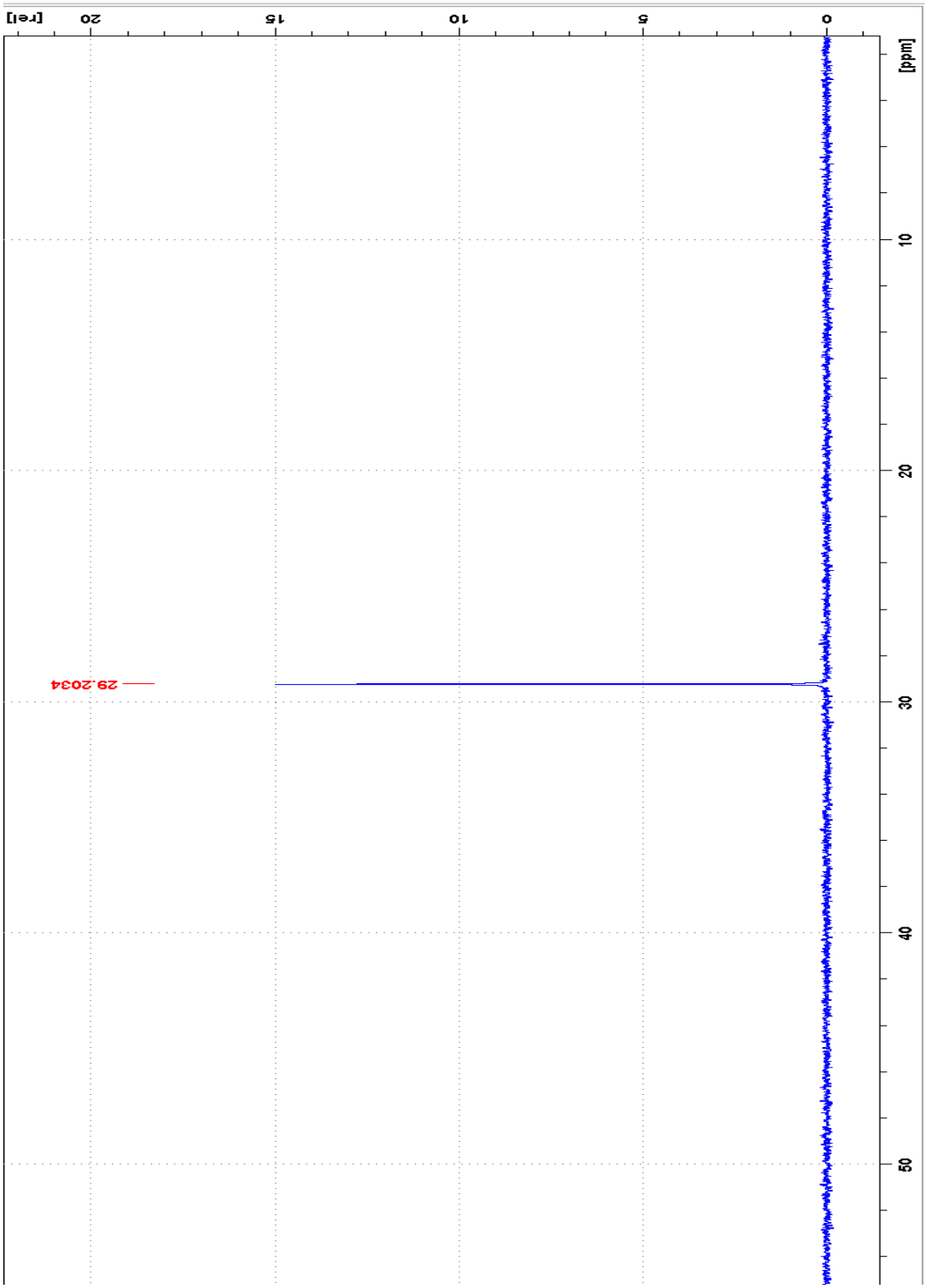

Figure 41. ^{13}C NMR of Oxazaphospholidinone **4a**.

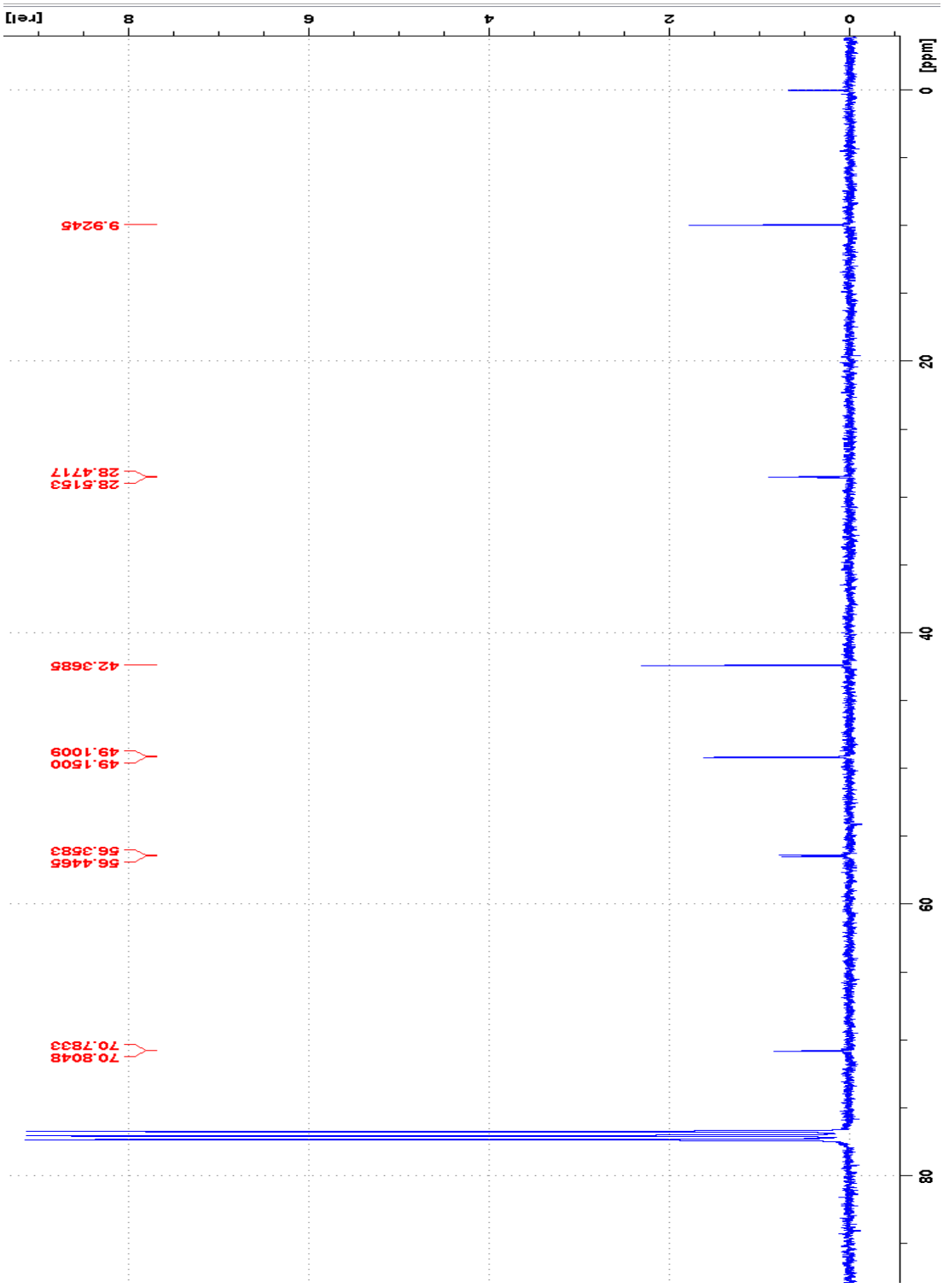

Figure 42. ^{1}H NMR of Oxazaphospholidinone **4a**.

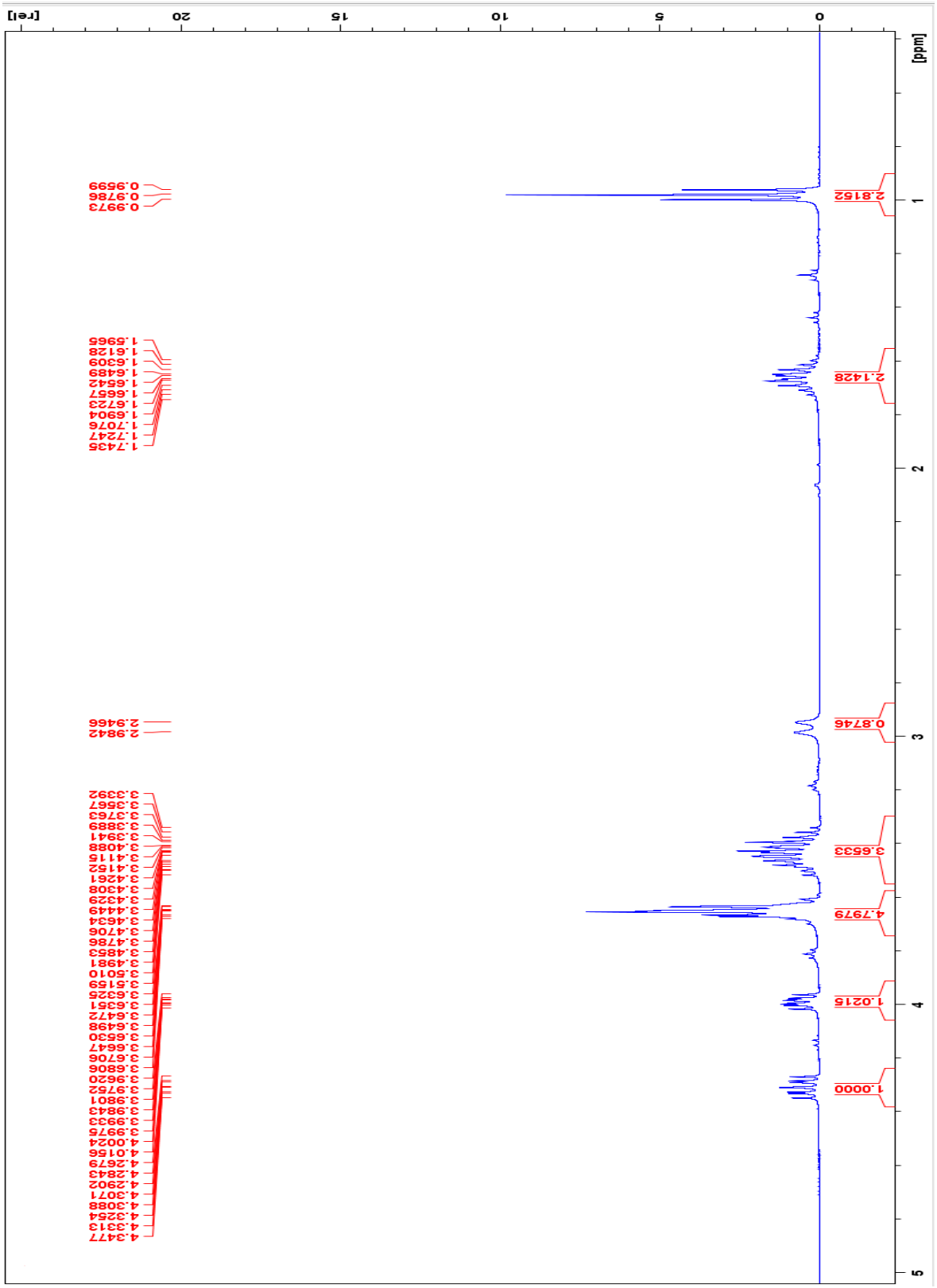

Figure 43. ^{31}P NMR of Oxazaphospholidinone **4a**.

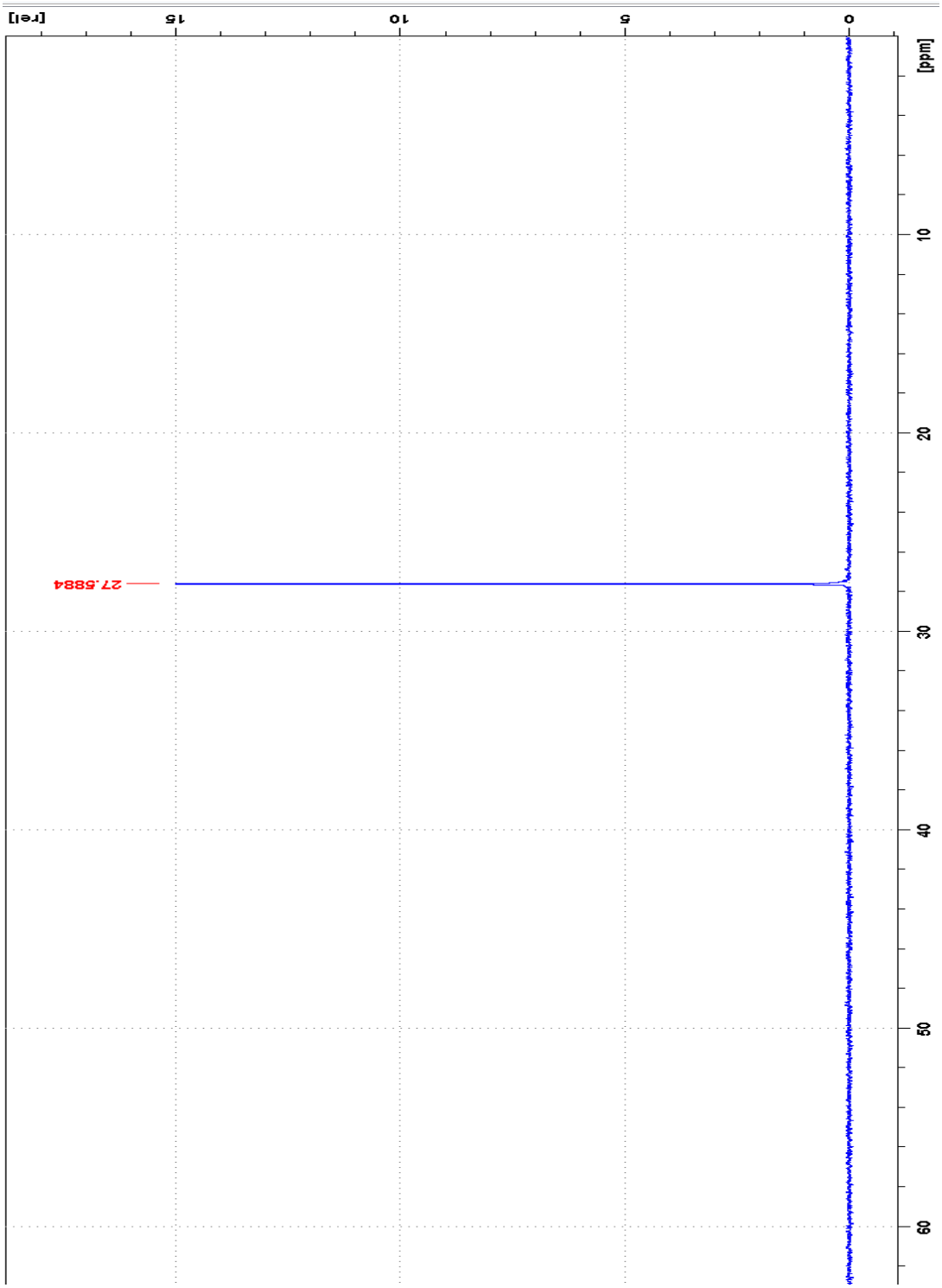

Figure 44. COSY NMR of Oxazaphospholidinone **4a**.

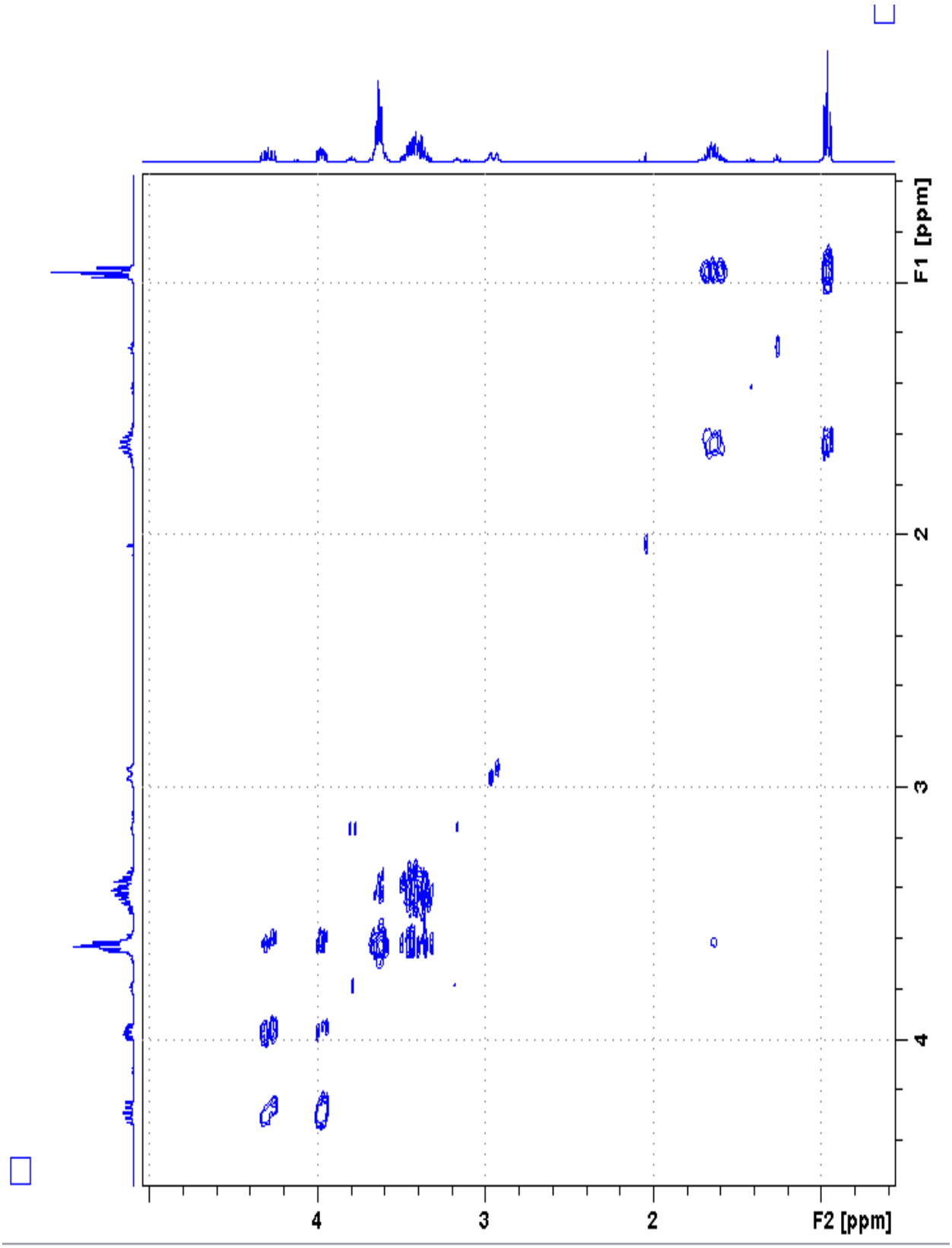

Figure 45. ^{13}C NMR of Oxazaphospholidinone **4b**.

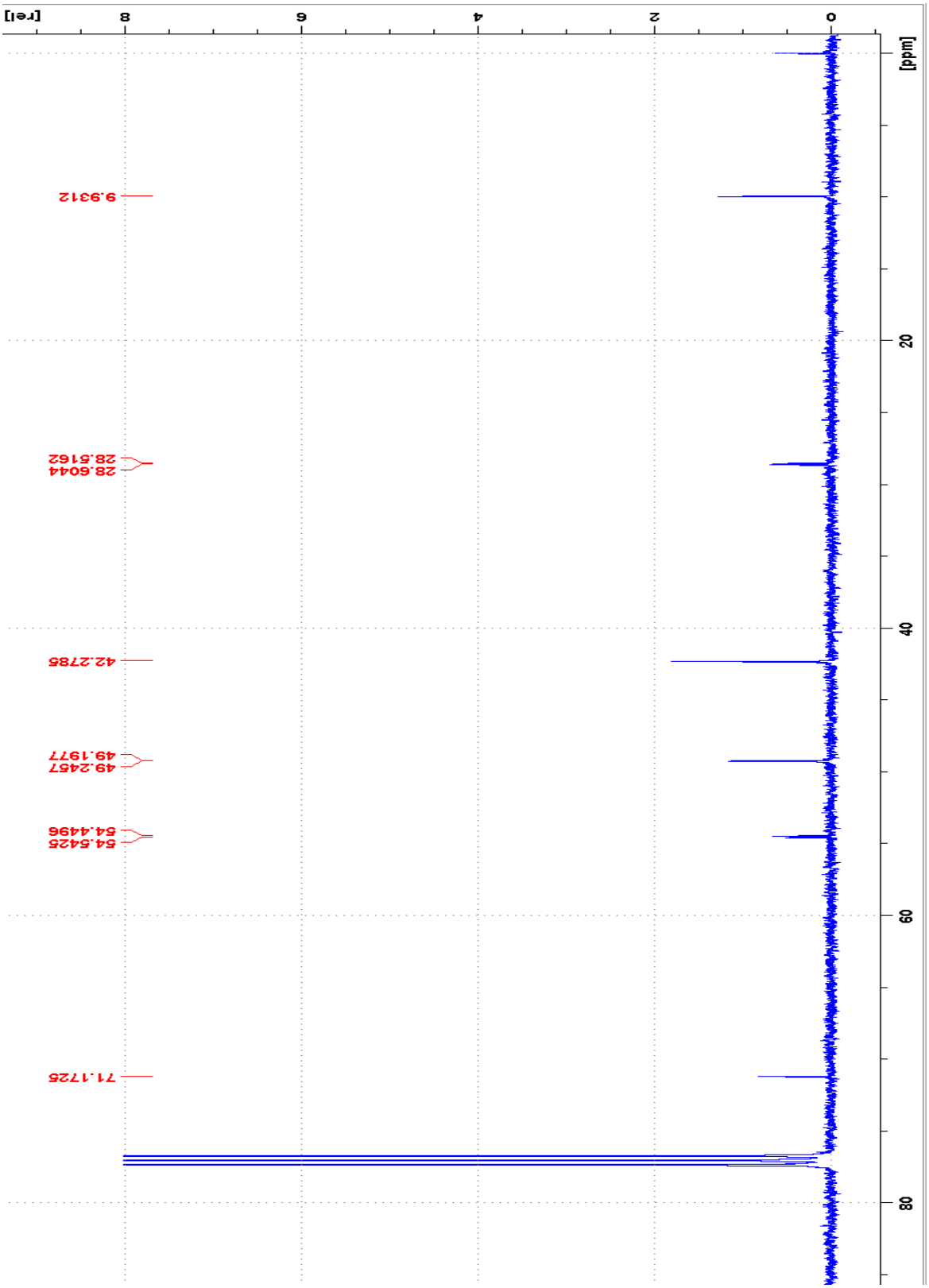

Figure 46. ^{1}H NMR of Oxazaphospholidinone **4b**.

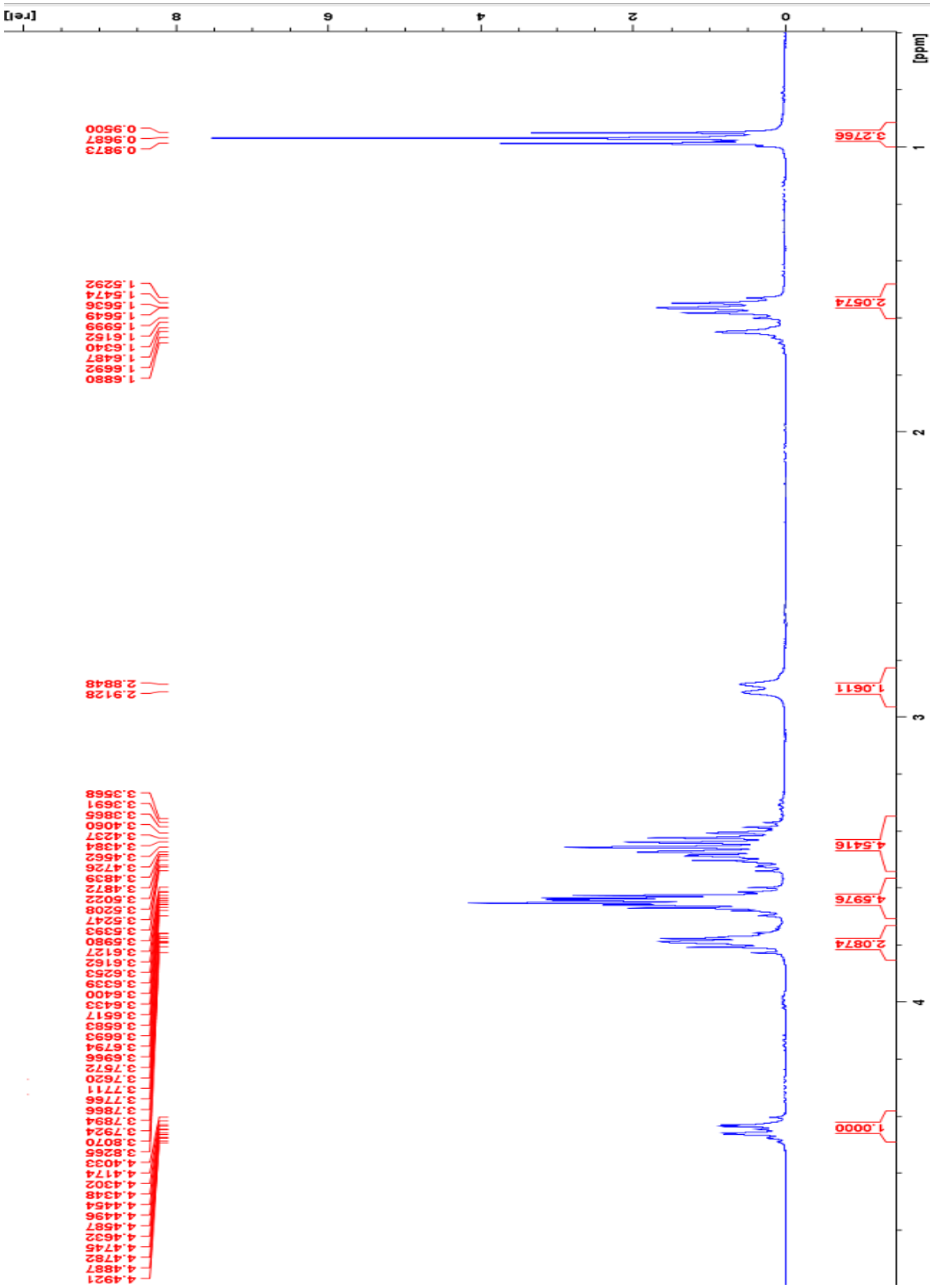

Figure 47. ^{31}P NMR of Oxazaphospholidinone **4b**.

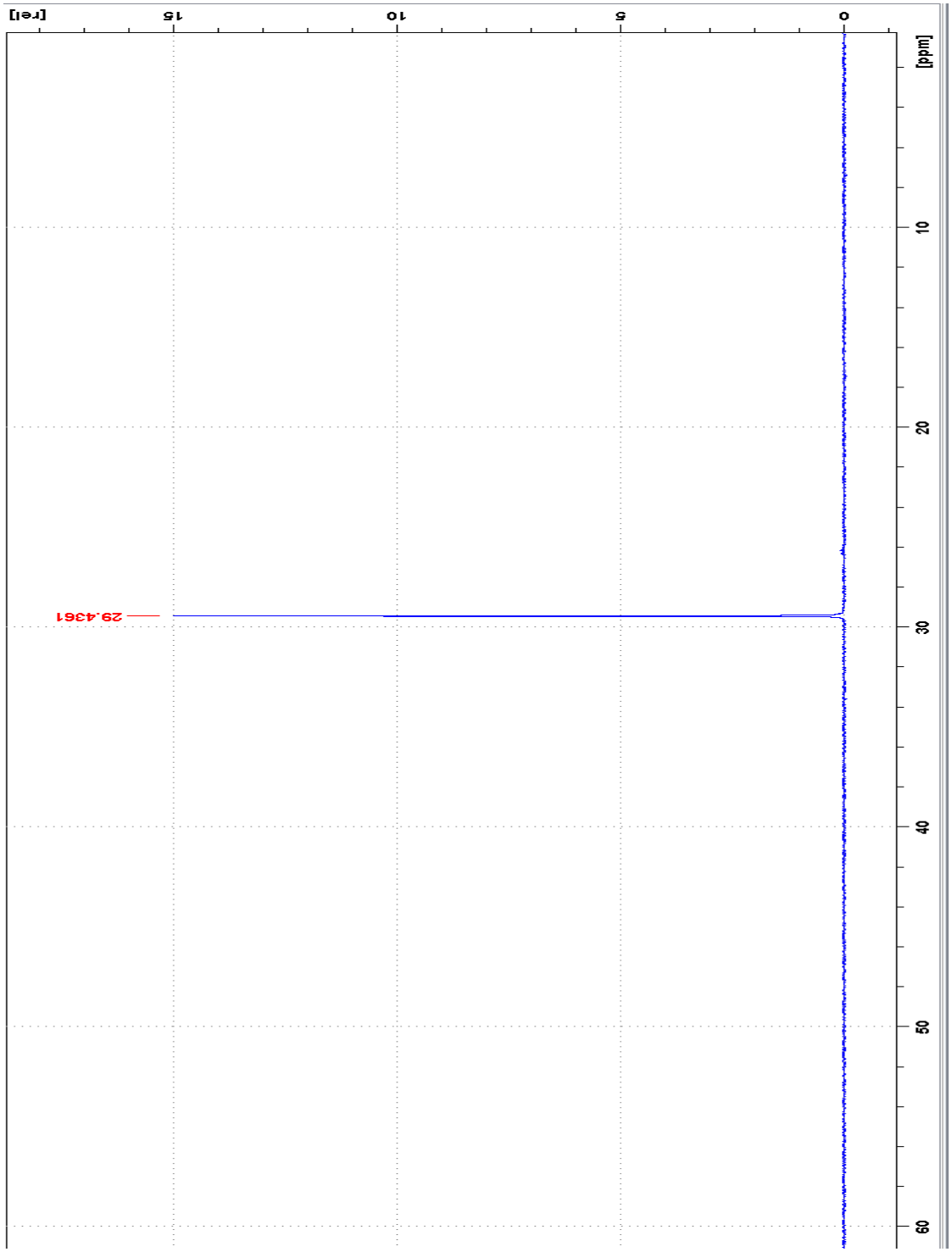

Figure 48. COSY NMR of Oxazaphospholidinone **4b**.

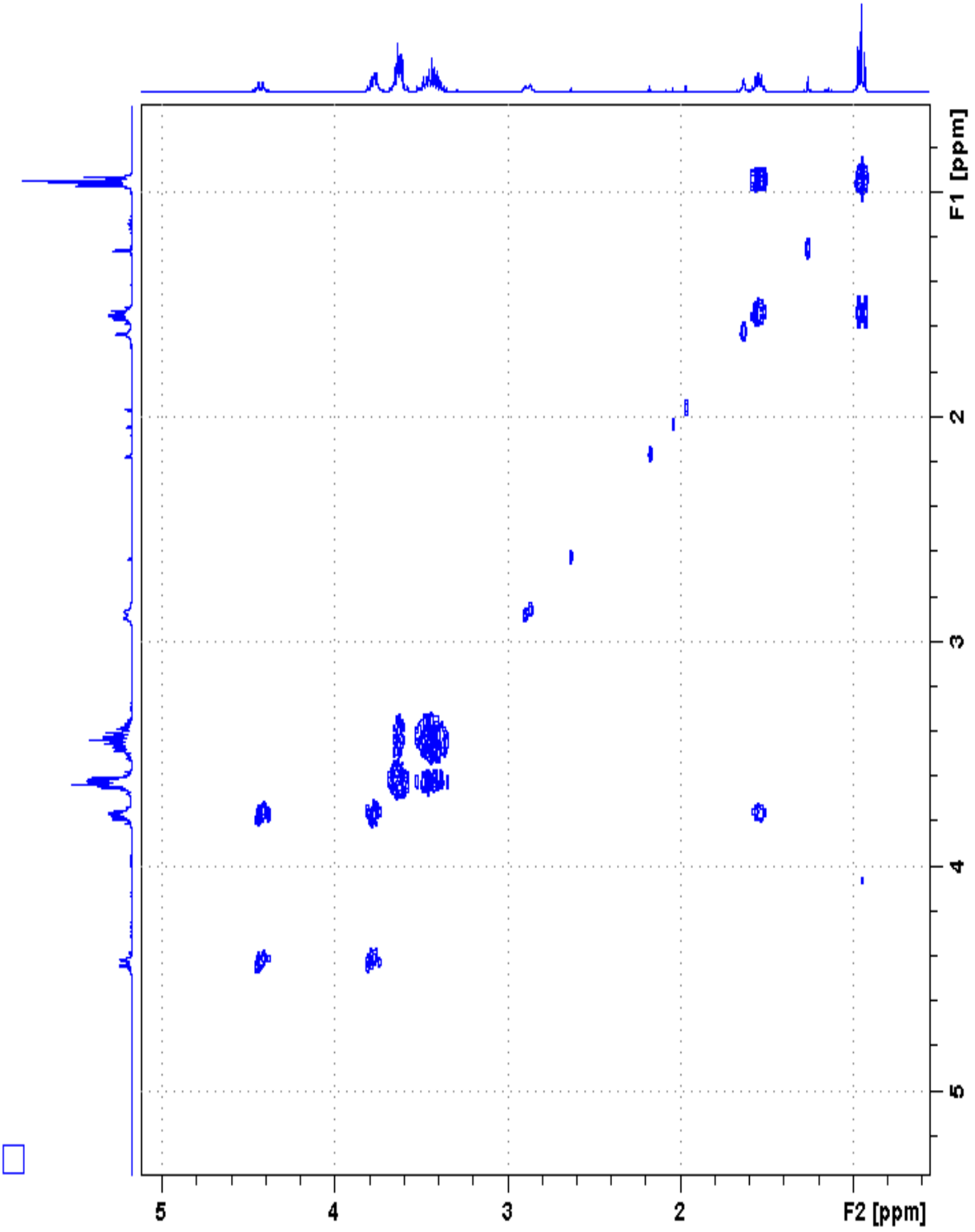

Figure 49. ^{1}H NMR of Oxazaphospholidinone **5a**.

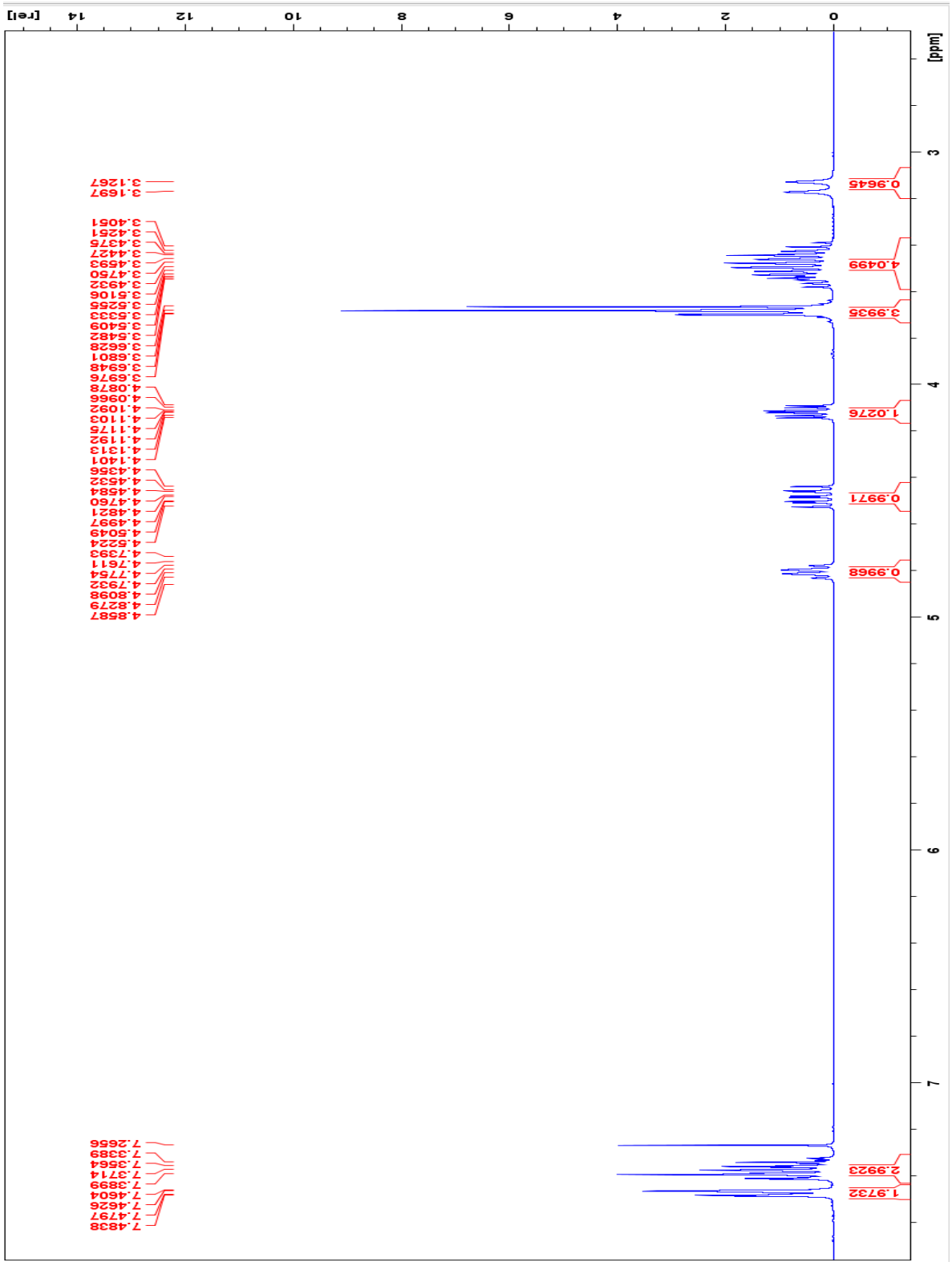

Figure 50. ^{31}P NMR of Oxazaphospholidinone **5a**.

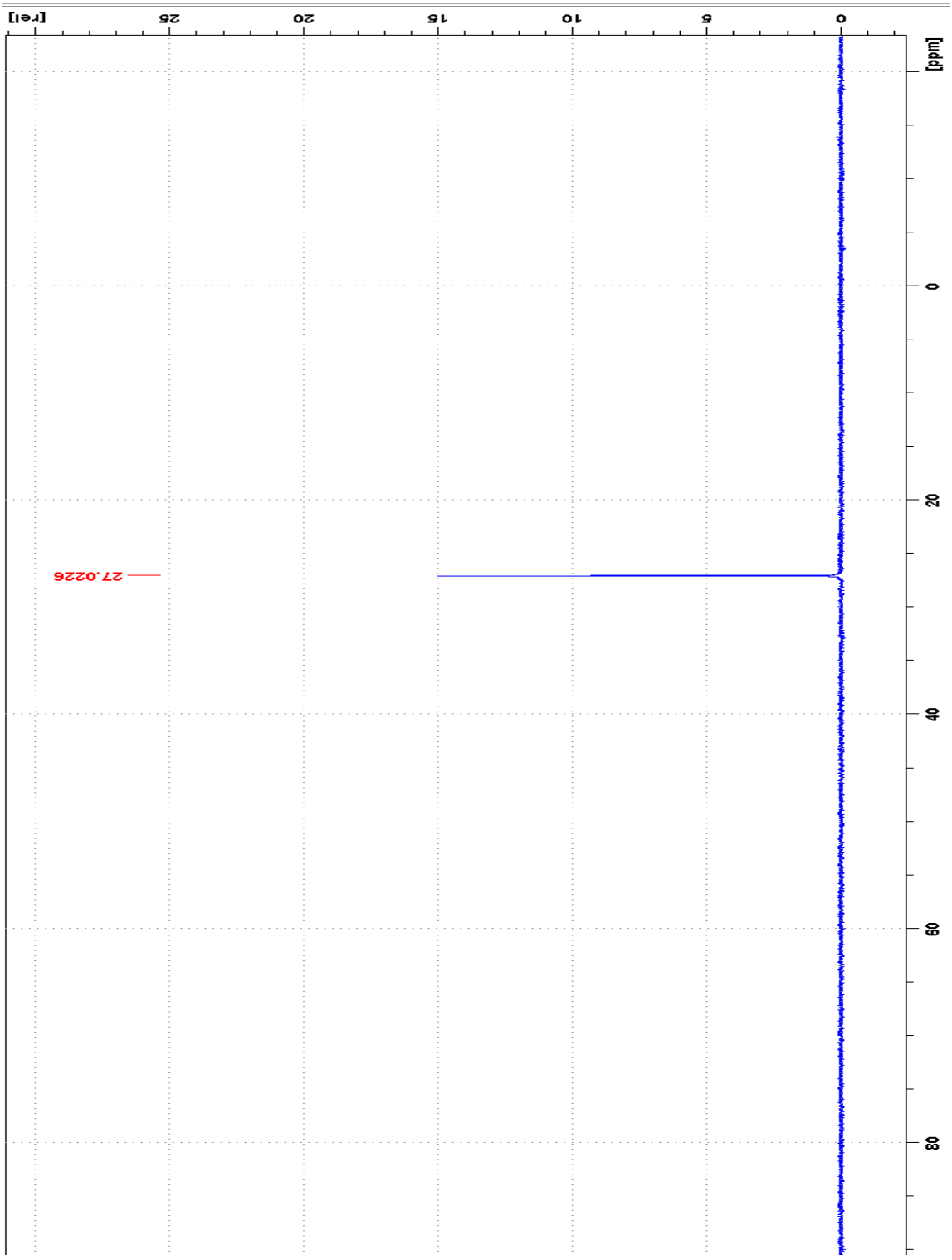

Figure 51. ^{1}H NMR of Oxazaphospholidinone **5b**.

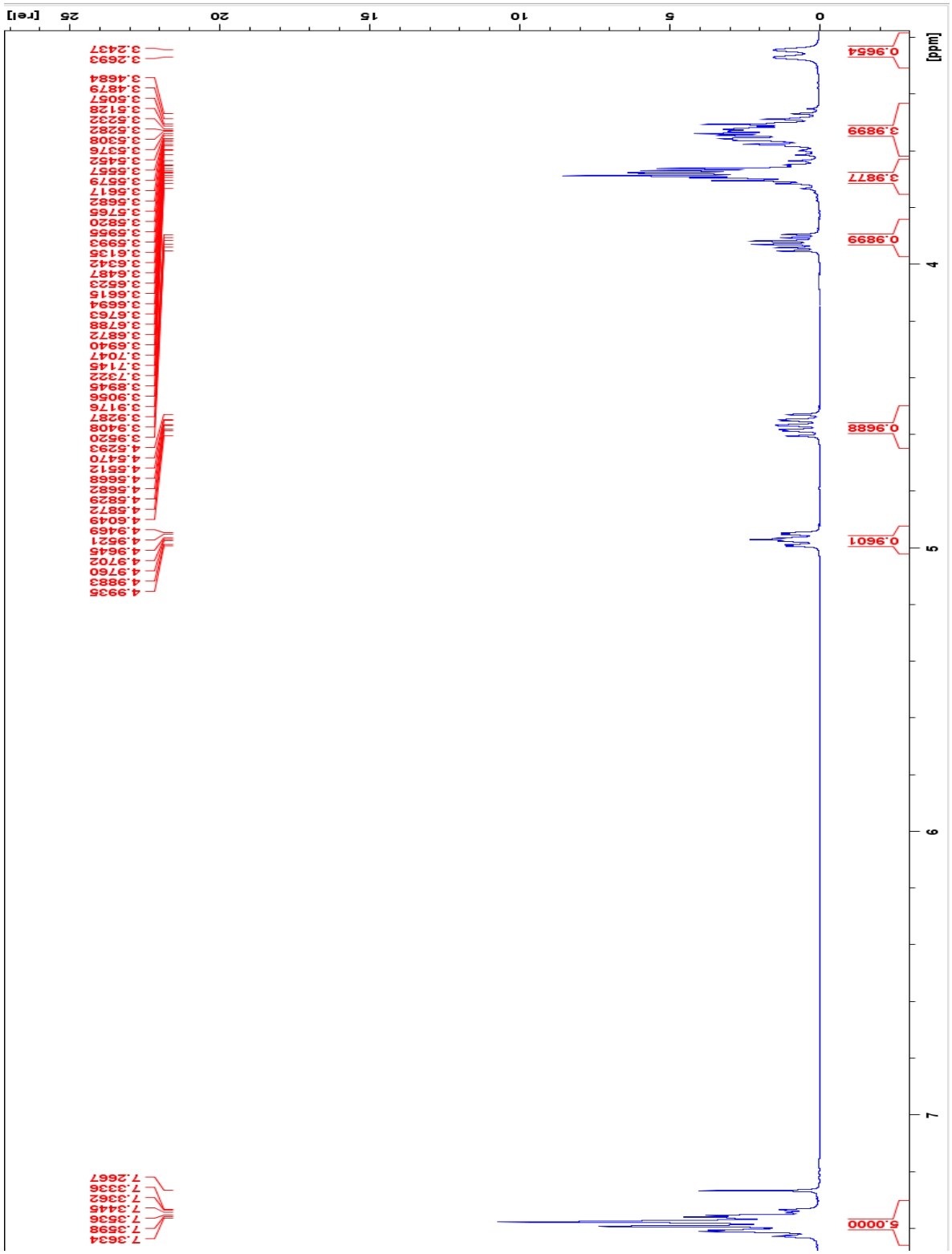

Figure 52. ^{13}C NMR of Oxazaphospholidinone **5b**.

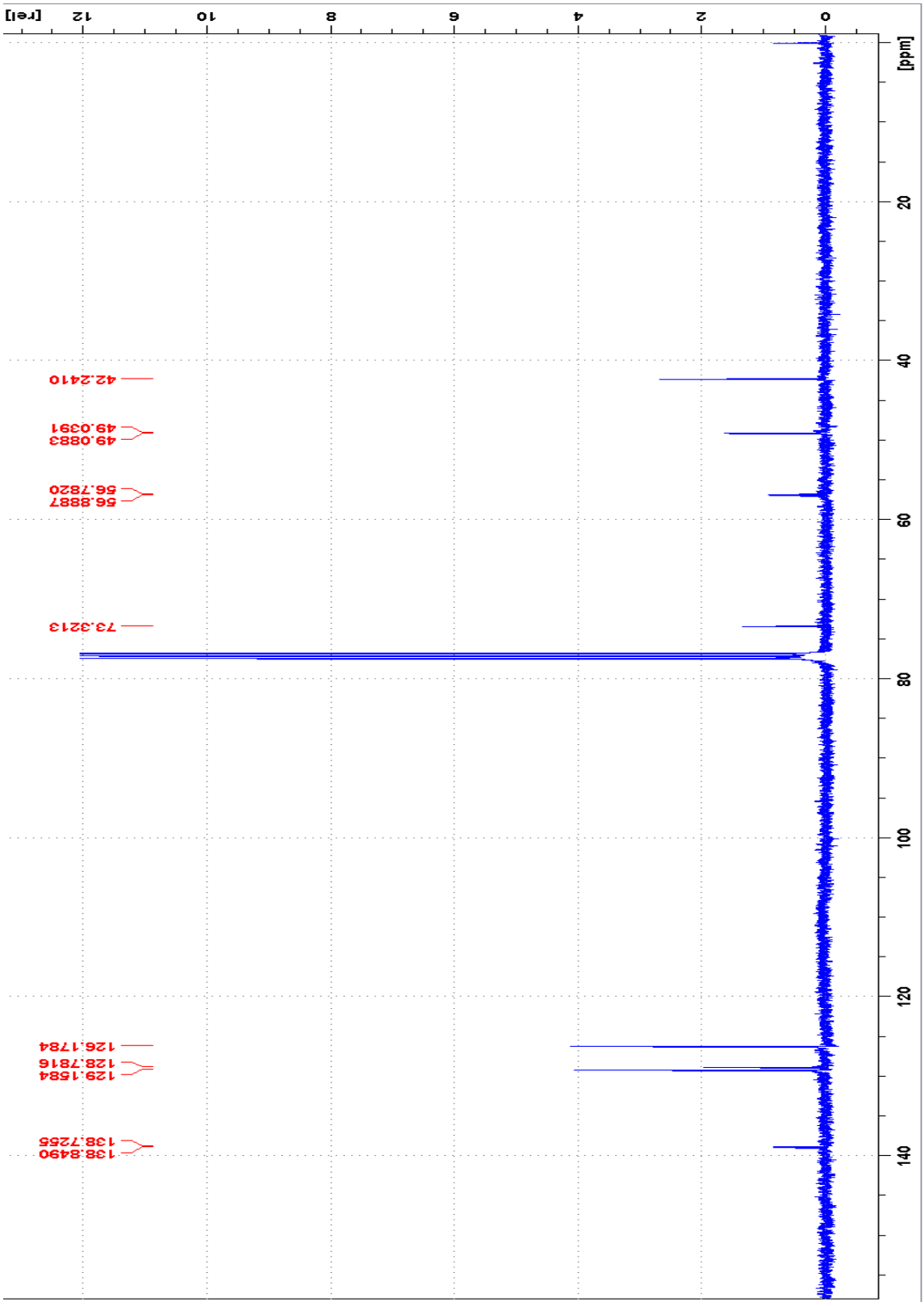

Figure 53. ^{31}P NMR of Oxazaphospholidinone **5b**.

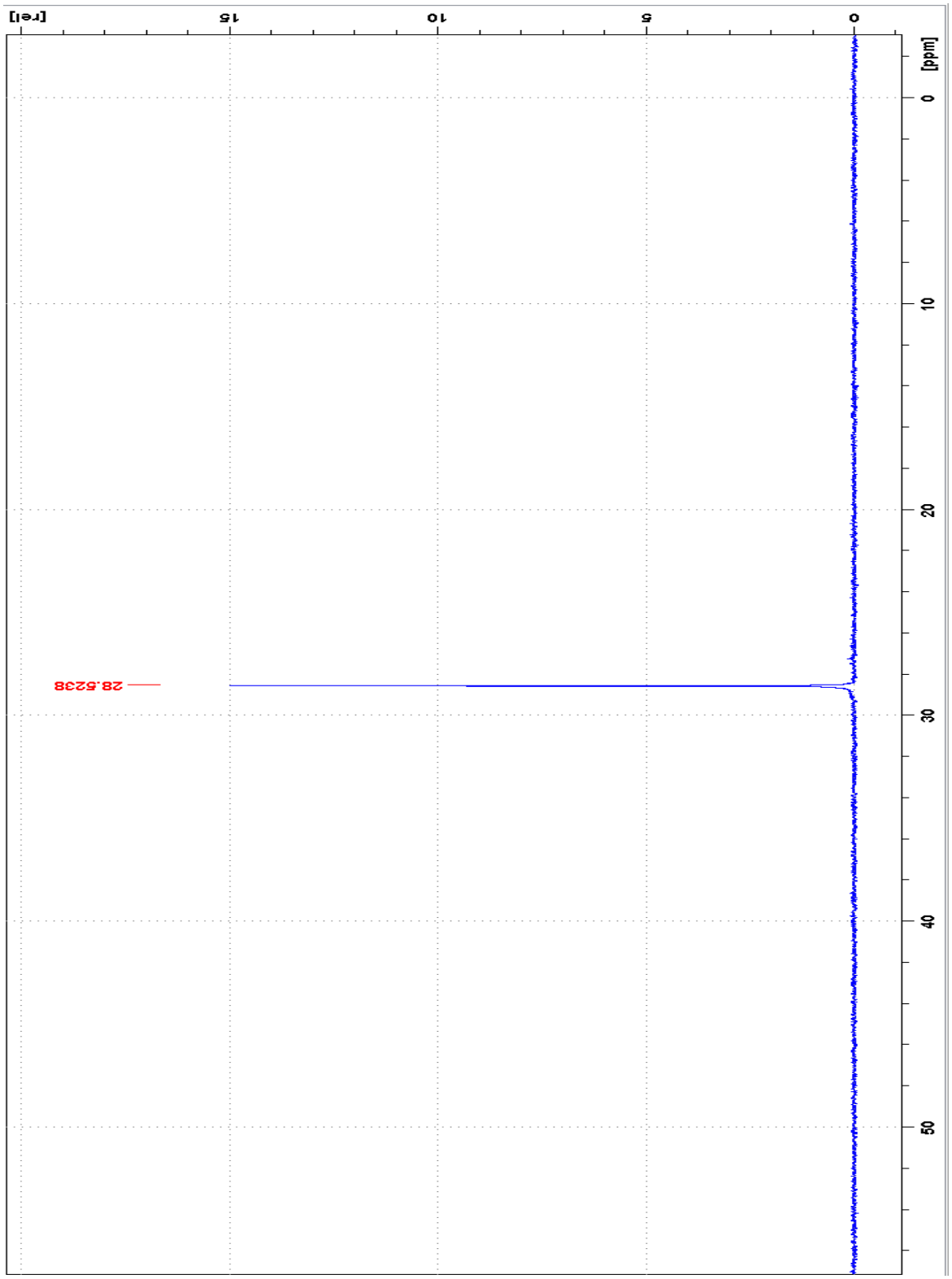

Figure 54. COSY NMR of Oxazaphospholidinone **5b**.

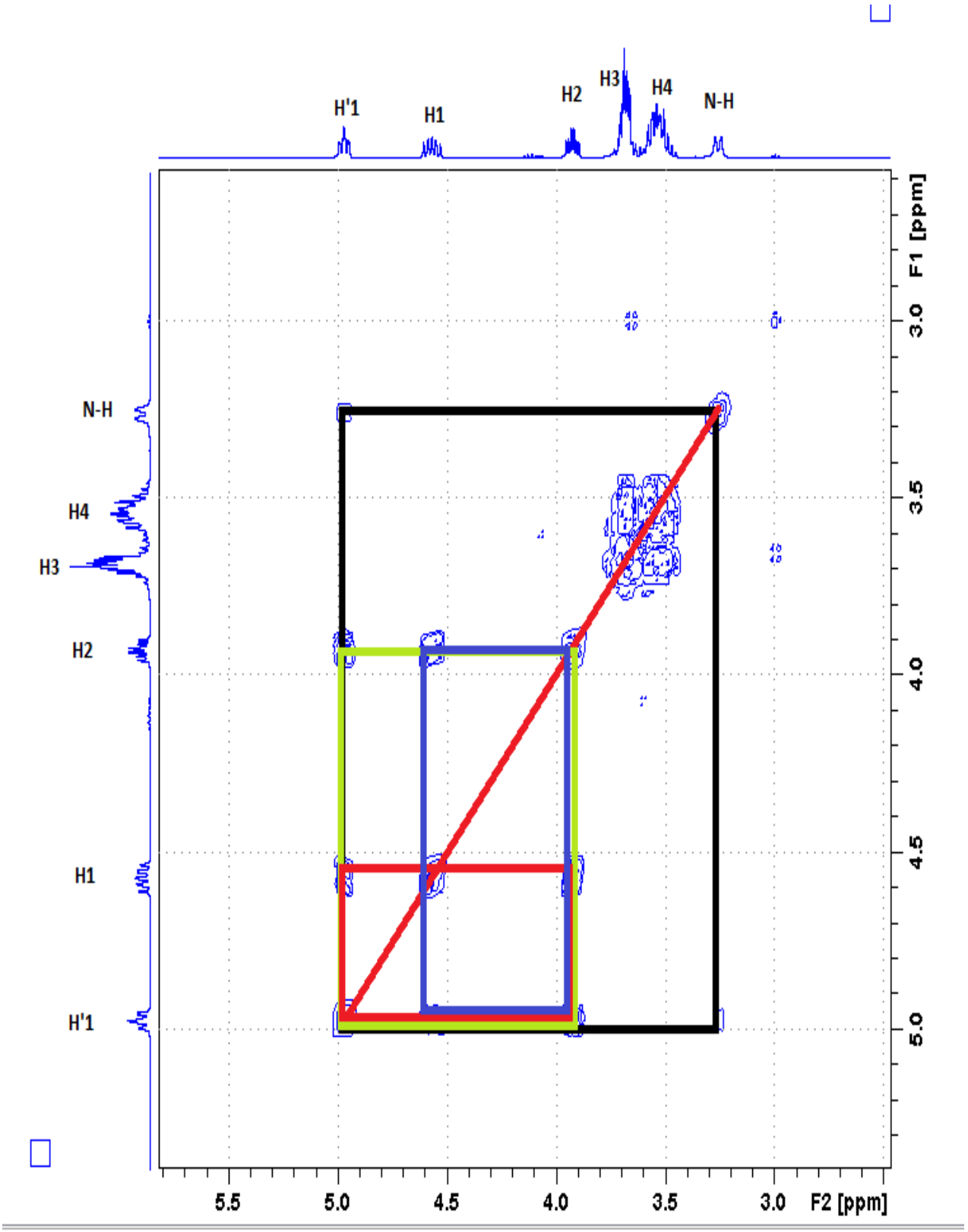

Figure 55. ^{31}P NMR of Oxazaphospholidinone **6a**.

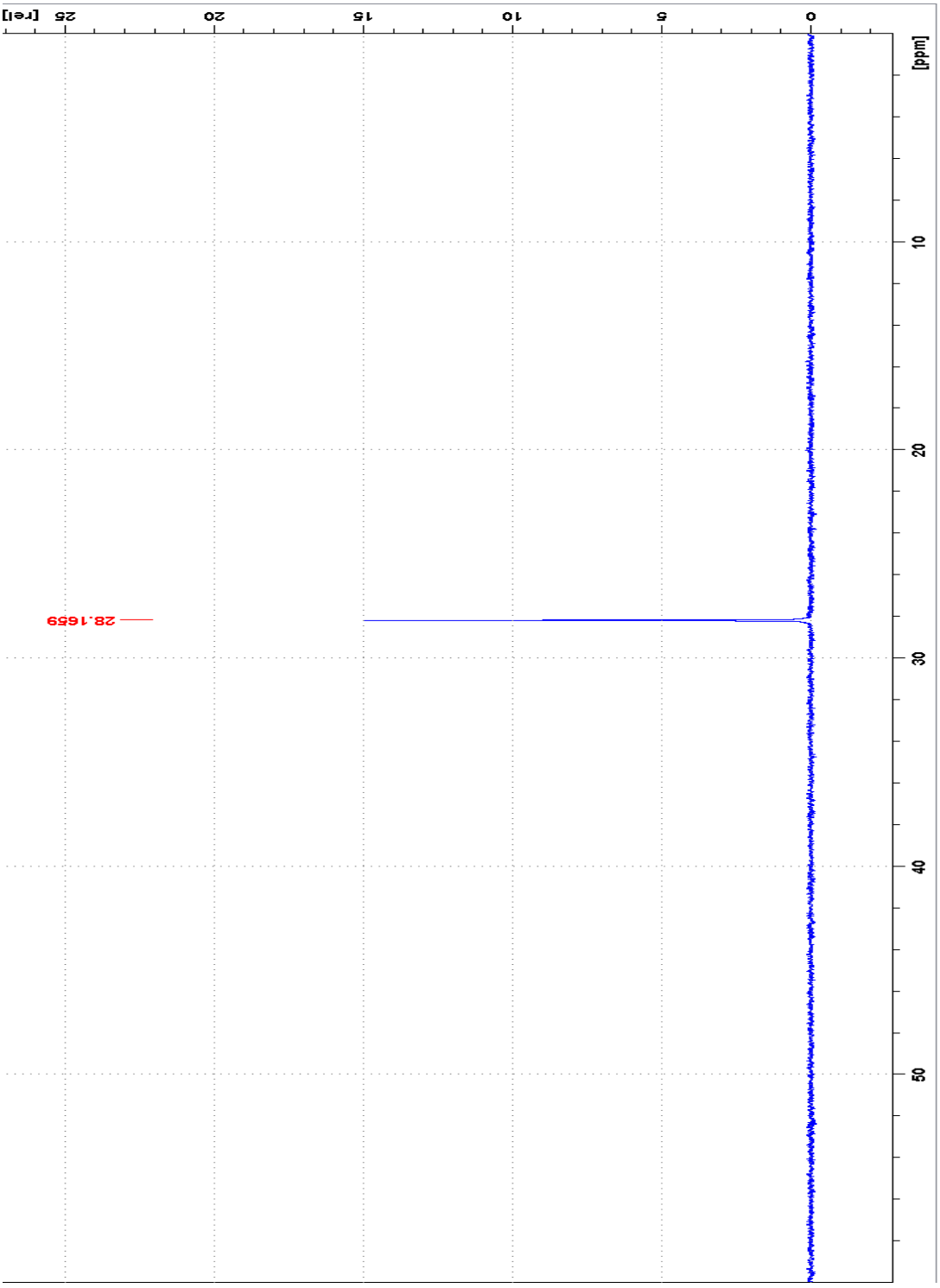

Figure 56. ^{1}H NMR of Oxazaphospholidinone **6a**.

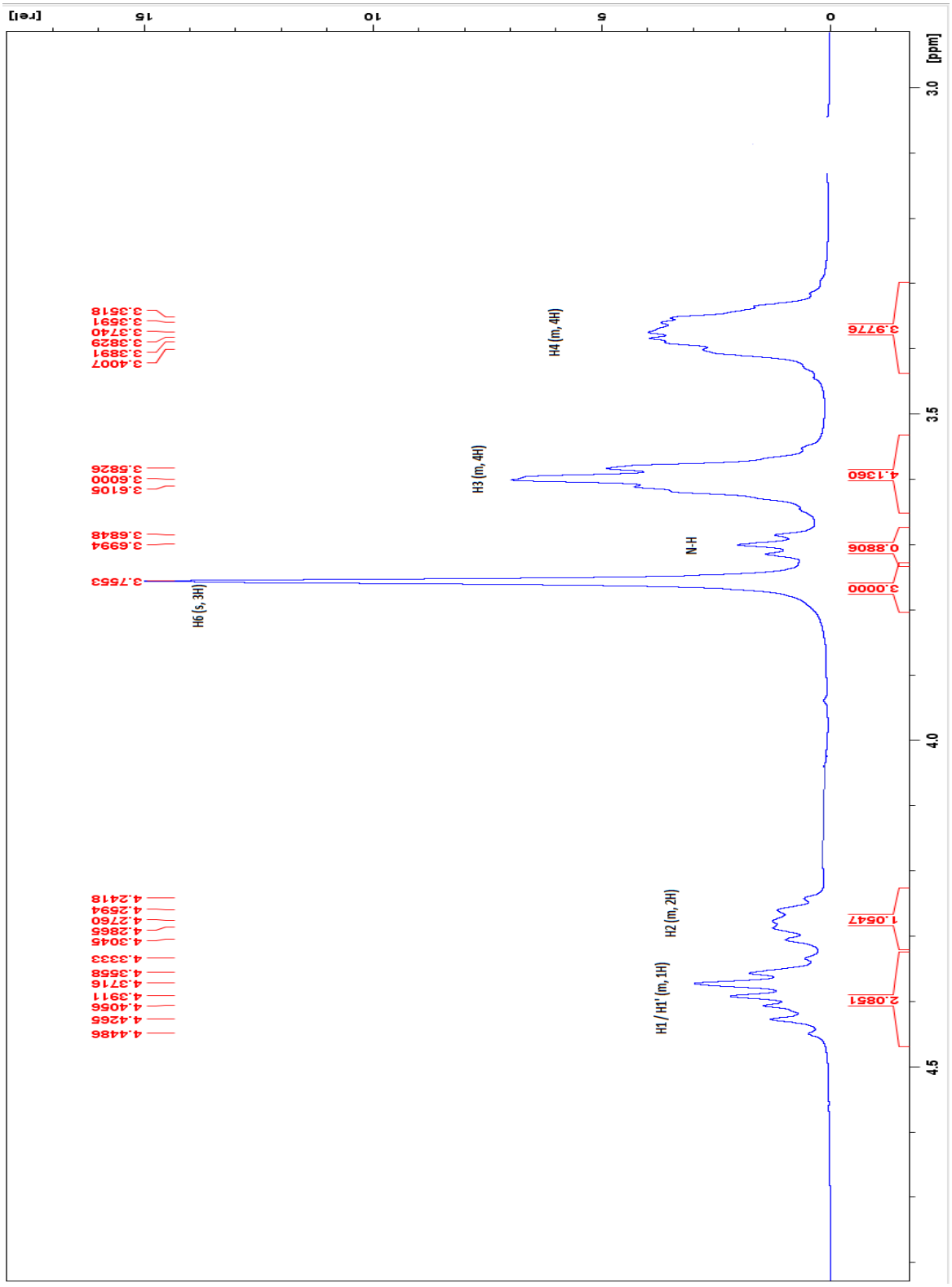

Figure 57. ^{13}C NMR of Oxazaphospholidinone **6b**.

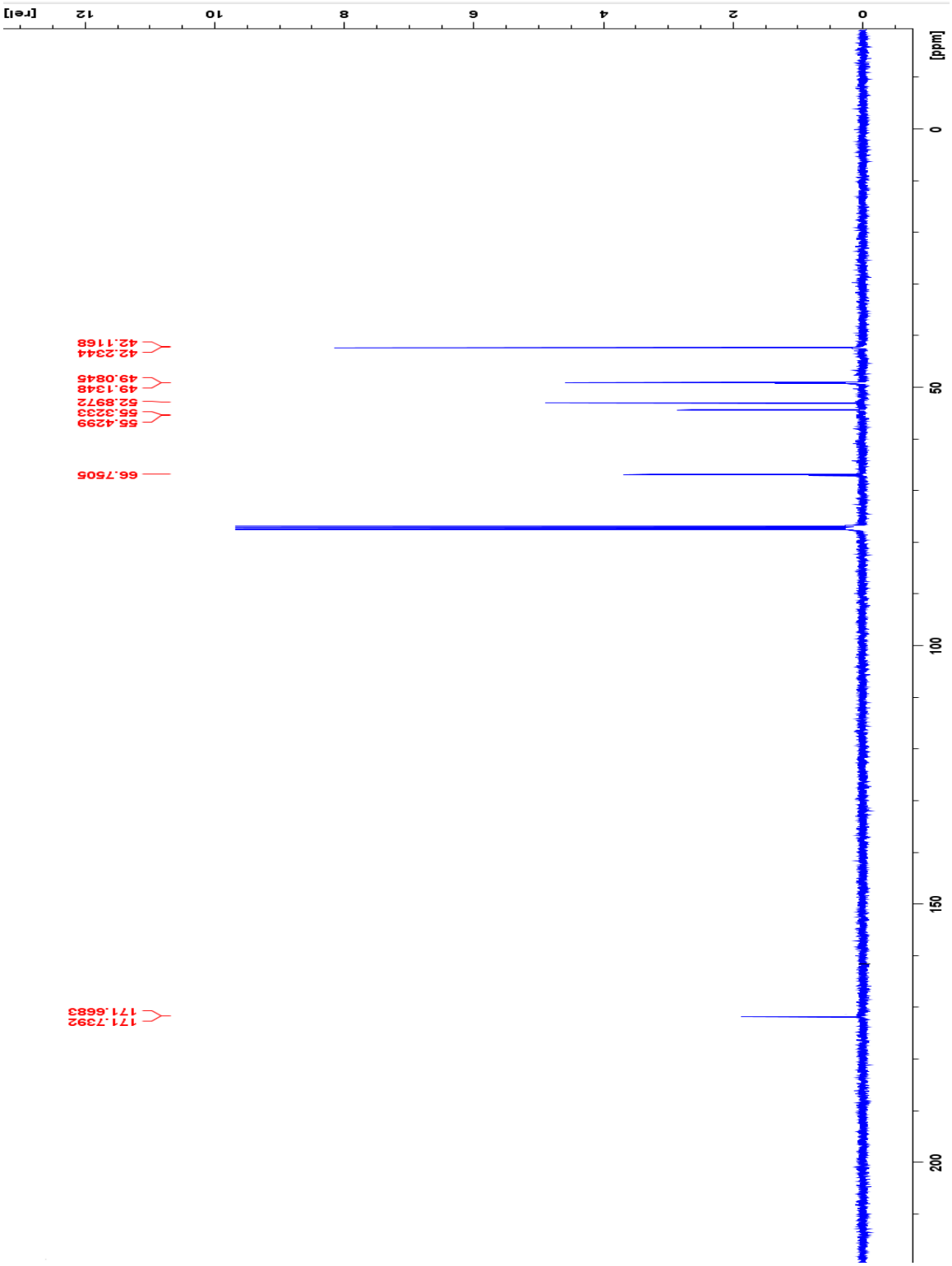

Figure 58. ^{31}P NMR of Oxazaphospholidinone **6b**.

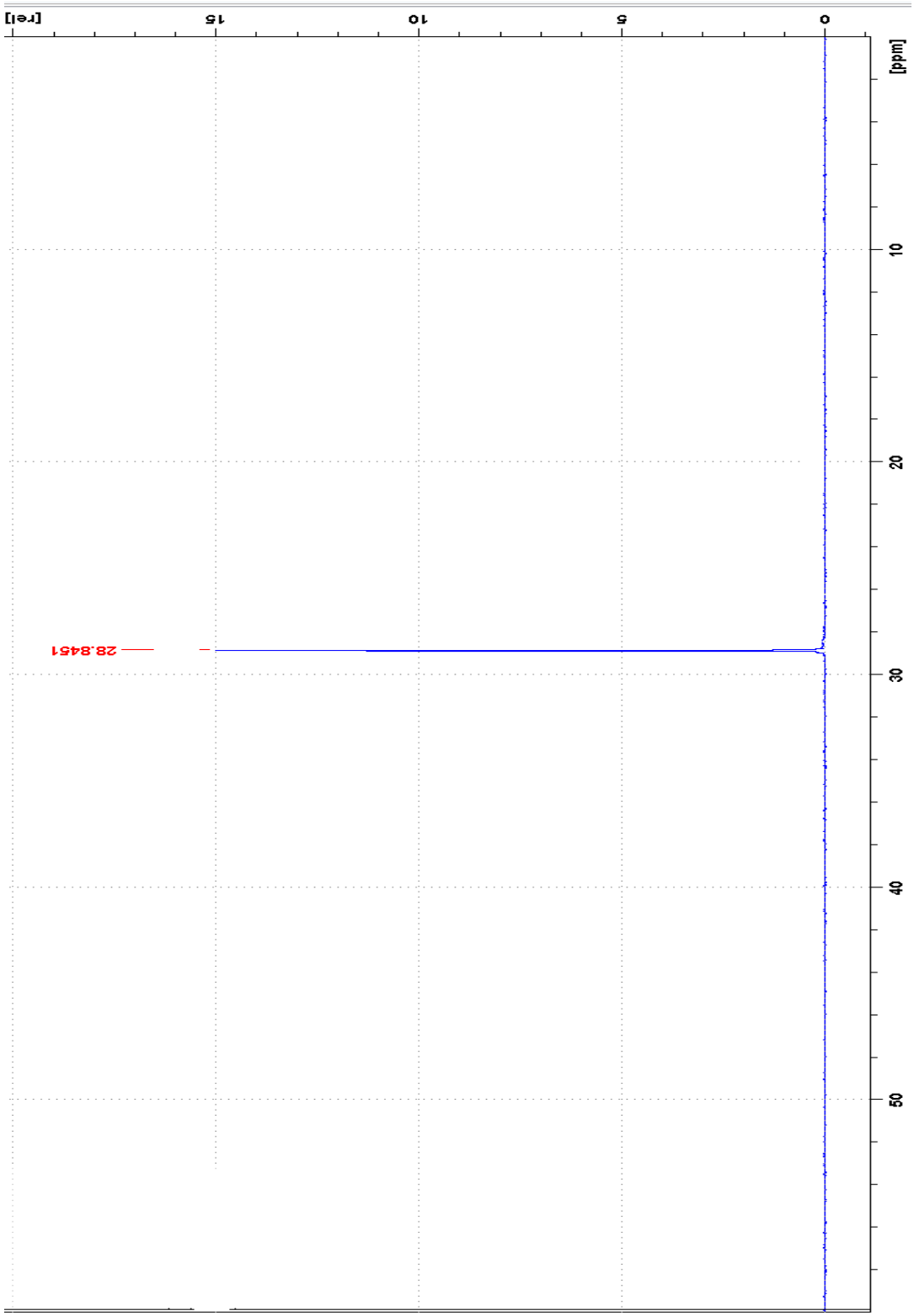

Figure 59. ^{1}H NMR of Oxazaphospholidinone **6b**.

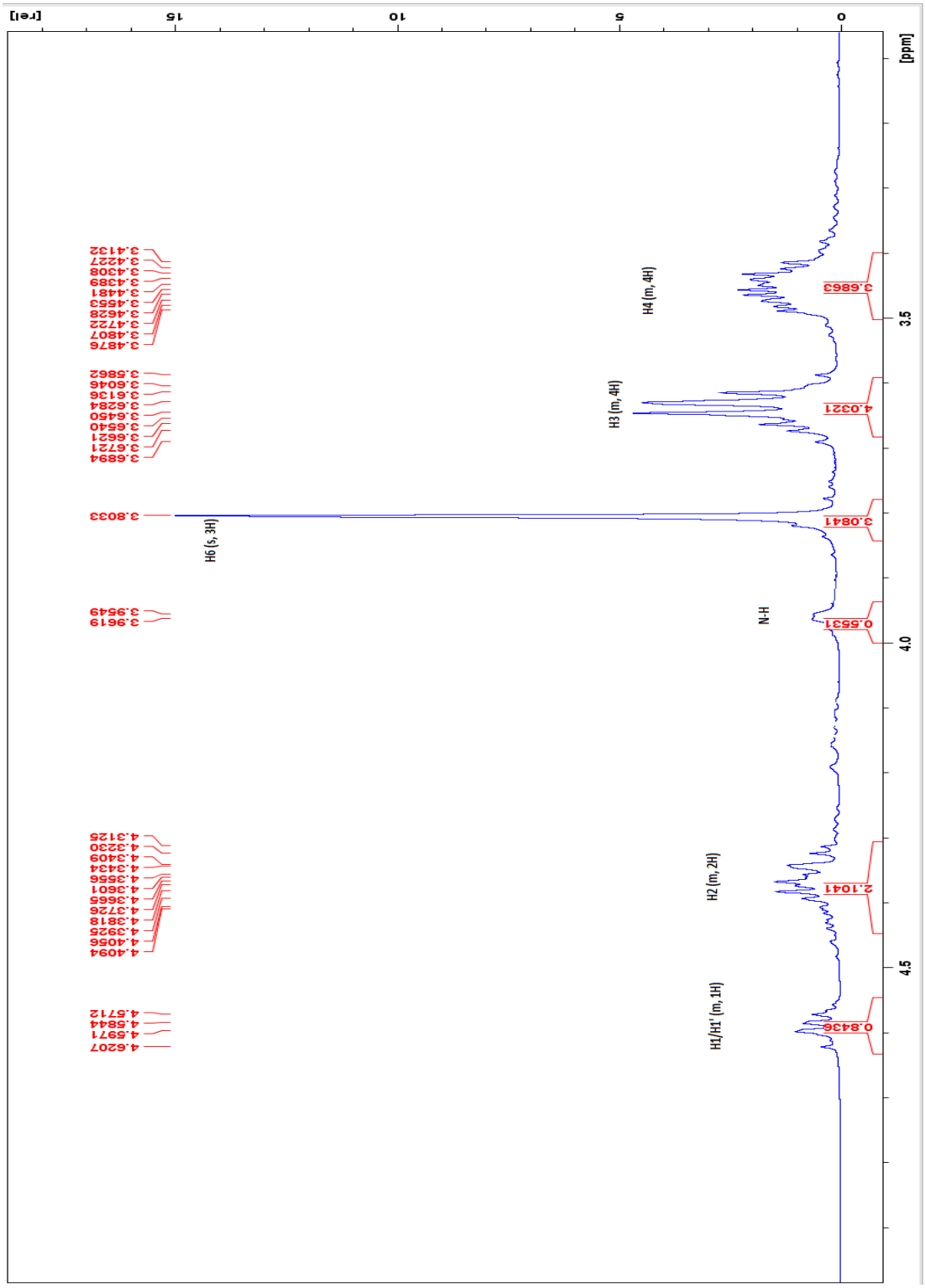

Figure 60. ^{13}C NMR of Oxazaphospholidinone **7a**.

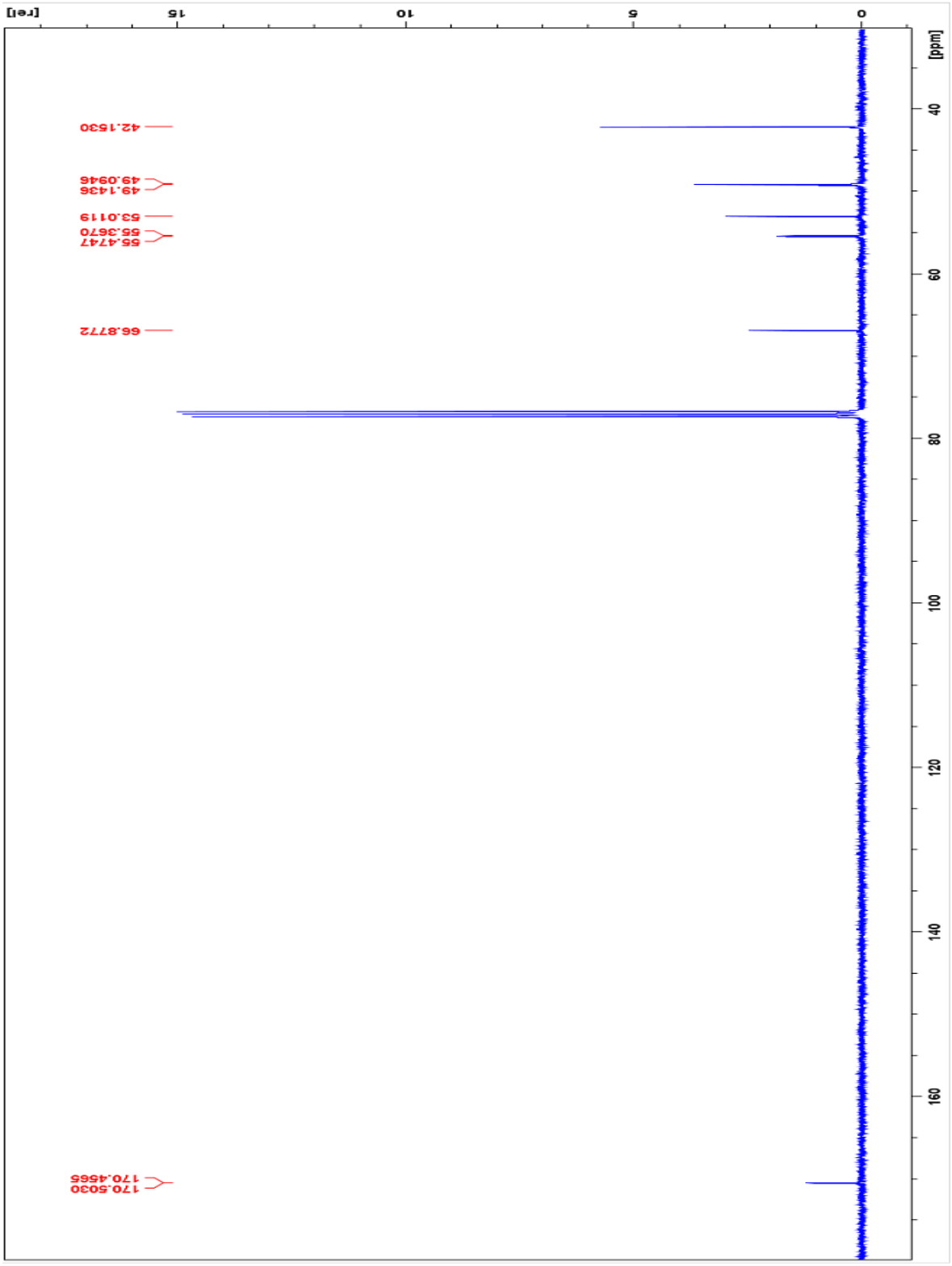

Figure 61. ^{31}P NMR of Oxazaphospholidinone **7a**.

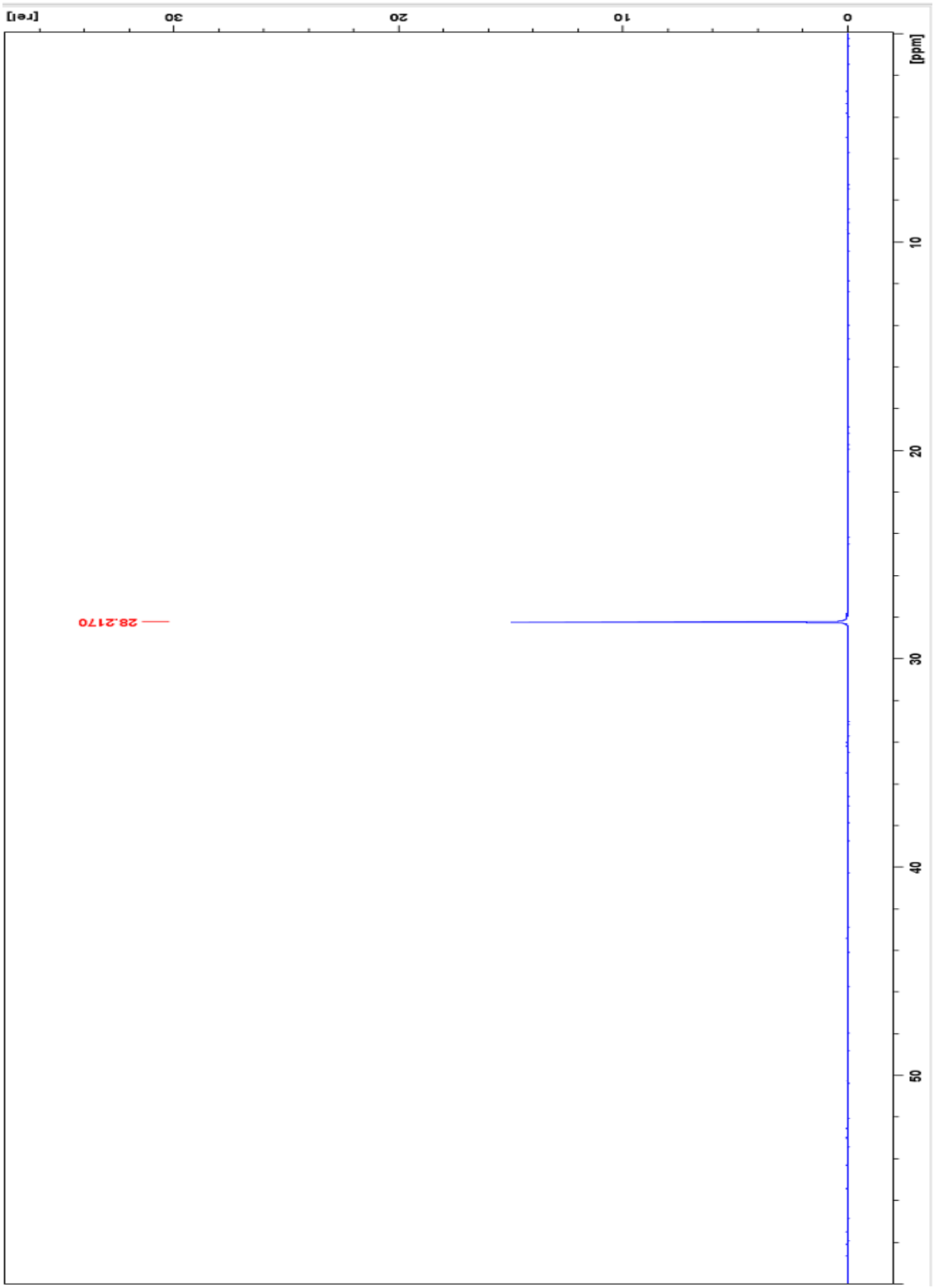

Figure 62. ^{1}H NMR of Oxazaphospholidinone **7a**.

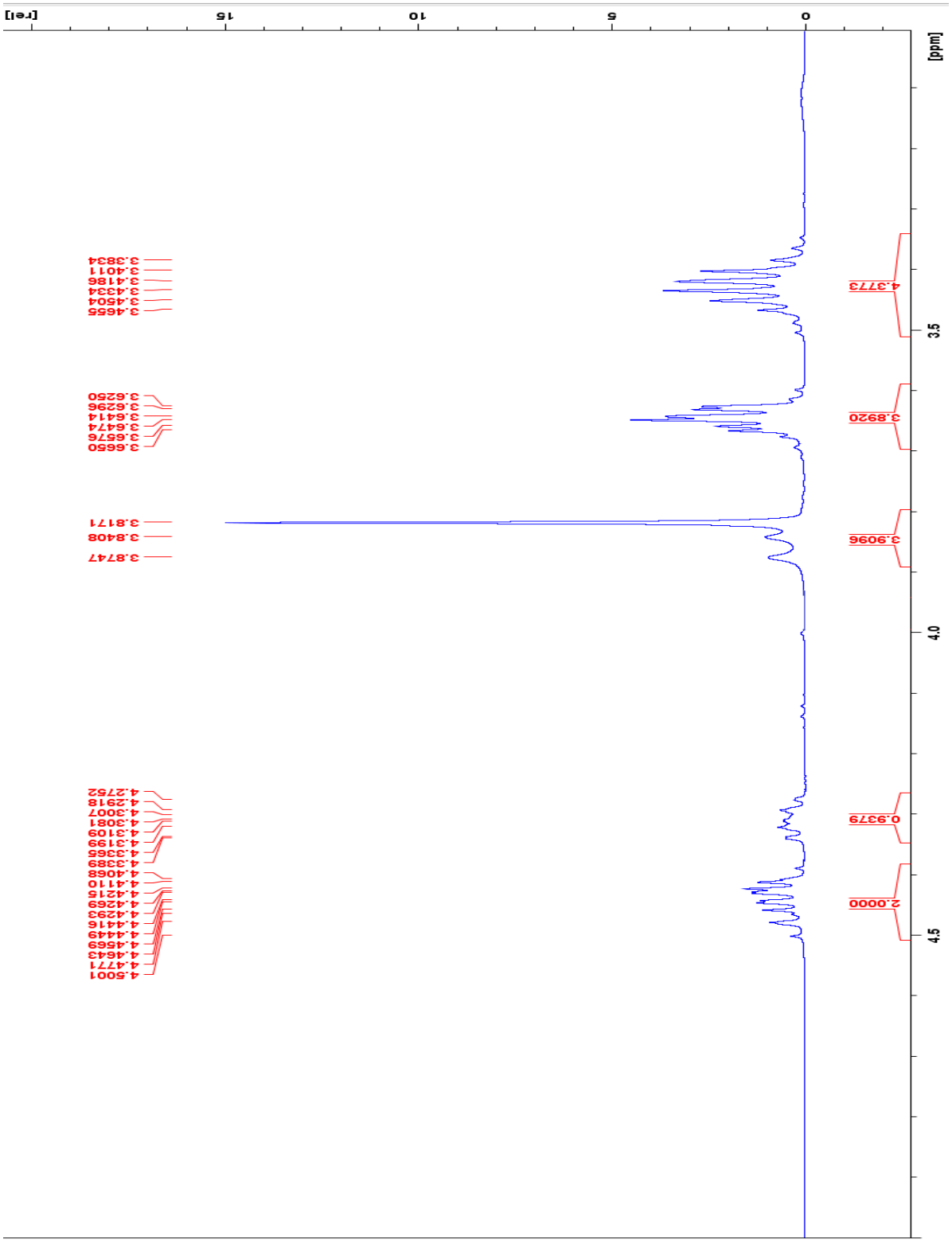

Figure 63. ^{13}C NMR of Oxazaphospholidinone **7b**.

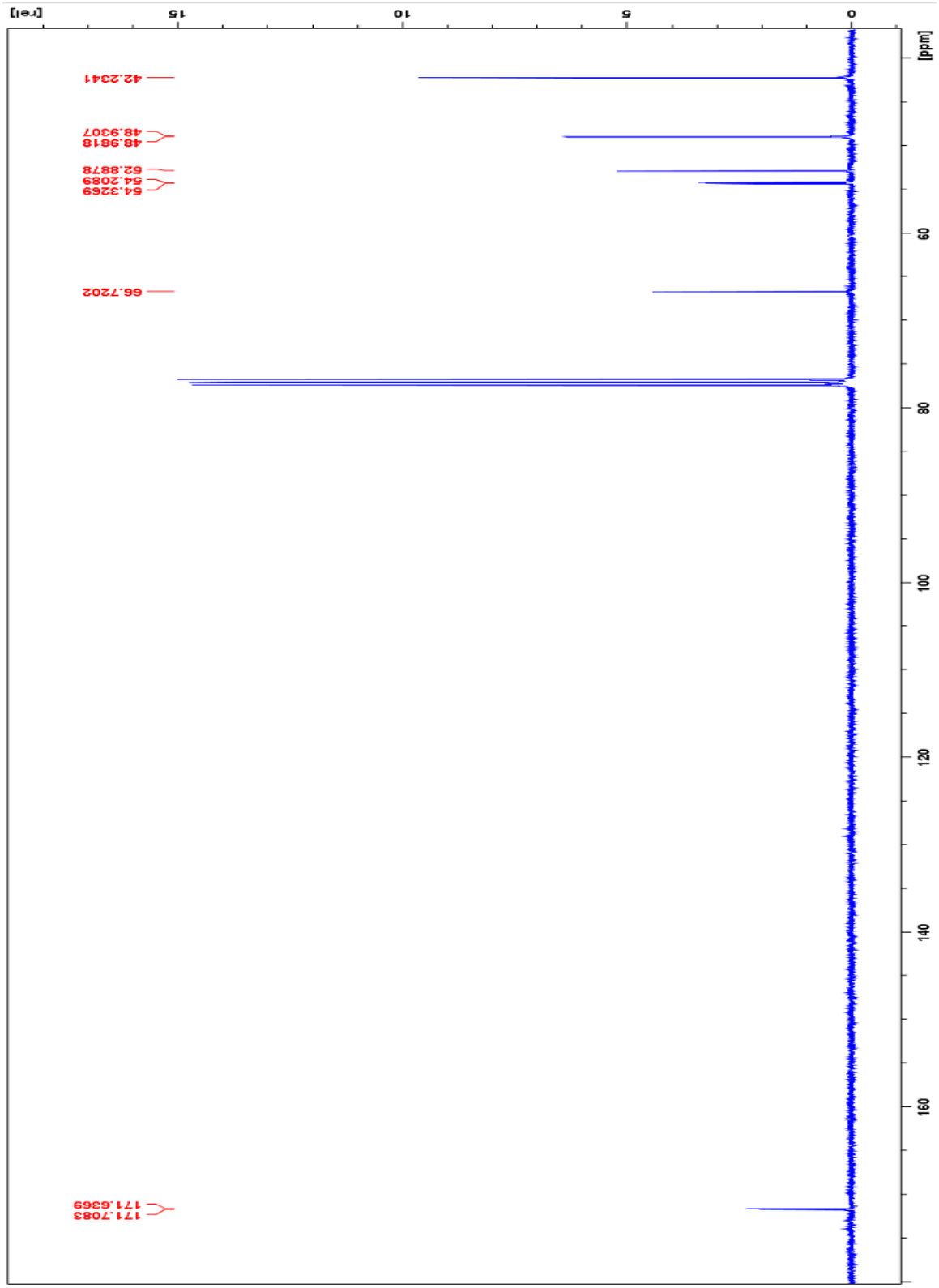

Figure 64. ^{31}P NMR of Oxazaphospholidinone **7b**.

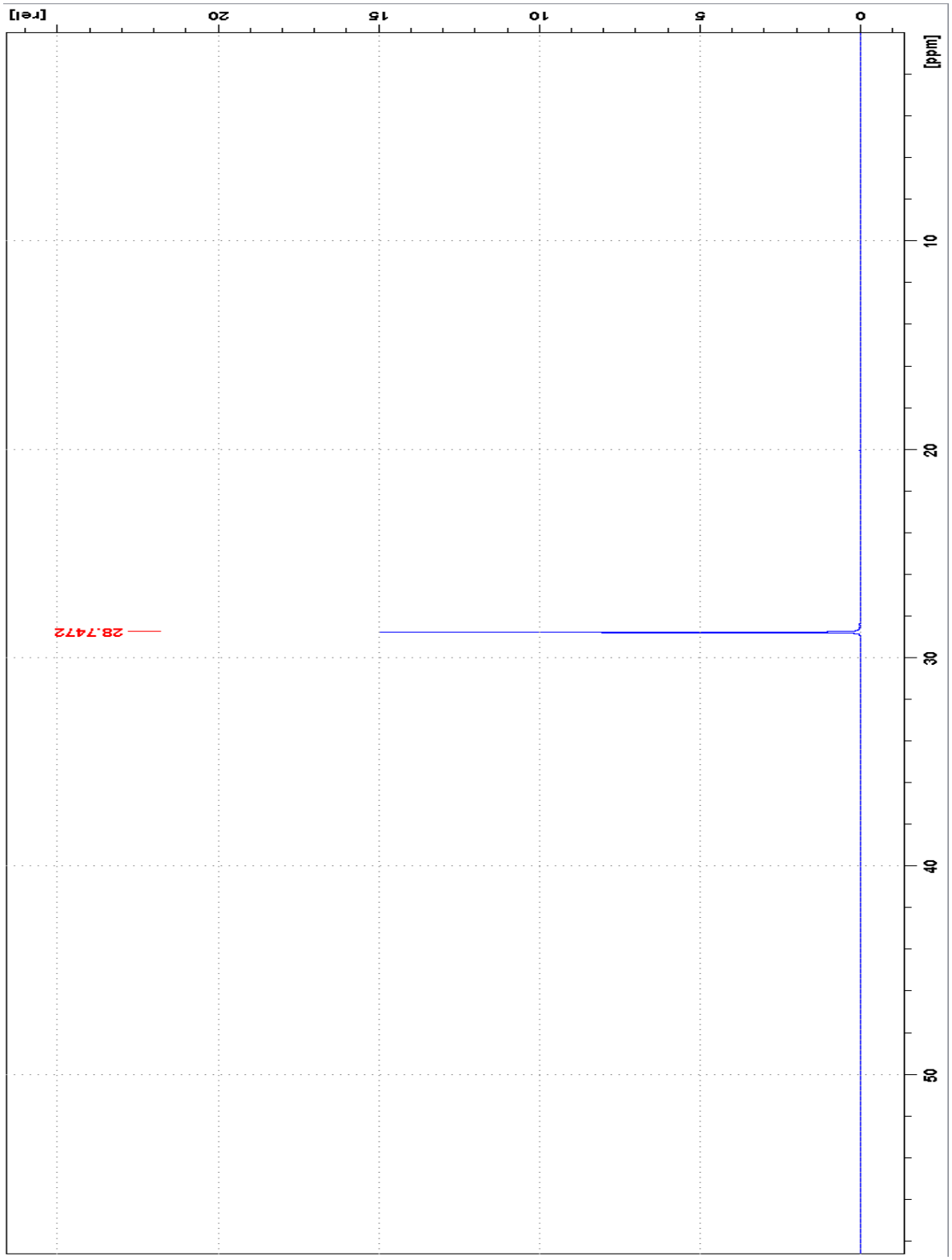

Figure 65. ^{1}H NMR of Oxazaphospholidinone **7b**.

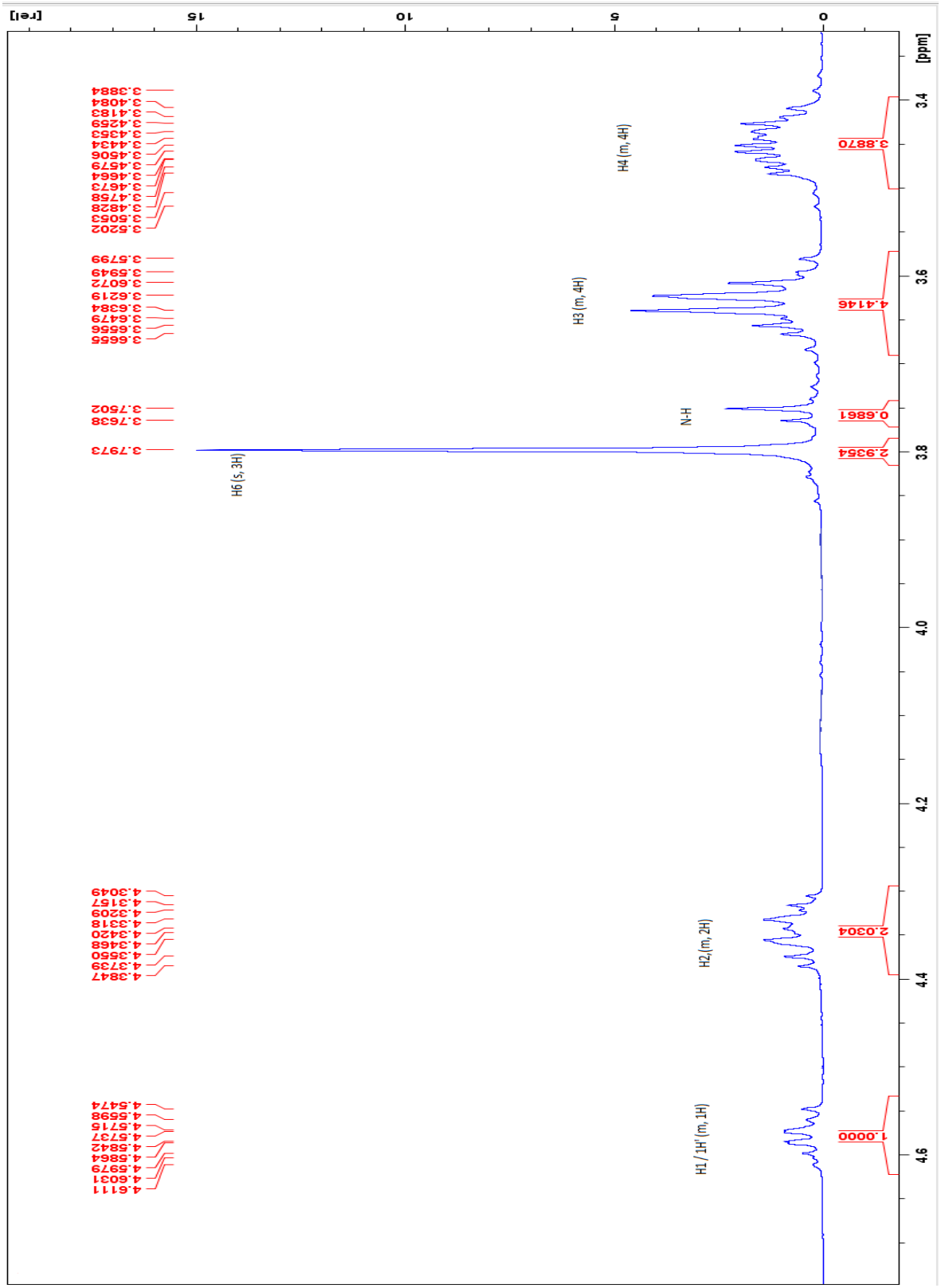

Figure 66. ^{13}C NMR of Oxazaphospholidinone **8a**.

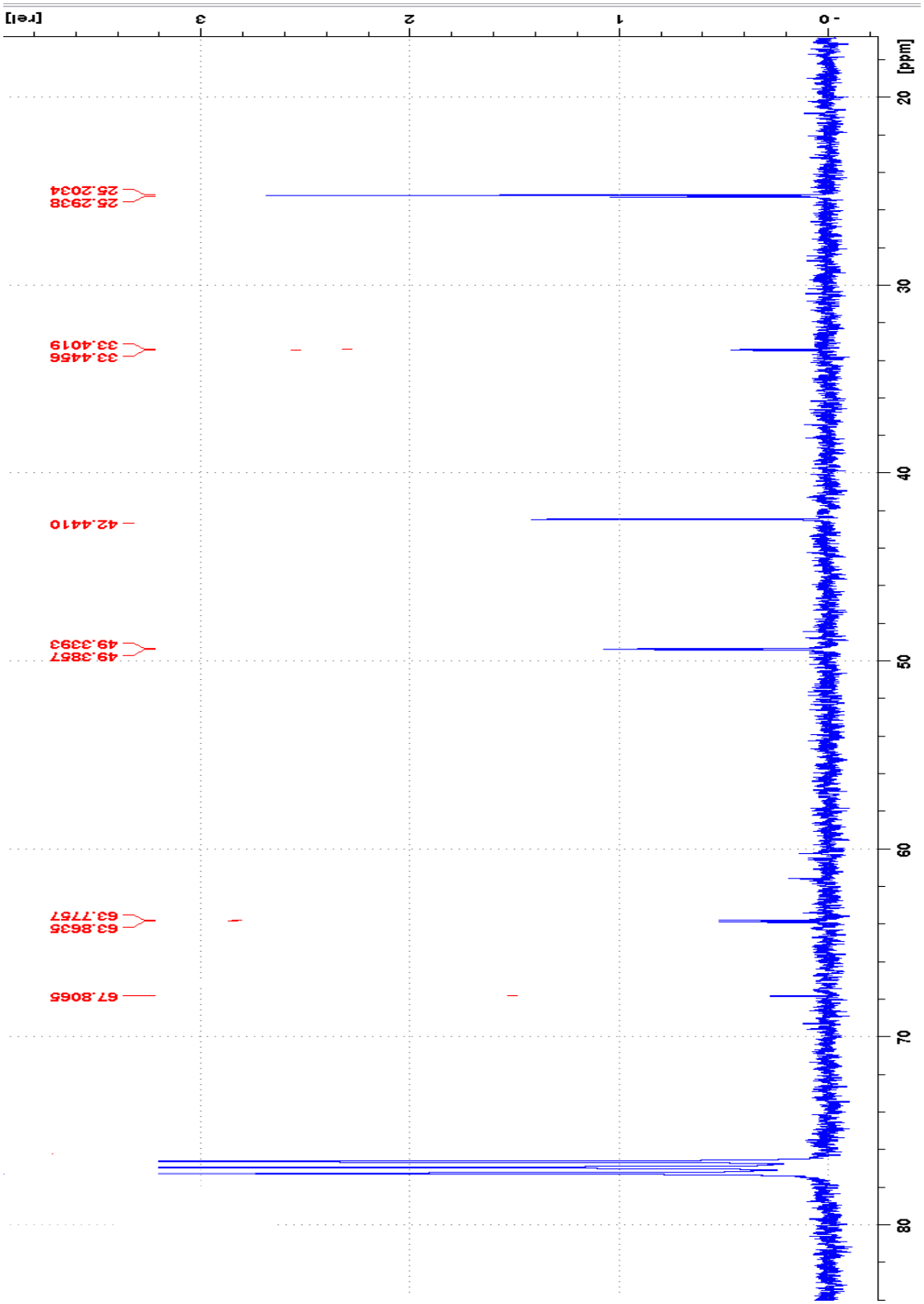

Figure 67. ^{31}P NMR of Oxazaphospholidinone **8a**.

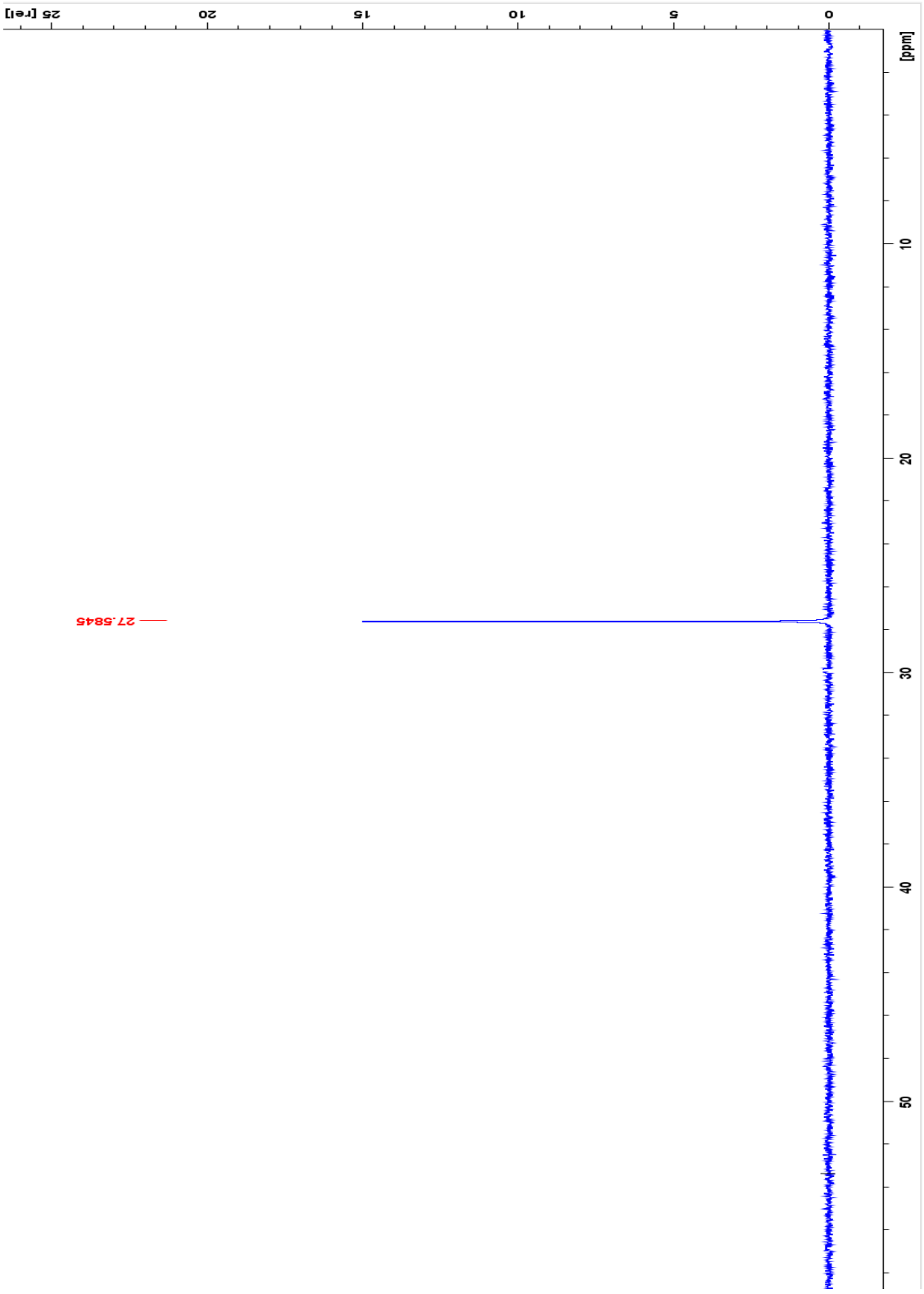

Figure 68. ^{1}H NMR of Oxazaphospholidinone **8a**.

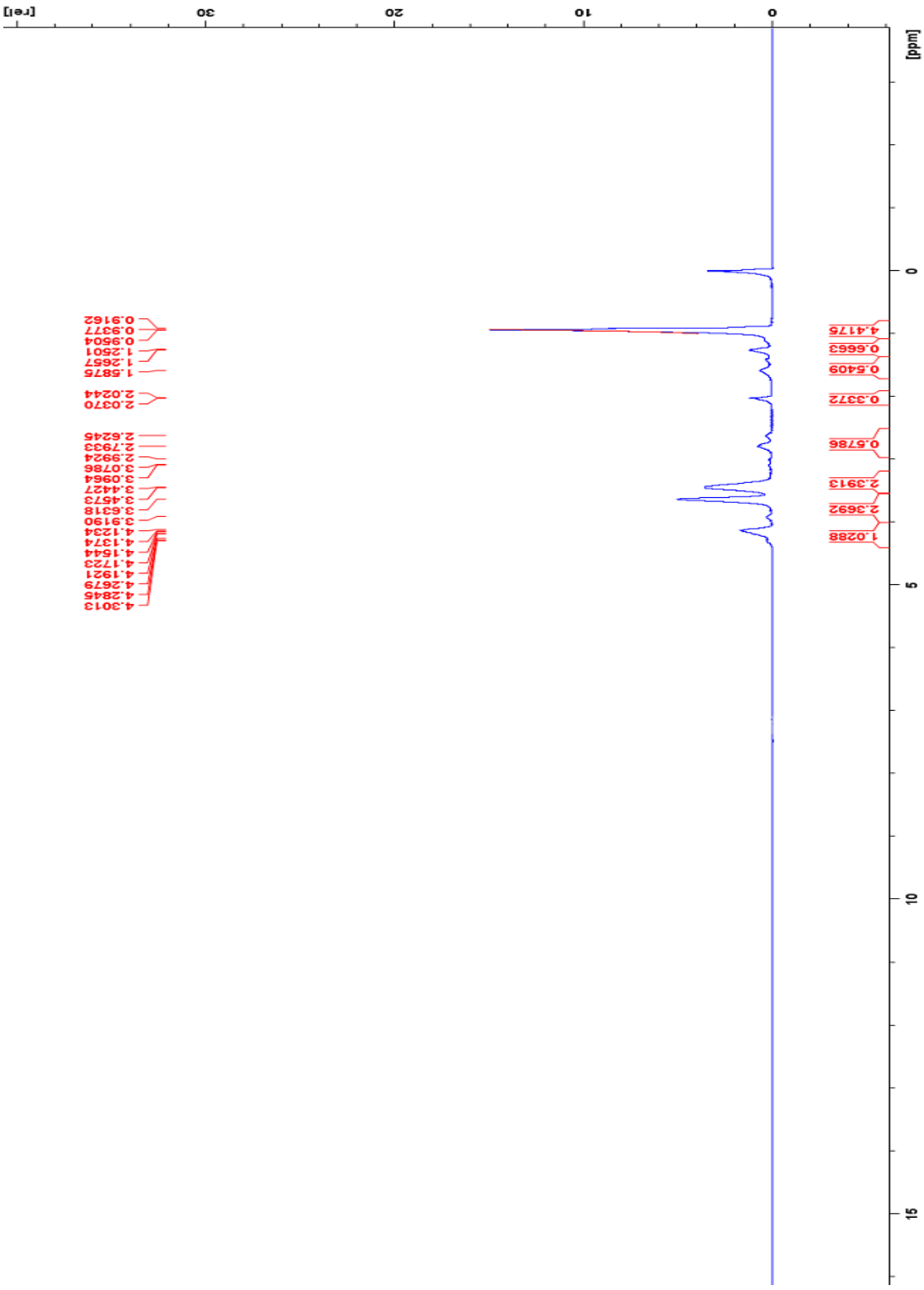

Figure 69. ^{13}C NMR of Oxazaphospholidinone **8b**.

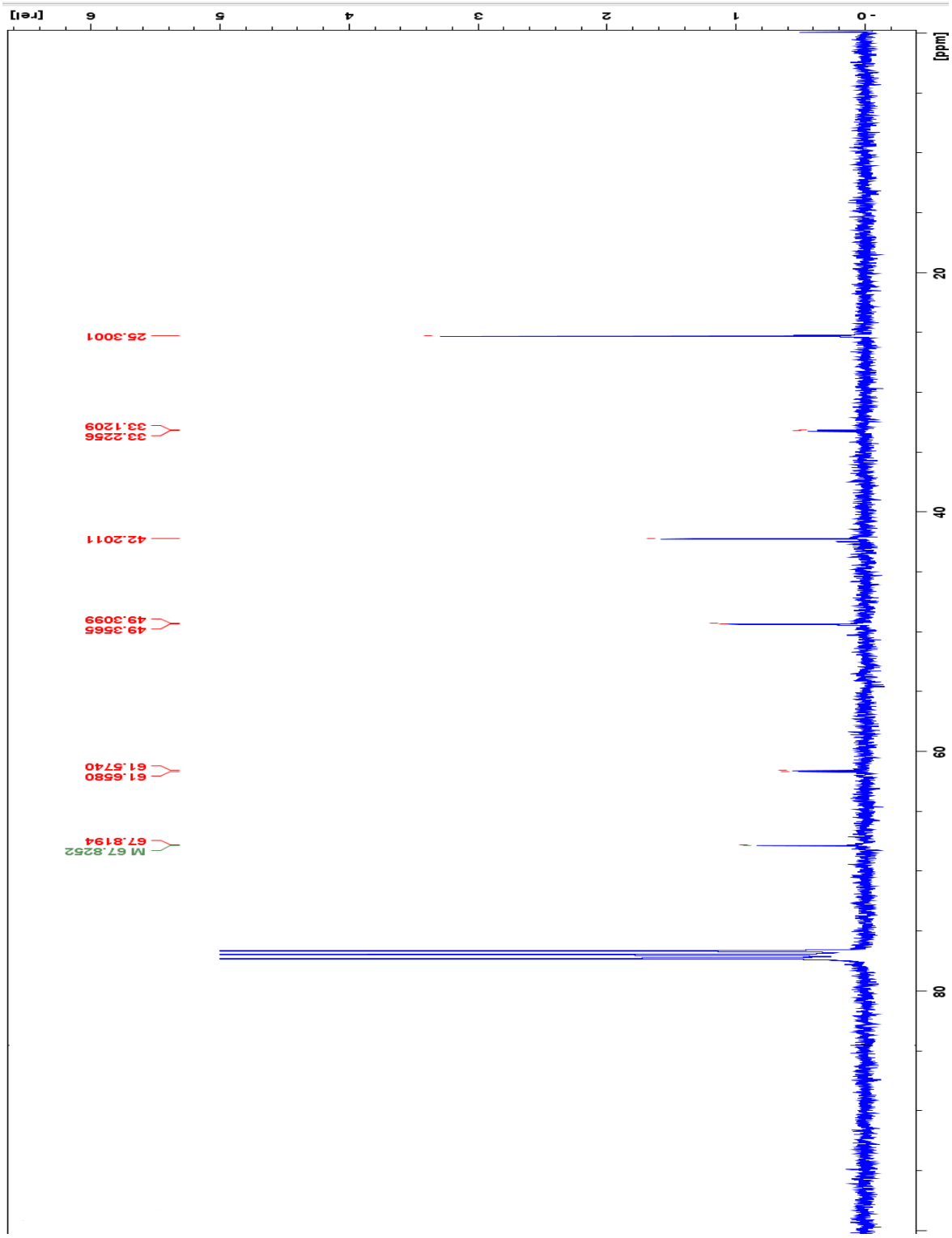

Figure 70. ^{31}P NMR of Oxazaphospholidinone **8b**.

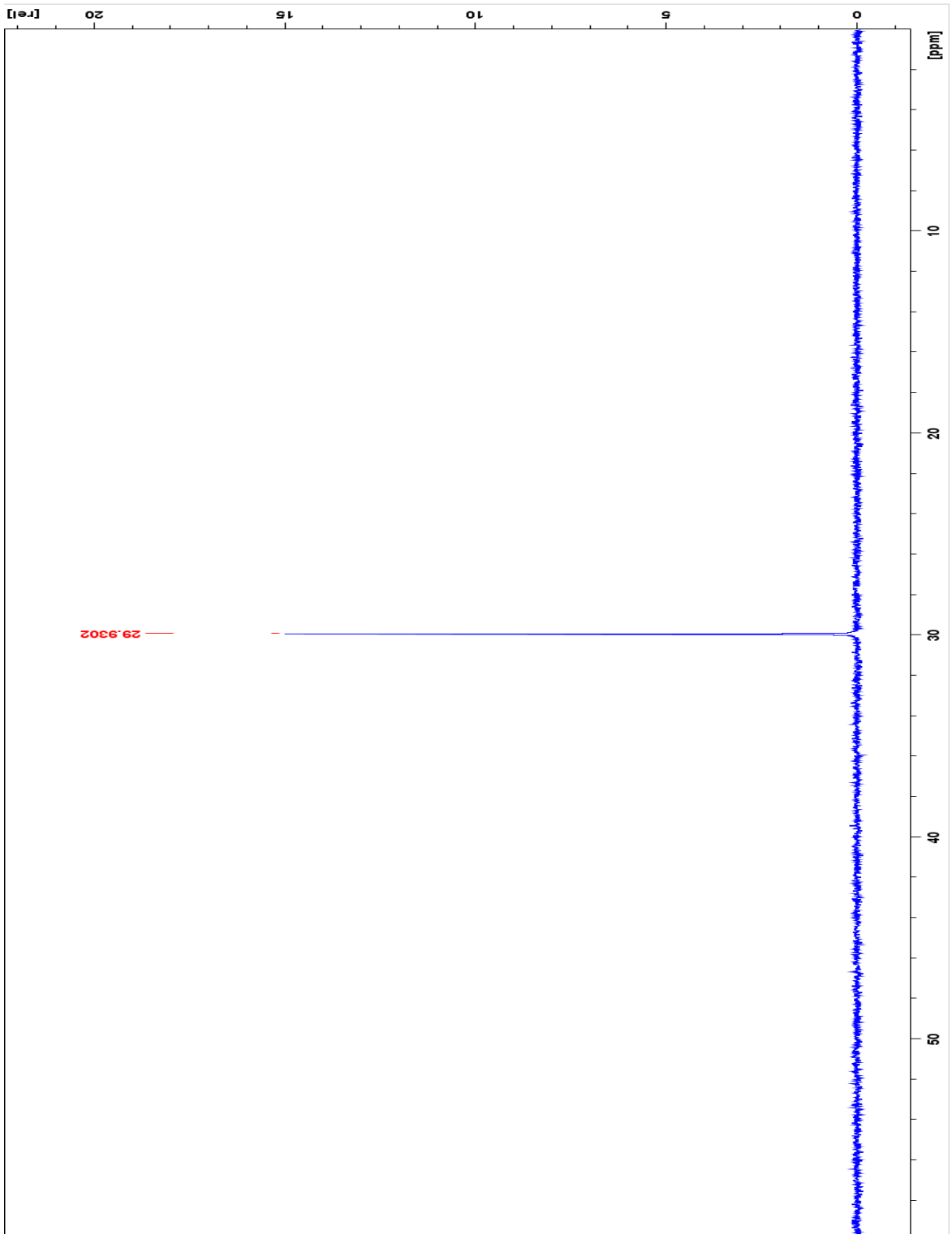

Figure 71. ^{1}H NMR of Oxazaphospholidinone **8b**.

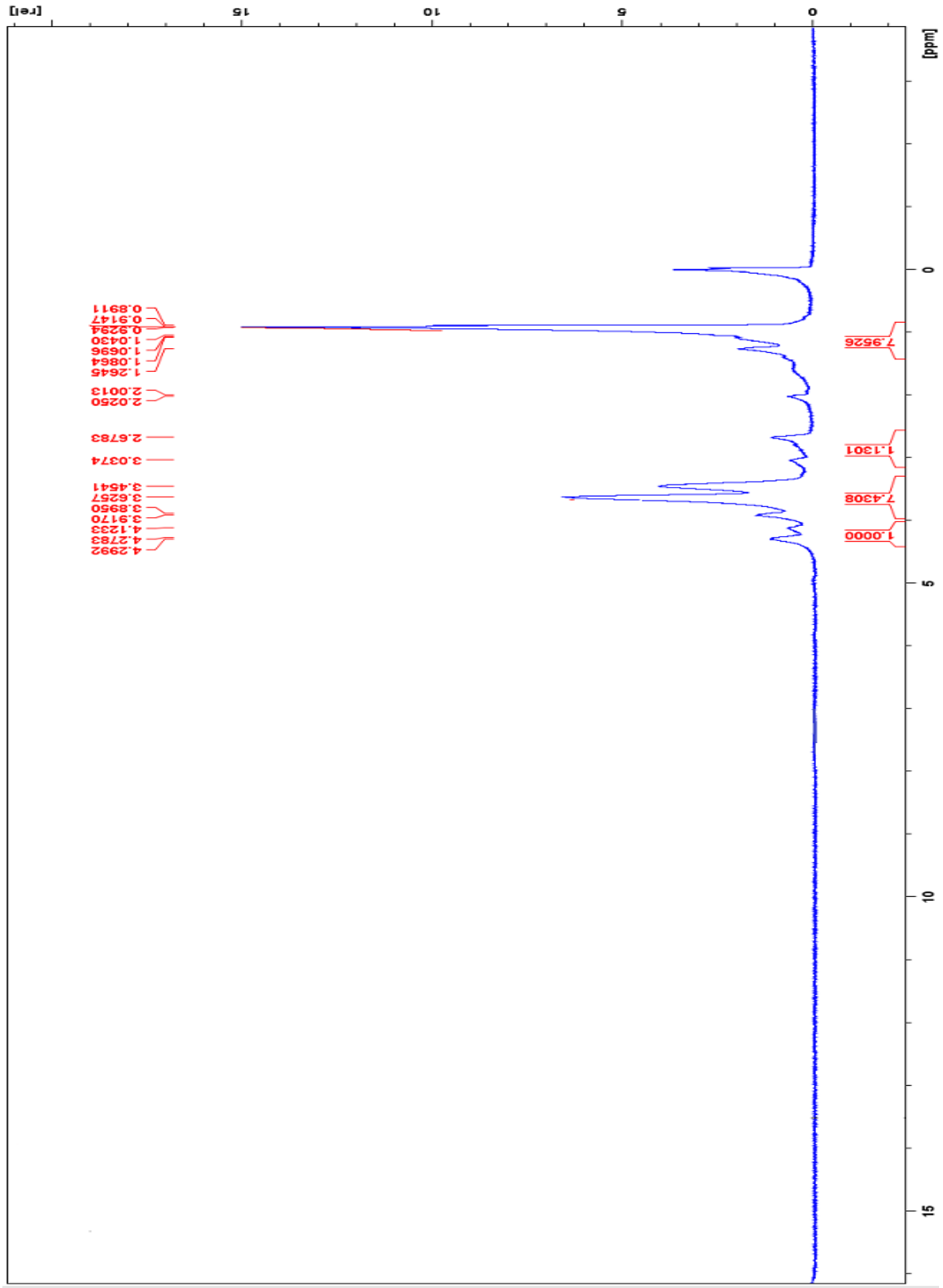

Appendix B

Preliminary X-Ray Crystallographic Data

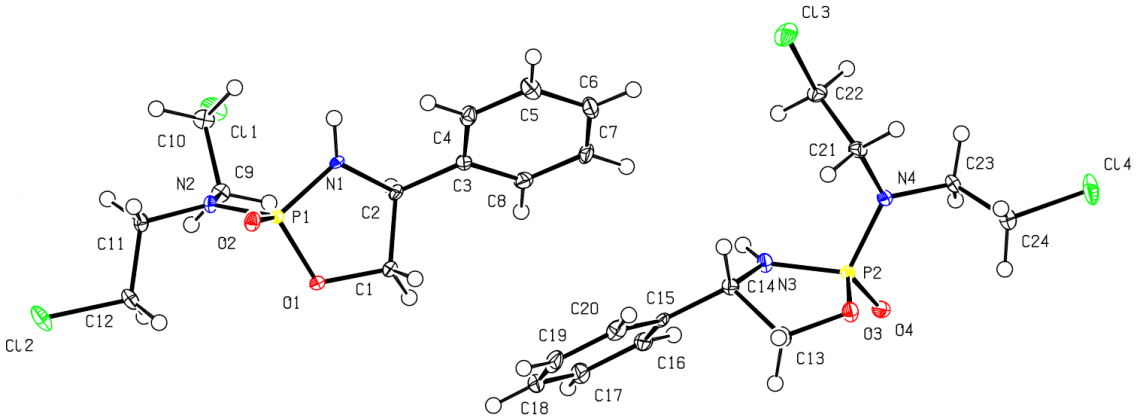

Table 11. Selected Bond Lengths (2*S*,4*S*)-2-[Bis(2-chloroethyl)amino]-4-phenyl-1,3,2-oxazaphospholidine 2-oxide (**5a**), Å.

P1-O1	1.5981(16)	P2-O3	1.6026(16)
P1-O2	1.4764(16)	P2-O4	1.4788(17)
P1-N1	1.6251(19)	P2-N3	1.6226(19)
P1-N2	1.6453(19)	P2-N4	1.644(2)
O1-C1	1.455(3)	O3-C13	1.455(3)
N1-C2	1.462(3)	N3-C14	1.461(3)
C1-C2	1.543(3)	C13-C14	1.542(3)
C2-C3	1.518(3)	C14-C15	1.513(3)
C3-C4	1.387(3)	C15-C16	1.380(3)
C4-C5	1.388(3)	C16-C17	1.396(3)
C5-C6	1.389(3)	C17-C18	1.376(3)
C6-C7	1.386(4)	C18-C19	1.386(4)
C7-C8	1.387(3)	C19-C20	1.383(3)
C8-C3	1.395(3)	C20-C15	1.390(3)
N2-C9	1.462(3)	N4-C21	1.466(3)
C9-C10	1.524(3)	C21-C22	1.522(3)
C10-Cl1	1.793(2)	C22-Cl3	1.797(2)
N2-C11	1.468(3)	N4-C23	1.471(3)
C11-C12	1.515(3)	C23-C24	1.517(3)
C12-Cl2	1.800(2)	C24-Cl4	1.800(2)

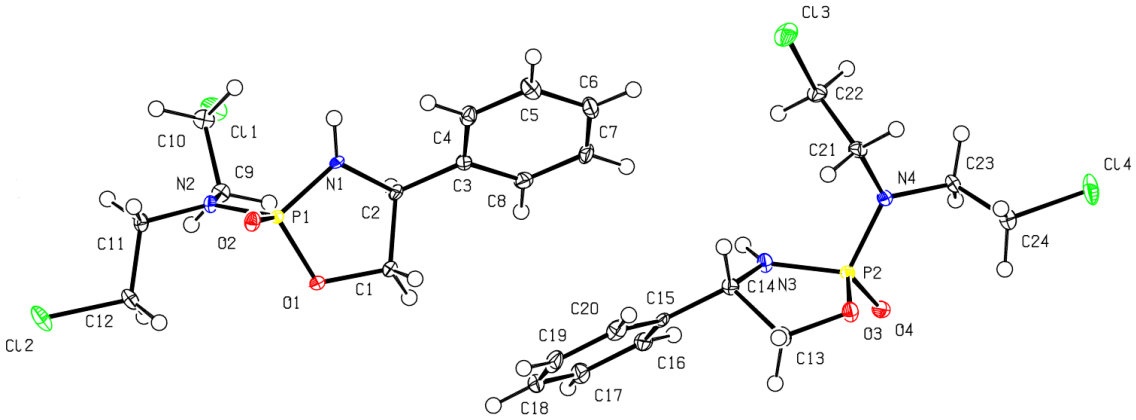

Table 12. Selected Bond Angles (2*S*,4*S*)-2-[Bis(2-chloroethyl)amino]-4-phenyl-1,3,2-oxazaphospholidine 2-oxide (**5a**), degrees.

N1-C2-C1	102.75(17)	N3-C14-C13	102.35(17)
N1-C2-C3	113.52(19)	N3-C14-C15	113.64(19)
N1-P1-N2	109.84(10)	N3-P2-N4	109.65(10)
N2-C11-C12	110.82(19)	N4-C21-C22	110.3(2)
N2-C9-C10	110.4(2)	N4-C23-C24	110.9(2)
O1-C1-C2	106.54(17)	O3-C13-C14	106.81(17)
O1-P1-N1	95.85(9)	O3-P2-N3	95.70(9)
O1-P1-N2	108.88(10)	O3-P2-N4	108.29(10)
O2-P1-N1	119.14(10)	O4-P2-N3	119.30(10)
O2-P1-N2	108.13(9)	O4-P2-N4	108.65(10)
O2-P1-O1	114.29(9)	O4-P2-O3	114.37(9)
C1-O1-P1	111.53(13)	C13-O3-P2	111.26(14)
C2-N1-P1	114.21(15)	C14-N3-P2	114.54(15)
C3-C2-C1	111.99(19)	C15-C14-C13	112.4(2)
C3-C4-C5	120.9(2)	C15-C16-C17	120.5(2)
C4-C3-C2	122.1(2)	C16-C15-C14	121.9(2)
C4-C3-C8	118.8(2)	C16-C15-C20	118.8(2)
C4-C5-C6	120.0(2)	C17-C18-C19	119.9(2)
C7-C6-C5	119.4(2)	C18-C17-C16	120.1(2)
C7-C8-C3	120.4(2)	C19-C20-C15	121.0(2)
C8-C3-C2	119.1(2)	C20-C15-C14	119.3(2)
C8-C7-C6	120.5(2)	C20-C19-C18	119.7(2)
C9-C10-Cl1	108.82(17)	C21-C22-Cl3	109.08(17)
C9-N2-C11	116.83(19)	C21-N4-C23	117.06(19)
C9-N2-P1	119.58(16)	C21-N4-P2	119.22(15)
C11-C12-Cl2	109.35(17)	C23-C24-Cl4	109.44(17)
C11-N2-P1	121.35(16)	C23-N4-P2	121.94(16)

Table 13. Atomic Coordinates ($x10^4$) and Equivalent Isotropic Displacement Parameters ($Å^2x10^3$) for (2*S*, 4*S*)-2-[Bis(2-chloroethyl)amino]-4-phenyl-1,3,2-oxazaphospholidine 2-oxide (**5a**).

	x	y	z	U(eq)
P1	8961(1)	5065(1)	10229(1)	8(1)
O1	7983(2)	3482(2)	9984(1)	12(1)
O2	10218(1)	4479(2)	10607(1)	12(1)
N1	8888(2)	5964(2)	9451(1)	10(1)
N2	8306(2)	6400(2)	10756(1)	10(1)
C1	7787(3)	3263(3)	9218(1)	12(1)
C2	7969(2)	5116(3)	8902(1)	10(1)
C3	8438(2)	4998(3)	8190(1)	10(1)
C4	9676(2)	5480(3)	8102(1)	14(1)
C5	10075(3)	5379(3)	7443(1)	17(1)
C6	9237(2)	4770(3)	6861(1)	18(1)
C7	7996(3)	4298(3)	6944(1)	19(1)
C8	7594(2)	4417(3)	7601(1)	15(1)
C9	7085(2)	7271(3)	10495(1)	12(1)
C10	7283(2)	9263(3)	10413(1)	14(1)
C11	8700(2)	6364(3)	11526(1)	12(1)
C12	8135(2)	4766(4)	11851(1)	18(1)
Cl1	5754(1)	10284(1)	10128(1)	19(1)
Cl2	8447(1)	4940(1)	12801(1)	23(1)
P2	5990(1)	-227(1)	4668(1)	10(1)
O3	6972(2)	-1832(2)	4882(1)	13(1)
O4	4685(1)	-791(2)	4349(1)	13(1)
N3	6198(2)	704(3)	5443(1)	12(1)
N4	6585(2)	1055(3)	4100(1)	10(1)
C13	7285(2)	-2004(3)	5647(1)	13(1)
C14	7185(2)	-128(3)	5959(1)	11(1)
C15	6853(2)	-175(3)	6703(1)	11(1)
C16	5620(2)	125(3)	6837(1)	15(1)
C17	5341(3)	54(4)	7527(1)	20(1)
C18	6297(3)	-324(3)	8081(1)	21(1)
C19	7542(3)	-611(3)	7954(1)	21(1)
C20	7812(2)	-536(3)	7268(1)	16(1)
C21	7848(2)	1874(3)	4309(1)	12(1)
C22	7699(2)	3832(3)	4480(1)	14(1)
C23	6065(2)	1059(3)	3342(1)	13(1)
C24	6455(2)	-613(3)	2984(1)	17(1)
Cl3	9263(1)	4800(1)	4723(1)	22(1)
Cl4	6030(1)	-396(1)	2039(1)	27(1)
H1	6912	2809	9050	15
H2	8419	2412	9076	15
H3	7137	5779	8846	12

H4	9360	6882	9367	13
H5	10258	5886	8498	16
H6	10923	5725	7390	21
H7	9511	4679	6411	22
H8	7416	3890	6547	23
H9	6738	4102	7650	18
H9A	6472	7064	10832	14
H9B	6716	6754	10033	14
H10A	7862	9480	10059	16
H10B	7681	9779	10870	16
H11A	8409	7466	11737	14
H11B	9649	6317	11634	14
H12A	8524	3662	11697	22
H12B	7197	4714	11689	22
H13A	8165	-2479	5778	16
H13B	6675	-2823	5829	16
H14	8018	512	5963	14
H21	5753	1634	5545	14
H21A	8363	1756	3919	15
H21B	8309	1254	4729	15
H22	4956	383	6456	18
H22A	7197	3956	4876	16
H22B	7232	4455	4063	16
H23	4490	267	7615	24
H23A	6387	2115	3114	16
H23B	5116	1135	3282	16
H24	6105	-387	8551	25
H24A	6012	-1656	3152	20
H24B	7392	-799	3107	20
H25	8206	-859	8336	25
H26	8666	-733	7183	19

Table 14. Experimental details

Crystal data		
Chemical formula	$C_{12}H_{17}Cl_2N_2O_2P$	
Formula weight	323.15 g / mol	
Temperature	85 K	
Wavelength	0.71073 Å	
Crystal system	Monoclinic	
Space group	$P12_11$	
Unit cell dimensions	a = 10.5334(4) Å	α = 90°
	b = 7.5226(3) Å	β = 98.6760(10)°
	c = 19.1042(7) Å	γ = 90°
Volume	1496.47(10) $Å^3$	
Z	2	
Density (calculated)	1.499 g/cm^3	
Absorption coefficient	0.614 mm^{-1}	
F(000)	668	
Crystal size	0.03 x 0.05 x 0.11 mm3	
Theta range for data collection	2.37 to 27.55°	
Index ranges	-13<=h<=13, -9<=k<=9, -23<=l<=24	
Reflections collected	51257	
Independent reflections	6886 [R(int) = 0.0629]	
Completeness to theta = 27.55°	99.70%	
Absorption correction	Multiscan	
Max. and min. transmission	0.9810 and 0.9380	
Refinement method	Full-matrix least-squares on F2	
Data / restraints / parameters	6886 / 1 / 344	
Goodness-of-fit on F2	1.528	
Final R indices [I>2sigma(I)]	R1 = 0.0300, wR2 = 0.0488	
R indices (all data)	R1 = 0.0370, wR2 = 0.0496	
Absolute structure parameter	0.04(2)	
Extinction coefficient	0.0024(6)	
Largest diff. peak and hole	0.339 and -0.281	

Computer programs: Apex3 v2016.1-0 (Bruker, 2014), PLATON v1.19, SAINT V8.37A (Bruker, 2016), SHELXL2018/3 (Sheldrick, 2015, 2018), SHELXLE Rev915 (Hübschle et al., 2011).